

**Impaired repression at a vasopressin promoter polymorphism
in a rat model of trait anxiety and depression**

Dissertation
der Fakultät für Biologie der
Ludwig-Maximilians-Universität zu München

Christopher A. Murgatroyd

28.09.2004

Mit Genehmigung der der Fakultät für Biologie der
Ludwig-Maximilians-Universität zu München

Berichterstatter: Prof. Dr. R. Landgraf

Mitberichterstatter:
Prüfungskommission: Prof. Dr. E. H. Weiss
Prof. Dr. C. N. David
Prof. Dr. B. Grothe

Weitere Mitglieder: Prof. Dr. M. Götz
Prof. Dr. R. Klein

Mitbetreuung durch den
promovierten Mitarbeiter: Dr. Dietmar Spengler

Dekan: Prof. Dr. Peter Dittrich

Tag der mündlichen Prüfung: 07.02.2005

**Impaired repression at a vasopressin promoter polymorphism
in a rat model of trait anxiety and depression**

CHRISTOPHER A. MURGATROYD

**Max-Planck-Institut für Psychiatrie
Kraepelinstr. 2-10
80804 München**

2004

*With thanks to my parents
and grandparents for
all their support*

CONTENTS

1	INTRODUCTION.....	1
1.1	HAB and LAB rats.....	1
1.1.2	Behaviour	2
1.1.3	Neuroendocrinology.....	3
1.1.4	AVP status.....	4
1.2	HAB and LAB mice.....	7
1.2.1	Behaviour	7
1.2.2	Neuroendocrinology.....	7
1.2.3	AVP status.....	8
1.3	Human affective disorders.....	9
1.3.1	Neuroendocrinology.....	10
1.3.2	AVP status.....	10
2	MATERIALS AND METHODS.....	12
2.1	Materials	12
2.1.1	Chemicals	12
2.1.2	Radiation	13
2.1.3	Restriction endonucleases	13
2.1.4	Modifying enzymes.....	14
2.1.5	Antibodies	14
2.1.6	Vectors	14
2.1.7	Plastics.....	15
2.1.8	Molecular biology kits	15
2.1.9	Cell lines.....	15
2.1.10	Primer sequences.....	15
2.1.11	Sequences and accession numbers	17
2.2	Methods.....	18
2.2.1	DNA Analysis	18
2.2.2	RNA analysis.....	23
2.2.3	Plasmids	28
2.2.4	Cell culture and transfection experiments.....	34
2.2.5	Protein preparation	36
2.2.6	Statistical analysis and computer software.....	41
3	RESULTS.....	42
3.1	Candidate gene approach	43
3.1.1	CRH.....	44
3.2	AVP.....	44
3.2.1	AVP levels in the PVN correlate with anxiety-related behaviour	45
3.2.2	Sequence analysis.....	46

3.2.3	Sequence and genotyping of the adjacent oxytocin gene.....	50
3.2.4	Association of AVP gene and anxiety in EPM test.....	51
3.2.5	Genotyping HAB AVP allele in an outbred population.....	54
3.2.6	<i>In vivo</i> tanscription analysis	55
3.2.7	Transcription factor element analysis	58
3.2.8	C(-592)T and cAMP responsive element.....	59
3.2.9	A(-1276)G and YY1.....	59
3.2.10	A(-1276)G and CArG box binding factor A (CBF-A).....	65
3.2.11	Reporter assays.....	73
3.2.12	CBF-A expression in the PVN	77
3.2.13	Model for the polymorphic CArG element leading to differential AVP expression.....	81
3.3	Genetic analysis of HAB and LAB mice lines.....	82
3.3.1	Marker analysis of mouse chromosome 2.....	82
3.3.2	AVP.....	83
3.4	Human AVP gene as a candidate gene for anxiety	89
3.4.1	Sequence analysis.....	89
3.4.2	C(-229)T promoter SNP.....	90
3.4.3	G(-558)T downstream SNP.....	91
4	DISCUSSION	93
4.1	HAB rat	93
4.2	HAB mouse	98
4.3	LAB mouse.....	98
5	SUMMARY.....	100
6	ABBREVIATIONS	102
6.1	Standard.....	102
6.2	Buffers and substances.....	102
6.3	Non standard	102
7	REFERENCE LIST	104
8	ACKNOWLEDGMENTS	121
9	CURRICULUM VITAE	122

1 Introduction

Anxiety disorders and major depression represent two of the most common and debilitating psychiatric disorders. Epidemiological studies show that anxiety disorders – including panic disorder, phobic disorders and generalised anxiety - can run in families (Hettema et al., 2001). Moreover, twin studies suggest that a genetic predisposition accounts for, at least, part of the familial nature of the disorders, with heritabilities of 30-40% (Kendler, 2001). However, despite decades of intensive research, the underlying genetic cause(s) of these remain elusive (Nestler et al., 2002). Functional studies have yet to identify a focal brain region or particular neurotransmitter system as the primary site of the abnormality and, furthermore, genetic studies have failed to provide evidence for specific culpability genes (Segurado et al., 2003) and allelic variations showing replicable associations in the general population (Lohmueller et al., 2003).

Current research lines in this field include identification of candidate genes in selectively bred animal models. The concept implies that, in these animal models, specific loci associating with a phenotype provide compelling candidate genes for complex human disorders. Indeed, recent animal studies have investigated the concordance of disease associating genes across species. For instance, in the case of hypertension, a remarkable degree of concordance of quantitative trait loci (QTL) regions in comparison of mouse with rat and human is beginning to emerge (DiPetrillo et al., 2004).

To gain insight into the molecular mechanisms underlying affective disorders, animal models were generated by selectively breeding Wistar rat lines for either high (HAB) or low (LAB) anxiety-related behaviour. This approach was followed up in mice also bred for either high or low anxiety-related behaviour. This concept of selectional inbreeding is postulated to concentrate loci playing major roles in the selected phenotype. In turn, the results from these two animal studies then provide a basis for extrapolating these findings to association studies in humans.

1.1 HAB and LAB rats

Criteria for animal models of depression have been intensively discussed in the last two decades, however, the criterion proposed by McKinney and Bunney (McKinney and Bunney, 1969) has been the most widely accepted. These authors propose that the validity of an animal model can be determined by the extent that (a) it is ‘reasonably analogous’ to the human disorder in its manifestations or symptomatology, (b) there is a behavioural change that can

be objectively monitored, (c) the behavioural changes observed should be reversed by the same treatment modalities that are effective in humans, and (d) the system should be reproducible between investigators. Taking these guidelines into consideration, it is proposed that the HAB rat represents a robust and unique model for human anxiety.

1.1.2 Behaviour

Ten-week old Wistar rats were selected for inbreeding using behavioural results from the elevated plus-maze (EPM) test. The EPM test is the most widely used apparatus for measuring anxiety in rodents (Pellow et al., 1985). The test is performed by placing a naive rat in the centre of an elevated plus-maze with two open and two enclosed arms, and allowing it to freely explore. It is accepted that the reluctance of rats to explore the open arms of the maze is caused by fear of open spaces. Furthermore, anxiolytic compounds increase, whereas anxiogenic compounds decrease, the percentage of time spent on open the arms (Pellow et al., 1985). The results from the EPM test were used to select mating pairs to establish the HAB and LAB lines. To date, HAB rats of both sexes spend less time in the open arms of the maze and enter this area less frequently. Specifically, HAB animals spend around 5% of the total time on the EPM test in the open arms compared to 50% in LAB animals.

The high anxiety phenotype in the HAB rats is not only detectable in the EPM test, but also in the open field, the modified hole board and in other tests of unconditioned anxiety such as the black and white box and the social interaction test (for a review see Henniger et al., 2000; Wigger et al., 2001). Furthermore, in a social defeat paradigm, HAB and LAB rats differed significantly in their coping behaviour - HAB rats emitting more ultrasound vocalisation calls and spending more time freezing in contrast to the LAB rats which showed increased locomotor activity and signs of aggressive behaviour towards a resident animal indicative of active stress coping (Koolhaas et al., 1999). Measuring ultrasound vocalisation in the rat pups revealed that the HAB rats vocalized significantly more than LAB animals (Wigger et al., 2001). This confirms, not only the early expression of the trait in the HAB rats development, but also of anxiety-related behaviour independent of locomotor activity (Tornatzky and Miczek, 1994).

While there were no differences in fighting, threatening, social grooming, self-grooming, sniffing, burying, and feeding or drinking, HAB rats displayed markedly less rearing, indicative of exploratory curiosity, but spent more time sleeping than LAB animals (Henniger et al., 2000). Again, all the tests performed confirmed that the difference in

Introduction

anxiety-related behaviour is independent of gender. It is of further importance to note that basal blood pressure and heart rate failed to differ between HAB and LAB rats.

In addition to the innate anxiety, HAB rats also present with a depression-like behaviour showing remarkably passive stress coping in the forced swim (FS) test (Keck et al., 2001). The FS test (Porsolt et al., 1977), which is considered to have predictive value for the efficacy of antidepressant treatments (Lucki, 1997), revealed that HAB rats floated much more and struggled far less than LAB animals. This preference of passive coping, in addition to the behavioural despair, is interesting when considering that anxiety and depression share many overlapping symptoms, often co-existing, in the clinic (for review see Gorwood, 2004).

The possibility of a genetic contribution or determinant underlying the anxiety-like behaviour was tested in the HAB line by examining the influence of postnatal factors in the divergent emotionality of HAB and LAB rats. In a cross-fostering experiment animals were reared, from the first postnatal day until weaning, by mothers of the opposite rat line and behaviourally characterized as adults. From this study it emerged that none of the anxiety parameters revealed variances between fostered controls and cross-fostered animals within either line (Wigger et al., 2001). Additionally, HAB mothers showed no deficits in their maternal behaviour making it highly unlikely that environmental factors (Meaney, 2001), or epigenetic programming stemming from maternal behaviour (Weaver et al., 2004) may contribute to the line-specific divergences detectable in the adults. Moreover, cross-breeding of HAB and LAB rats resulted in F1 offspring displaying intermediate anxiety-related behaviour on the EPM test, perhaps again supporting a role of genetic factors in the behavioural differences between HAB and LAB rats (Wigger et al., 2001).

1.1.3 Neuroendocrinology

Hyperactivity of the hypothalamic–pituitary–adrenal (HPA) axis is one of the key findings described in major depressive and affective disorders (Holsboer, 2000). Corticotropin-releasing hormone (CRH) and vasopressin (AVP) are the main regulators of this stress system acting synergistically in stimulating adrenocorticotropin (ACTH) release from the anterior pituitary which subsequently causes the release of cortisol (humans) or corticosterone (rodents) from the adrenal gland, which, in turn, regulates CRH and AVP production via negative feedback (figure 1A). HPA axis function can be examined by conducting a neuroendocrine challenge test that attenuates or enhances cortisol/corticosterone (CORT), ACTH or CRH release. This test entails administration of the synthetic corticosteroid, dexamethasone (DEX), to the subject and measuring CORT levels 12h later. If CORT levels

are not decreased then the subject is said to suffer from DEX non-suppression. A further improvement on this test is the combined DEX/CRH challenge test in which the HPA axis is both stimulated by the administration of CRH and inhibited with DEX (Holsboer et al., 1987), resulting in a far greater sensitivity (for review see Heuser et al., 1994). When the DEX/CRH test was performed in the two rat lines it became evident that HAB rats were DEX non-suppressors (Keck et al., 2002). It was further speculated by the authors that this phenomenon pointed towards an enhanced activity and critical involvement of the neuropeptide AVP, which was supported by the observation of increased basal synthesis and release of AVP within the paraventricular nucleus (PVN) of the hypothalamus in the HAB rats, as described in more detail below.

Anxiolytic and antidepressive drugs generally yield contradictory results when administered to normal rats indicating that - in parallel to the situation in humans - the efficacy of an anxiolytic may depend on the animal's basal level of anxiety (Liebsch et al., 1998; Will et al., 2003). Indeed, HAB rats responded to diazepam with a 20-fold increase in the percentage of time spent on the open arms of the EPM test, in contrast to a 2.5-fold increase in LAB rats (Liebsch et al., 1998). Of further note, diazepam functions in the rat by stimulating basal HPA axis activity (Vargas et al., 2001). As previously stated, the behaviour of the HAB rats is indicative, not only of anxiety-related, but also depression-like symptoms and accordingly responded to, the classical antidepressive selective serotonin re-uptake inhibitor (SSRI), paroxetine, with a more active stress-coping strategy in the FS test, in contrast to the LAB rats which failed to respond (Keck et al., 2003). Similarly to diazepam, paroxetine again attenuates HPA axis overactivity (Nickel et al., 2003).

As previously described, the HAB rats are DEX non-suppressors, however, periferal administration of the AVP V1-receptor antagonist $d(\text{CH}_2)_5\text{Tyr}(\text{Me})\text{AVP}$ in HABs, resulted in a reduced level of anxiety/ depression-related behaviour (Keck et al., 2002). This indicates that AVP has major effects in both the neuroendocrine system and in the anxiety-related behaviour.

1.1.4 AVP status

CRH and AVP are the main regulators of the HPA stress system; being released from the hypothalamic parvocellular neurons of the PVN. *In situ*-hybridisation analysis of the hypothalamic PVN in HAB and LAB rats revealed that CRH mRNA expression was similar between the lines under both basal and stress conditions. The most striking molecular finding, however, and the focus of the present study, relates to AVP mRNA expression, which was

Introduction

found to be significantly higher in the parvocellular and magnocellular neurons of the PVN of HAB rats under both basal and stress conditions (figure 1B) (Wigger et al., 2004). Furthermore, the HAB rats presented with a significantly higher AVP release from the PVN in microdialysate experiments (figure 1C) (Wigger et al., 2004).

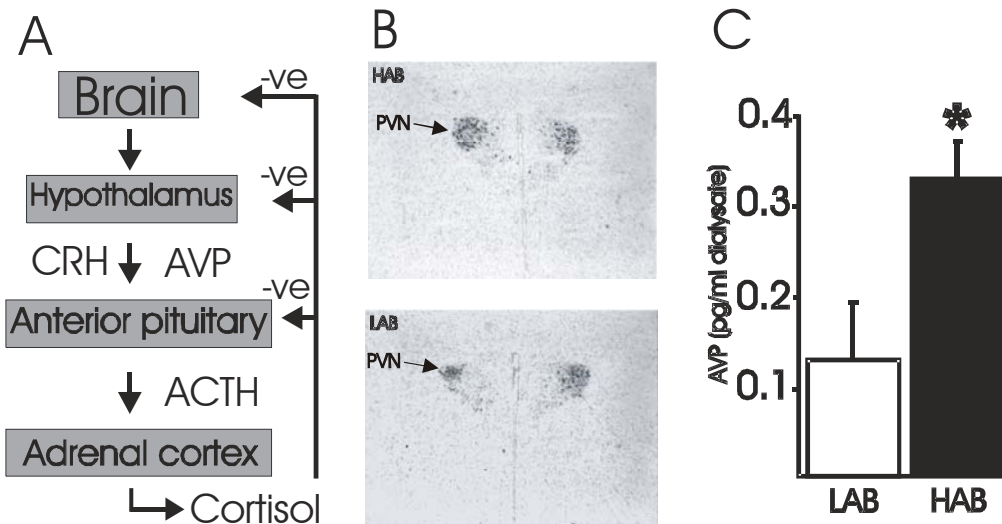


Figure 1. Scheme of HPA axis and differential AVP expression between HAB and LAB animals. (A) Schematic diagram of the HPA axis. (B) *in situ*-hybridisation experiments using a radiolabelled AVP mRNA-specific oligonucleotide in the PVN (Wigger et al., 2004) reveal an increase in expression of AVP mRNA in the HAB rat line. (C) Microdialysate measurement of AVP peptide in the PVN reveal a significant increase in AVP peptide release from the PVN in the HAB line rats. *, Significantly different ($p < 0.05$).

Measurements of oxytocin - the structurally and functionally related neuropeptide - failed to reveal differences between the HAB and LAB rats in either mRNA or protein content in the PVN or release in the dialysate. When comparing the levels of AVP between the various AVP-containing hypothalamic nuclei strict tissue-specificity emerged whereby AVP overexpression occurred only in the parvocellular and magnocellular neurons of the PVN, whereas no elevations were present in other AVP expressing nuclei in the hypothalamus, namely the supraoptic nucleus (SON) and the suprachiasmatic nucleus (SCN).

Taking together the aforementioned evidence; (a) higher AVP mRNA expression, and release in the parvocellular and magnocellular neurons of the PVN in HAB rats, (b) an AVP V1a receptor antagonist results in reduced anxiety/depression related behaviour, and (c) hyper-reactive HPA axis and Dex/CRH results in the HAB animals are driven by AVP overexpression which paroxetine treatment normalized, it was hypothesized that AVP plays a major role in the anxiety/depression related behaviour and neuroendocrine features of the HAB. Therefore, to pursue further this issue, and to gain insight into the molecular

Introduction

mechanism underlying the anxiety in our rat lines, we decided to investigate the AVP locus as a candidate gene for anxiety and depression.

The structures of AVP and oxytocin were determined by du Vigneaud in 1954, and earned him the nobel prize in 1955 (du Vigneaud, 1954). AVP is a cyclic nonapeptide that is synthesised centrally in the hypothalamus. The peptide is released in response to a variety of stimuli including increasing plasma osmolarity, hypovolaemia, hypotension and hypoglycaemia (Dunn et al., 1973;Laszlo et al., 1991) and has powerful antidiuretic and vasoconstrictor effects (Hofbauer et al., 1984). AVP has also been implicated in learning and memory (Engelmann et al., 1996), however, it is the role of AVP in the regulation of the HPA axis that forms the main focus of this study (for review see Scott and Dinan, 2002;Gazdar et al., 1980;Landgraf, 2001). Although the cell-specific expression and physiological regulation of the AVP gene has been described in some detail (for review see Burbach, 2002), much less is known about the regulatory elements and transcription factors bound within the promoter that control these processes. The AVP promoter is positively regulated by the cAMP signalling pathway (Verbeeck et al., 1990), and two cAMP responsive elements (CRE) have been identified at -227 to -220bp and -123 to -116bp in the rat promoter (Iwasaki et al., 1997). Furthermore, an AP1 site has also been identified in the rat promoter (Grace et al., 1999), although its functional role in AVP expression remains to be established (Coulson et al., 1999b). A number of E-box motifs localise to the region -157 to -23bp, which are predicted to be bound by members of the basic helix-loop-helix (bHLH) transcription factor family. Among these Clock, Bmal1, Sim1 and Arnt2 behave as transactivators, involved in controlling either circadian rhythm or neuronal development (for review see Burbach, 2002). Expression of the AVP gene is suppressed by adrenal glucocorticoids through a putative glucocorticoid response element (GRE) which maps to -622 to -608bp in the rat promoter (Iwasaki et al., 1997). Both GR-DNA dependent and independent mechanisms for repression have been assigned to this element (Kim et al., 2001). In addition, AVP gene expression also appears to be regulated by other members of the nuclear hormone receptor family, notably by androgen (Adan and Burbach, 1992) and oestrogen receptors (Shapiro et al., 2000).

In addition to the upstream AVP promoter, regulatory regions located downstream to the gene are also suggested to control the cell-specific expression of AVP. Specifically, a 178bp sequence immediately downstream of exon 3, has been demonstrated to contribute to tissue-specific expression of green fluorescent protein reporter constructs in hypothalamic slice-explant cultures (Fields et al., 2003).

Introduction

In this study we sought to examine the molecular mechanisms underlying the differential expression and release of AVP in the PVN of HAB and LAB lines. We show that the promoter of the AVP gene in the HAB animal, containing a number of SNPs, works in *cis* to produce higher levels of AVP. In this promoter region we discovered that the disruption of a CArG element in the HAB rat, located 1276bp upstream from the AVP start codon, plays a major role in this promoter overexpression by disrupting the binding of CBF-A which, in turn, acts as a repressor for AVP expression. We, therefore, conclude that constitutive overexpression of AVP in the PVN of HAB rats is critically dependent on the HAB allele. The relevance of AVP to the anxiety-related behaviour was further investigated in an association study involving the F2 offspring from a HAB/LAB and HAB/outbred cross, which supported a possible involvement of the AVP gene in controlling behaviour on the EPM and FS tests. Therefore, we speculate that this allele might contribute to the behavioural and endocrine correlates of trait anxiety and depression in this rat line.

1.2 HAB and LAB mice

Above findings prompted us to examine, in addition, the relevance of AVP as a candidate gene for anxiety in other mammals. Therefore, to address this topic, mice have recently been subjected to selective bi-directional inbreeding on the EPM test for either high (HAB) or low (LAB) anxiety-related behaviour. In this protocol 'outbred' CD1 mice were employed on the basis that a population of outbred animals should display a higher degree of variance in behaviour, which might facilitate the bi-directional selective inbreeding strategy (Kroemer et al., submitted).

1.2.1 Behaviour

Within a few rounds of selective inbreeding, HAB and LAB mice lines - in a similar fashion to the rats - differed markedly and consistently in their anxiety-like behaviour on the EPM test. In addition to this deficit in emotionality, the HAB mice were also impaired in their stress coping, depression-like, behaviour in the FS test, resembling again the aforementioned HAB rat line. Results of the tail suspension (TS) test which, similarly to the EPM test, also measures behavioural despair (Chermat et al., 1986), again support the presence of a passive stress coping behaviour in the HAB mice.

1.2.2 Neuroendocrinology

The smaller blood volume of mice compared to rats prevents application of the DEX/CRH test in the HAB and LAB mice lines in the same manner as it was performed in the rat lines.

Introduction

Therefore, HPA axis functioning in these animals has yet to be characterised. The behavioural responses to antidepressant and anxiolytic drugs in the HAB mice appeared to differ from the HAB rat line because HAB mice revealed no responses to paroxetine, and, furthermore, administration of the benzodiazepine diazepam resulted in no anxiolytic effects (Landgraf R, unpublished data). The HAB mice did, however, react mildly to imipramine (Landgraf R, unpublished data), which is a tricyclic antidepressant whose mechanism of action, in contrary to paroxetine and diazepam, is thought to involve the transmitter-uptake mechanism of monoaminergic neurons (Mongeau et al., 1997).

1.2.3 AVP status

The most striking feature of the mice lines, in the context of this study, was the finding that AVP mRNA expression, as well as release of the neuropeptide, are higher in the PVN of HAB mice when compared to LAB mice (figure 2) (Landgraf R, unpublished data).

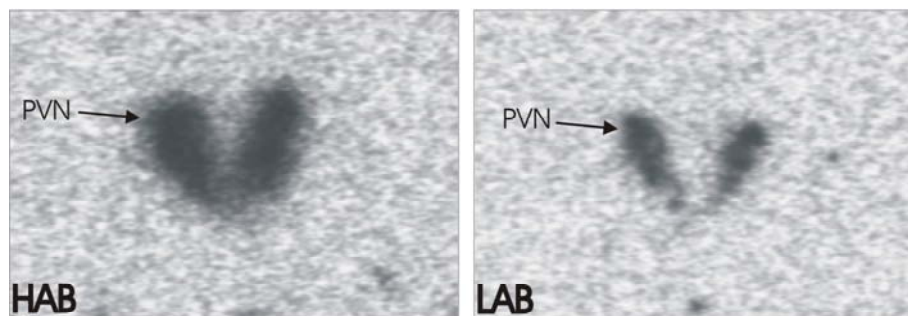


Figure 2. *In situ*-hybridisation experiments for AVP mRNA in the PVN of HAB and LAB mice reveal a 3 to 4-fold increase in expression in the HAB line mice (Landgraf R, unpublished data).

The finding that selective inbreeding in two separate species of rodents on the same behavioural paradigm resulted in a similar behavioural endophenotype, accompanied in parallel at the molecular level by a dramatic overexpression of AVP, represents a remarkable outcome. In addition to the AVP overexpression in the HAB mice, it should be noted that the LAB mice contained a stark reduction in AVP expression in the PVN when compared to HAB and normal anxiety-related behaviour (NAB) mice, in contrast to the LAB rats (see below). It was, therefore, speculated that AVP might play a role in the behavioural and neuroendocrine features typical of trait anxiety and depression in the two mice lines providing an impetus for us to investigate the mouse AVP gene as a vulnerability candidate. Indeed, sequencing of the AVP gene and promoter led to the finding of line-specific differences which we speculate underlie the expression differences seen in the PVN between the LAB

and HAB mice in a similar way to that seen in the anxious rat line. Furthermore, it is possible that the conserved amino acid change in the signal peptide might play a role in AVP post-translational regulation by altering the processing and release of AVP. In this respect it was of further interest to note that subsequent metabolic studies in the LAB mice revealed a defect in their osmotic regulation, being acutely prone to a hyperosmotic challenge (Landgraf R, unpublished data). This supports the theory that this altered signal peptide leads to the observed reduction in AVP, resulting in a diabetes insipidus (DI) -related phenotype.

1.3 Human affective disorders

The impact of depression and anxiety disorders worldwide is overwhelming (figure 3). The World Bank report on the global burden of disease ranked major depression fourth among all medical illnesses in terms of its disabling impact on the world population (Murray and Lopez, 1996) It was further estimated that, by the year 2020, depression would be second only to ischemic heart disease with anxiety disorders ranking close behind (for review see Hirschfeld, 2001). Indeed, between 10% and 20% of adults in any given 12-month period will visit their primary care physician during an episode of mental illness (Kirmayer et al., 1993).

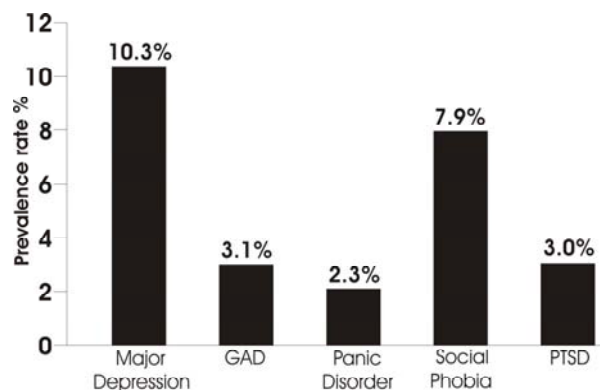


Figure 3. Prevalence of major depression and anxiety disorders in the community. Adopted from (Kessler et al., 1994;Kessler et al., 1995). Values based on 12-month comorbid prevalence data. GAD= generalized anxiety disorder, PTSD= posttraumatic stress disorder.

The debilitating nature of the disease, as well as representing a burden to the individual concerned, results in an increasingly higher strain on the state. In fact, 24% of high medical utilizers, the top 10%, have been found to suffer from major depression and 22%, from an anxiety disorder (Katon et al., 1990), representing, respectively, a cost of 82 and 53 billion dollars a year in the US (Uhl and Grow, 2004).

1.3.1 Neuroendocrinology

Disturbances in HPA axis regulation seem to play a profound role in the development, course and remission of major depression and affective disorder. Patient studies consistently evidence a close correlation between a stable remission of the clinical symptoms and a normalization of HPA regulation (for review see Holsboer, 2003). Furthermore, the finding that healthy probands, with a family history of mood disorder, show abnormalities on the Dex/CRH test (Holsboer et al., 1995), supports the theory that culpability genes can contribute to the development of mood disorders via HPA axis function.

1.3.2 AVP status

The overall aim in this research, as to almost any animal research, was to extrapolate findings from the rat and mouse models to the human, thereby aiding in the development of diagnostic markers and therapeutic tools. Therefore, this study progressed towards the direction of analysing the AVP gene in humans to determine to what extent, if any, AVP might act as a marker for human affective disorders. It is well known that AVP has an important role in the regulation of the HPA axis in patients. It is, therefore, of interest in this regard to note the previous literature linking increased numbers of CRH neurons co-expressing AVP mRNA in the PVN of depressed patients (Purba et al., 1996) and aged subjects (Raadsheer et al., 1993) reflecting a hyperactivity of these neurons and subsequent HPA axis. Furthermore, numerous studies reported higher levels of AVP in the plasma of depressed patients (Inder et al., 2001; van Londen et al., 1997; van Londen et al., 1998), and in the cerebral spinal fluid (CSF) of patients presenting with a range of affective disorders such as depression (Frank et al., 2000; Gold et al., 1981; Pitts et al., 1995; Sorensen et al., 1985), psychotic depression (Gold PW, unpublished data 1986), obsessive compulsive disorder (Altemus et al., 1992; Altemus et al., 1994), anorexia nervosa (Gold et al., 1983), bulimia nervosa (Frank et al., 2000; Demitrack et al., 1992), aggression (Coccaro et al., 1998) and chronic pain disorder (Wahlbeck et al., 1996). Moreover, reductions in CSF concentrations of AVP have been reported in patients with major depression upon treatment with antidepressants such as fluoxetine (De Bellis et al., 1993), clomipramine hydrochloride (Altemus et al., 1994), and clonidine (Peskind et al., 1987). A recent study using a non-peptide AVP 1b receptor (AVPR1b) antagonist has pointed to a role for AVP in the modulation of emotional processes via the V1b receptor (Griebel et al., 2002). Following on, a further study revealed that a haplotype, involving a number of

Introduction

genetic variations in the AVPR1b gene, associated in patients with affective disorders (van West et al., 2004).

We, therefore, concluded this study by providing a framework to address the question of the relevance of the AVP gene to affective disorders in the human by elucidating and characterising SNPs in the promoter 5' of the AVP gene and downstream 3' to the gene. These markers, together, provide a useful basis for a prospective case/control association study.

2 Materials and Methods

2.1 Materials

2.1.1 Chemicals

Consumable	Supplier	Consumable	Supplier
1kb ladder	Fermentas	3MM-Papier	Wattman
Agar	GibcoBRL	Agarose (low-melting point)	Gibco
Agarose (peqGOLDuniversal)	Peqlab (Erlangen)	Ammoniumperoxodisuphate	Sigma
Ampicillin	Roth	Antibiotic/antimycotic	Gibco
Boric acid	Biomol	Bovine serum	Invitrogen
Bradford assay	Biorad	Bromophenol blue	Biorad
BSA	Sigma	Chloroform	Roth
Chloroform (RNase free)	Merck	Coomasie blue	Biorad
Developing emulsion (slides)	Kodak	Developing solution (film)	Kodak
Developing solution (slides)	Kodak	DMSO	Sigma
DNA marker (1kb)	NEB	DNA marker λ HindIII	GibcoBRL
dNTPs (set of 4)	Fermentas	DTT	Sigma
DMEM (-Na.pyruvate)	Gibco	EDTA	Sigma
Ethanol	Merck	Ethidiumbromide	Biomol
Ficoll 400	Sigma	Fixing solution (films)	Kodak
Fixing solution (slides)	Kodak	Foetal bovine serum	Gibco
Formaldehyde	Merck	Formamide	Sigma
L-Glutathione reduced	Sigma	Glutathionine Sepharose	Amersham
Glycerine	Sigma	Glycerol	Biomol
Glycine	Biomol	Glycogen	Fermentas
Guanidine thiocyanate	Merck	IGEPAL	Sigma
IPTG	Fermentas	Isoamylalkohol	Merck
β -mercaptoethanol	Merck	Methanol	Merck
Milk powder	Regilait (France)	MOPS	Sigma
Nitrocellulose film BA-S85	Schleicher&Schuell	N-lauroyl-sacosine	Sigma
Oligonucleotides	MWG /Invitrogen	Optimem1 medium	Gibco
Paraformaldehyde	Sigma	PBS	Gibco
Phenol	Appligene	Phenol pH 7.5	Appligene
Ponceau	Sigma	2-propanol	Merck
2-propanol (RNase free)	Merck	Protein marker	NEB
Poly(d(I-C))	Roche	Polaroid instant film	Polaroid
Polyacrylamide–rotiphorese 30	Roth	Polyacrylamide –rotiphorese 40	Roth
Potassium chloride	Sigma	Roti-Histokit II	Roth

Materials and Methods

RPMI 1640 (+L-glutamine)	Gibco	Salmon testes DNA	Sigma
Sarcosyl	Sigma	SDS	Biomol
Siliconising fluid	Sigma	Sodium acetate	Merck
Sodium chloride	Merck	Streptavidin Agarose	Novagen
Taurine	USB (USA)	TEMED	Sigma
Toluidine blue	Sigma	Transfer Ribonucleic acid	Sigma
Tris	Riedel-deHaen	Triton X-100	Roth
Trypsin	Gibco	Tryptone	Roth
Urea	Roth	Ultima Gold	Packard
X-Gal	Sigma	X-ray film (Biomax)	Kodak
Xylencyanol	Chroma-gesellschaft	Yeast extract	GibcoBRL

2.1.2 Radiation

Nucleotide	Activity	Supplier
35S-thio-rUTP	12.5 mCi/mM	NEN
(35S)UTP- α S	10mCi/ml	Hartmann Analytica
32P α dCTP	1x9,25 MBq	Amersham
α -33P dATP	1x9,25 MBq / 1x250 μ Ci	Amersham
(33P)ddNTPs) Redivue (set of 4)	10mCi/ml	Amersham
γ 32P-ATP	1x9,25 MBq	Amersham

2.1.3 Restriction endonucleases

Enzyme	Supplier	Enzyme	Supplier	Enzyme	Supplier
AcI	NEB	BbvI	NEB	BsmAI	NEB
DraIII	NEB	BamHI	Fermentas	EcoRI	Fermentas
EcoRV	Fermentas	Eam11041(Ksp6321)	Fermentas	HindIII	Fermentas
KpnI	Fermentas	HaeIII	NEB	HincII	NEB
NlaIII	NEB	PvuI	Fermentas	MaeIII	NEB
MseI	NEB	SacI	Fermentas	SfaNI	NEB
SmaI	Fermentas	SphI	Fermentas	Tth1111	NEB
XbaI	Fermentas	XhoI	Fermentas		

2.1.4 Modifying enzymes

Enzyme	Supplier	Enzyme	Supplier
T3-RNA polymerase	Roche	T4-DNA-Ligase	Roche
T4 DNA polymerase	Fermentas	T4 polynucleotide kinase	Fermentas
T7-RNA polymerase	Fermentas	CIAP	Fermentas
DNA pol. I, klenow fragment	NEB	DNA polymerase (<i>Taq.</i>)	Fermentas
DNA polymerase(Pfu)	Fermentas	DNaseI	Fermentas
Proteinase K	Boehringer Mannheim	Proteinase K (RNase free)	Sigma
Ribonuclease A	Sigma	RNase	Sigma
RNase inhibitor	Fermentas	S1 Nuclease	Amersham
Streptokinase	Sigma		

2.1.5 Antibodies

2.1.5.1 Primary antibodies

Antibody	Epitope	Host	Supplier
YY1 (H-10)X	full length human YY1(monoclonal)	Mouse	Santa Cruz
α -N-CBF-A	1st 75aa mouse CBF-A (polyclonal)	Rabbit	gift Leanderson et al.
Anti-GST	Shistosomal GST (polyclonal)	Goat	Pharmacia
Anti-Flag	M2 (monoclonal)	Mouse	Sigma
Anti-His	His ₆ (monoclonal)	Mouse	Roche

2.1.5.2 Secondary antibodies

Antibody	Epitope	Host	Supplier
Anti-rabbit	rabbit IgG	Goat	Perbio
Anti-goat	goat IgG	Donkey	Santa Cruz
Anti-mouse	mouse IgG	Goat	Santa Cruz

2.1.6 Vectors

Vector	Supplier
pBSKII	Stratagene
pGL2basic	Promega
pGEX-2TK	Pharmacia

2.1.7 Plastics

Consumable	Supplier	Consumable	Supplier	Consumable	Supplier
Filtertips	Sarstedt	PCR plates/caps (96)	ABgene	Cell culture plates	Greiner
Pipette tips	Sarstedt	Scalpels	Merck	Micro test plates	Greiner
Cuvette 1mm	Biorad	X-ray cassette	Kodak	Gel chambers	Biorad

2.1.8 Molecular biology kits

Consumable	Supplier	Consumable	Supplier
Chemagenic DNA tissue	Chemagen	Chemagenic stand 2x12	Chemagen
NucleoSpin Tissue	Macherey Nagel	NucleoSpin plasmid quickprep	Macherey Nagel
DNAeasy extraction kit	Qiagen	RNeasy	Qiagen
Thermosequ. Radio. Term. cycle sequencing	USB	Thermosequ. (33P) Term. cycle sequencing	Amersham
ExoSAP-IT	USB	Lumi-light Western blotting substrate	Roche
Lipofectamine TM	Invitrogen	OneStep RT-PCR	Qiagen
Picogreen DNA quantification reagent	Molecular probes	GeneRacer superscriptII and zero blunt TOPO cloning	Invitrogen
Bio-spin 6 columns	Biorad	silver stain kit	SIGMA

2.1.9 Cell lines

Name	Derived tissue	Morphology	Supplier	Reference
Saos-2	prim. Osteosarcoma	epithelial	DSMZ	(Fogh et al., 1977)
Neuro2a	murine neuroblastoma	neuronal	ATCC	(Klebe RJ, 1969)
Lu-165	small cell lung can.	SSLC	Terasaki. T	(Terasaki et al., 1994)
HeLa	cerv.epith.adenocarcin.	epithelial	ATCC	(Scherer, 1954)
3T3	murine embryo	fibroblast	ATCC	(Todaro, 1963)

2.1.10 Primer sequences

2.1.10.1 SSCP primer pairs

Rat CRF **1f**, tca gta tgt ttt cca cac ttg gat; **1r**, cga ccc tct tca gaa agc ac; **2f**, tat tag gca aat gct gcg tg; **2r**, agc tca ggc agc aca aag tt; **3f**, cca agg gag gag aag gta gg; **3r**, gcg ggt atg gga cac aat aa; **4f**, tca atc caa tct gcc act ca; **4r**, aaa gct cat atg gtg cga gc; **5f**, cgg cga ata gct taa acc tg; **5r**, aag gtg ggg gag aga ggt aa; **6f**, agg aag tcc cgc tac acc tt; **6r**, atc aga atc ggc tga ggt tg; **7f**, ccg ttg aat ttc ttg caa cc; **7r**, tga gat cca gag aga tgg gc;

Materials and Methods

8f, gga gag gga gag gcg gtc; **8r**, ttg tgc atg cta att aag ggg; **9f**, gaa gat gta cag gga gag agc c; **9r**, cca aat tga cca agg atc aga; **10f**, agg ggt ggc tag gac aaa at; **10r**, gga caa att gca ggg cta gt.

Rat AVP **1f**, tca atg cca gct ttc tgc ta; **1r**, agt cct agg tga gcc cac ag; **2f**, ata gta cca gcc tca ggg ca; **2r**, gcc aca gtc atg gag tca ag; **3f**, gca tgt gtc aca act gtc ctt t; **3r**, tga gca ttt cag cag ctc tc; **4f**, gca gac ctg cta gtc ctt gg; **4r**, gct gtc agc agt gat tca gg; **5f**, gat tgc aca gca cca atc ac; **5r**, agc atc atg gcg agc ata g.

Rat Oxytocin **1f**, ctg ctt gag gag aag gct ga; **1r**, ggt tgg tcc act ttg gta cg; **2f**, aag ggg tgg gca act aga ac; **2r**, ttg acc tgg gac tgt ctg tg; **3f**, gtg agt tca agc cca gcc ta; **3r**, cat ctg agg gct gga gaa ct; **4f**, gca aga gca act caa cca c; **4r**, tgg tct aca gac cta gtt c; **5f**, gtc ttc ctg cca tgg ttt gt; **5r**, tgc tgg gaa caa aat tca ga; **6f**, ggg gag atg gct taa tgg tt; **6r**, tgc atg gga aga atg cta ca; **7f**, cac aca cta ggc agg cag tc; **7r**, gct ggc ctt gaa ctc aca gt; **8f**, agc tga tgg cct gtg ttt tc; **8r**, ggc tca gtg gtt agg agc ac; **9f**, agg gcc ttt ggt aga gca gt; **9r**, atg agg ttg gat agc gca ag.

2.1.10.2 Sequencing primers

Rat AVP **1f**, cgg gcg ctc tag agg atc; **1r**, aag gta gtg gtg cac tat cag; **2f**, gac tgg agt cct cac acc; **2r**, atg tac aga tat aca tgc aaa c; **3f**, tgc cac cat cat cag gct g; **3r**, tga gtc cat tcc ttt gtc tc; **4f**, gta atc cca gca gac atg tg; **4r**, ggc agc ttc cac cag att g; **5f**, gga gtt aaa cta tgt taa atc ag; **5r**, atc aca tcc act aga gct ttg; **6f**, gca cac agg cag cat ggc; **6r**, ttc taa ggc agt cgt tta gtc; **7f**, cta tgt agt aag gtc aag gtc; **7r**, cca ccg cca cag tga ttg; **8f**, ctg acc tcc ctg att gca c; **8r**, tga taa gta tct ctc att ttc tg; **9f**, gcc aca taa agg aca gtg tc; **9r**, tca gag act tac ctc tcc g; **10f**, gga cat gcc act caa ggg; **10r**, tac agg cgt gca tca ccg; **11f**, aat act cta gga aga aga caa; **11r**, gaa aca gct tcc ttg gtc a; **12f**, gac aca gtg tgc ctc tat g; **12r**, gct ctc ctg gac ctt ctg; **13f**, gtt agc agc cac gtt gtc; **13r**, aca tac aat aca gat ctg; **14f**, cca tgc cca agt gga gc; **14r**, gct gga acg agg cca ag; **15f**, cca gca acg caa agc agc; **15r**, aat aga gac aga cac cag g.

Rat Oxytocin **1f**, aac gga tct gtg att cag gg; **1r**, cct agg ttt gat tcc cag ca; **2f**, cac tgg aac tgg gat aag t; **2r**, ccc cag gag ctg tca tta aa; **3f**, aat caa gga gct ggg gag at; **3r**, gat gcc ctc ttc tgg tgt gt; **4f**, tga tgg cct gtg ttt tct ca; **4r**, gag ctc aaa agg gac aca gc; **5f**, tag aag aag ggc tga gct gc; **5r**, agg gga tgc tct ctg aag gt; **6f**, ctt ggc cta ctg gct ctg ac; **6r**, atc atc aca aag cag ggc tc.

Mouse AVP **1f**, cta gaa gcc gtg ggc tag gt; **1r**, ggg gag agc ttg gga ata gtg; **2f**, cat tgc cac cat agc ttt cc; **2r**, gtt agc agc cac gtt gtc; **3f**, caa gag aag gga cac cat ag; **3r**, ttc cttt ggt cag aag aaa cct; **4f**, att tct gct cga cct cag ag; **4r**, act ctg tgc tct cct gga c; **5f**, atc gcc aga gca cca gca ac; **5r**, cac ccc aga aat aga gac ag.

Human AVP **1f 5'**, tgg cct gag tat agg agg c; **1r 5'**, aag gga cac aga at gaga g; **2f 5'**, gtg tca tgt ctt gca ctt tc; **2r 5'**, cag ttc tgg aag tag cac g; **3f 3'**, cca gtc atc cgc agc ccg a; **3r 3'**, ttt gtg ttt cag tct cct g; **4f 3'**, cac tta gtc tgt aac gtg a; **4r 3'**, gag gcg aga gca gag tg.

Mouse chromosome 2 markers **1f**, ccc aag gtt cat aat gaa ttc c; **1r**, agc agg tct caa tgc cag g; **2f**, aat gga aag cta agc acc tac; **2r**, gag ggc ttc act gca tgt g; **3f**, ctg ctc cac ttg cat gca ac; **3r**, cct ggg aga aac atg agg ag; **4f**, tga gga gct gtc aca tta gg; **4r**, ctg aac att taa tca ctt ctc c; **5f**, ctg tcc tgc att agc tgt ctg; **5r**, act gat gtg gcc aca gtc c; **6f**, ggc ttt aat gtc agt caa acc; **6r**, gaa gaa ctt gtg tgg aaa gag; **7f**, acc aac att caa agt cct tgg; **7r**, gac atg gtg gat gga taa cag; **8f**, aac caa cag aaa gag aag agc; **8r**, taa agg ctt gtt cta cca ctg; **9f**, gtt gtc aag agt gga gat gga c; **9r**, cct gac aca aga cca gtg ag; **10f**, cac cca gcg agt atg tca tc; **10r**, aaa cat atc tgc agg atg aat g; **11f**, tgc agg tcc ctg tct tgt g; **11r**, aat gac atc tca gaa agc cac; **12f**, cca aag gta tca cca aga ac; **12r**, tga aat tca aca tca atg atg; **13f**, att ttc tct gca tag ctt tg; **13r**, tcc tga agt tgc att gtt tg; **14f**, ctt taa gct tcc ttc tga agc; **14r**, ctt gct tga gtt cct gtc.

Materials and Methods

pBSKII vector T7, gta ata cga ctc act ata ggg c; T3, aat taa ccc tca cta aag gg; **M13 forward**, gta aaa cga cgg cca gt; **M13 reverse**, gga aac agc tat gac cat g.

pGL2 UPS, ctt atg gta ctg taa ctg; **DS**, gat aga atg gcg ccg ggc c.

2.1.10.3 *In vivo* transcription assay primers

Rat AVP f, ccg aca tgg agc tga gac; r, tga gcc tag tga ctg gat tcc c.

Rat oxytocin f, atc teg gac tga aca cca acg c; r, ctg tgc aca atc cat atc ggg ac.

2.1.10.4 RFLP primer pairs

Location	Polymorphism	Primers	Restriction Enzyme
Rat AVP intron	T(+549)C	f; TGA GAA CGG GTT AAA CTG GG r; GGG ACA TAC TCC GCT CAG AC	Acil
Rat AVP promoter	A(-455)C	f; ACA ACT GTC CTT TTT ATT CTT T r; AAT CAT ACT TGA GCA TTT CA	Eam1104I
Rat AVP promoter	A(-534)G	f; GCA TGT GTC ACA ACT GTC CTT T r; TGA GCA TTT CAG CAG CTC TC	MaeIII
Rat AVP promoter	C(-590)T	f; GCA TGT GTC ACA ACT GTC CTT T r; TGA GCA TTT CAG CAG CTC TC	SfaNI
Rat AVP promoter	T(-2452)C	f; GTG ATT TCA GGT TAG AAC CC r; CAC TTT GGC GTC TAC GTG C	HaeIII
Rat oxytocin exon	C(+18)T	f; GCT GTG TCC CTT TTG AGC TC r; CTT GGC CTA CTG GCT CTG AC	BsmAI
Human AVP 3'	G(-558)T	f; GCC TCA GGT TCA AGA AGG r; CCA AGG CAG TGC TCG TGT	MseI
Human AVP promoter	C(-229)T	f; CTG AAT CCA GAG CGC TGC r; GCA TCC TGG TGC ACA CAG	NlaIII
Mouse AVP exon	C(+6)T	f; GTT AGC AGC CAC GTT GTC r; CTC TTG GGC AGT TCT GGA AG	BstNI

2.1.11 Sequences and accession numbers

Rat AVP gene (X59496), promoter (AF112362), 3' region (X01637); **Mouse AVP** gene (M88354), promoter (AL731707); **Human AVP** gene (X62890), promoter (AL160414); **Rat CRH** gene and promoter (M54987); **Rat oxytocin** gene (X59496,) promoter (X12792). **Mouse YY1** mRNA (AB080317); **Mouse CBF-A** mRNA (D90151); **Mouse chromosome 2** polymorphic regions (C77491, AI747202_153, AI663983_10, AI325259_167, AW046744_208, AA410094_61, AI225831_18, AB015595_12, AW541238_50, AF091998_162, R7484970, L25602_11, AI385582_268, AL808143, C80276_113, AU015228_19, AB012611_76, AL808143_5, AL831753_5, AI118379).

2.2 Methods

2.2.1 DNA Analysis

2.2.1.1 DNA extraction

DNA was purified from either 0.5cm tail tips of live rats, or from the spleens of rat autopsies using the NucleoSpin Tissue kit (Macherey-Nagel). Extraction from the tail generally gave a DNA yield of ~20µg from rats (0.5cm) and mice (0.5-1cm), whereas the spleen (~20mg) gave somewhat higher amounts of ~30µg. A further, more cost-efficient, extraction protocol was developed to allow the analysis of large numbers of animals during the selectional breeding. Tail tissue of mice and rats were digested in 700µl of tail buffer (Tris-HCl pH 8, 0,5M EDTA, 7M NaCl, 20% SDS) in the presence of 40µg proteinase K at 55°C overnight. 300µl of NaCl (7M) was added to the DNA, which was vortexed for 10min and centrifuged at 14,000rpm in a benchtop centrifuge for 10min. The upper aqueous layer was then added to 500µl isopropanol, which was mixed and centrifuged at again at 14,000rpm in a benchtop centrifuge for 5min to pellet the DNA. The pellet was then washed in 70% ethanol, dried and dissolved in TE buffer. DNA was also purified from samples of clotted blood using streptokinase. Streptokinase is a proteolytic enzyme, produced by haemolytic streptococci, that is capable of dissolving blood clots by converting plasminogen to plasmin. Briefly, a small amount (50µl) of clotted blood was incubated at 37°C overnight in the presence of 10U streptokinase, after which a spin column tissue extraction protocol (Qiagen) was followed.

Due to the relatively small size of rats and the presence of fur, collection of blood by hypodermic needle is not possible. Furthermore, it is not practical to take tail tips from rats over the age of 2 years due to the discomfort it causes. Therefore, a new method was designed in this study, circumventing these problems, utilizing faeces from the rats, which contain cells from the intestines as the source of DNA. Faeces are generally not a good source of pure DNA for the use in PCR procedures due to the presence of contaminating chemicals, which inhibit polymerases, and the high concentration of bacteria DNA. A method was devised involving the solid-phase chromatography principle of the spin column methods, but using streptavidin-coated magnetic poly(vinyl alcohol) (M-PVA) -beads to bind the DNA, allowing for more stringent washing steps. Briefly, faeces were taken from cages and DNA extracted following the Chemagenic kit instructions, except that the numbers of washes were increased by 5-fold, and DNA resuspended in 100µl water.

This method, surprisingly, resulted in a measurable quantity of DNA (figure 4A), though it is expected an overwhelming portion of this emanates from bacteria. However,

accepting the possibility of the very low levels of DNA, PCR amplification using 1 μ l of the DNA in a 25 μ l PCR reaction (39 cycles with a 55 $^{\circ}$ C annealing temperature) still proved possible (figure 4B).

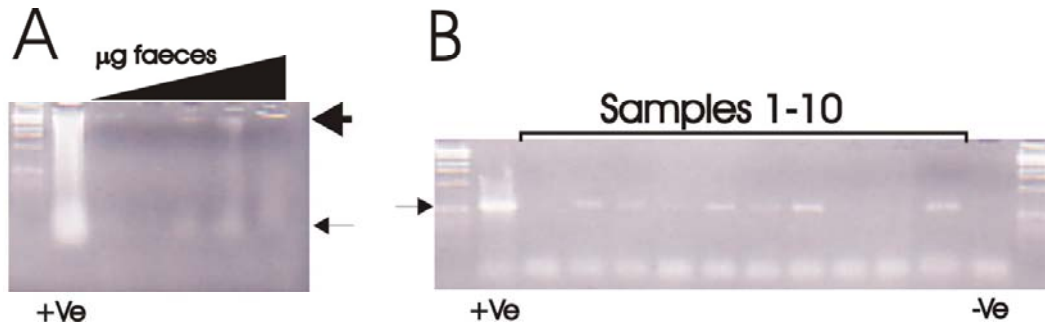


Figure 4. DNA extraction and PCR results from rat faeces. (A) Agarose gel loaded with 3 μ l of spin column (tail tip) extracted DNA obtained from tail tip (+ve) and 3 μ l of faeces extracted DNA with increasing amounts of starting material (one wash of faeces with water, five washes, 0.005g, 0.05g and 0.1g). (B) PCR amplification reactions for a 550bp product (arrow) using the samples described in figure 4A performed in parallel. The first lane contains the spin column extracted DNA, the last lane the -ve control. Both gels, of A and B, are representative of three independent experiments.

Naturally, the PCR reactions were less efficient in the faeces extractions than the tail tip extractions, both in the quantity of PCR product and the success rate in PCR reactions. It also seems that using less starting material does not effect the functioning of the PCR, suggesting that the failure of the PCR was not caused by lack of starting material, but perhaps by contaminants still present in the DNA extract or an overwhelming concentration of bacterial DNA in the final DNA sample.

However, the finding that this method does result in enough detectible PCR product to allow restriction fragment length polymorphism (RFLP) analysis is testament to the use of this method as a real option for DNA extraction. Moreover, if DNA is required simply for the presence of genotyping one allele then this method represents an alternative to collecting tail tips or sacrificing animals solely for this purpose.

2.2.1.2 PCR

PCR was conducted on DNA extractions in order to amplify DNA for the use in sequencing, single strand conformation polymorphism (SSCP) analysis, cloning and RFLP genotyping. Amplification reactions were carried out in a total volume of 25 μ l in the presence of 50ng of DNA, 10x PCR Buffer (with MgCl₂), 0.2mM of each dNTP, 0.5 μ M of each primer and

Materials and Methods

0.25U of *Taq* (*Thermus Aquaticus*) DNA polymerase enzyme. For certain analyses outlined in this study, such as the *in vivo* transcription experiments, the DNA polymerase Pfu (*Pyrococcus furiosus*) was used, which is a high fidelity polymerase with a very low rate of nucleotide misincorporation. This enzyme also results in the production of blunt ended PCR products in contrast to *Taq*, which produces PCR products with a one base 3'-overhang. Annealing temperature and numbers of cycles were optimised for each primer. After an initial denaturation step at 94°C for 2min, 30-35 cycles of 1min at 94°C, 1min at an optimised annealing temperature, 1min at 72°C were carried out, and a final extension period of 10min was performed at 72°C. Optimised annealing temperatures and numbers of cycles for each primer pair used in RFLPs are presented in *Materials*. Primers, used to amplify regions from sequences deposited at GeneBank, were designed according to rules laid out by Innis and Gelfand (Innis and Gelfand, 1990); primers should be 18-25bp in length, GC content should be 40-60%, repetitive stretches of bases should be avoided, no 3' complementarity between primers, if possible two cytosine or guanine residues should be present at the 3' end of each primer and the opportunity for internal secondary structure should be kept to a minimum. PCR fragments were analysed on agarose gels stained with ethidium bromide (EtBr) to check the quantity and quality of amplified product.

2.2.1.3 SSCP

Twenty HAB and twenty LAB rats were used to search for polymorphisms in the coding and promoter regions of the AVP gene, oxytocin gene, and the CRH gene. Primers were designed for SSCP analysis to produce overlapping PCR products of around 300bp long. 3-5µl of PCR product, depending on the concentration, were mixed with an equal volume of loading dye (10mM NaOH, 20mM EDTA, 95% formamide, 0.025% Bromophenol blue and 0.025% Xylene cyanol), denatured at 95°C for 2min and immediately chilled on ice. Then 3-5µl of the mixture was loaded on to a non-denaturing 0.5x TBE 8% polyacrylamide gel. Electrophoresis was carried out at room temperature in 0.5x TBE buffer using the MiniProtean gel apparatus at 80V for 2-3h. After electrophoresis the gels were either stained in EtBr and DNA visualised under a UV light, or were silver stained. SSCP reactions were repeated where any suspected band pattern differences were evident, and PCR products revealing differences in band patterns were sequenced.

2.2.1.4 Sequencing

Plasmid inserts were sequenced using ThermoSequenase Cycle sequencing kit in conjunction with α -33PdATP. PCR products corresponding to genomic regions were sequenced using the ThermoSequenase radiolabelled termination cycle sequencing kit and [α -33P]ddNTP. Although both protocols are based on the same traditional chain termination sequencing method (Sanger, 1977), the first method used for plasmid sequencing involves alkaline denaturation of samples, which proved inefficient for the separation of linear DNA fragments produced in PCR. Furthermore, the use of [α -33P]ddNTP in the second protocol, ensures the radiolabel is incorporated in the 3' end, allowing longer stretches of DNA sequences to be read more cleanly with the occurrence of fewer compressions and BAFLs (Bands across four lanes). Primers used for sequencing (refer to section 2.1.10.2) were either complementary to inserted sequences or complementary to sequences found in the parent vector backbone.

Sequencing of plasmids was conducted by firstly denaturing 2-4 μ g of vector DNA (prepared from either maxi-preps or spin columns) in the presence of 1mM NaOH/0.001mM EDTA in a final volume of 20 μ l. The DNA is then precipitated in 3M NaAc (pH 5.2) and ethanol, washed in 70% ethanol and annealed with 2pM primer in the presence of sequenase buffer. The elongation reaction is performed by adding DTT, 1x label mix, α -33PdATP and 1.3U T7-Sequenase, which is terminated by the addition of ddNTP(G,A,T,C), and finally, formamide loading buffer. This reaction was performed on micro test plates.

PCR products were cleaned-up prior to sequencing by treating with ExoSAP-IT. ExoSAP-IT utilizes two hydrolytic enzymes, Exonuclease I and Shrimp Alkaline Phosphatase, to remove unwanted dNTPs and primers from PCR products. Exonuclease I removes residual single-stranded primers and any extraneous single-stranded DNA produced in the PCR. Shrimp Alkaline Phosphatase removes the remaining dNTPs from the PCR mixture. Following this, 100-200ng DNA was included in the ThermoSequenase radiolabelled termination cycle sequencing reaction, which was performed as described in the manufacturers protocol. This reaction was performed in PCR tubes. Sequencing products from both reactions were, thereafter, treated the same. The reactions were heated to 75°C for 2min, to denature the DNA, and loaded onto an 8% denaturing polyacrylamide gel (see *Materials*). The gels were run in 0.5x TBE at 3,000V and 40-50W for between 1-3h at a temperature of 50°C. The gel is then transferred and dried on blotting paper and exposed to X-ray film in a cassette for between 12-36h. The film was then developed in an automatic developer (Kodak), or developed manually by soaking in developing solution for 1-5min and fixing in fixing solution for 2min.

2.2.1.5 RFLP analysis

Polymorphisms detected in genomic DNA from the sequencing reactions described above were analysed, using the online DNA analysis program contained in webcutter2 (refer to section 2.2.6), to determine if a polymorphism affected a DNA site for a restriction endonuclease. Any polymorphisms resulting in differential digestion by a restriction endonuclease were used to genotype animals for the presence of the polymorphism concerned. This procedure using RFLP is far more cost and labour efficient than sequencing for the presence of a genotype in large numbers of animals. Primers are designed spanning the restriction site, to give a PCR product of between 300-500bp in length. Ideally, the polymorphism is usually located off centre, to allow for electrophoresis separation of both digested products; this and the presence of nearby restriction sites determines the positions on which the primers are designed. The DNA concentration of PCR products prior to enzyme digestion is estimated by agarose gel electrophoresis. Around 1µg DNA is digested in a reaction containing reaction buffer (with or without BSA) and between 1 and 5U restriction endonuclease. The reaction is then made up to an appropriate volume of between 10 and 20µl with distilled water. The digestion reactions are incubated at the optimal temperature required by the enzyme for between 8 and 24h. Generally, the whole digestion reaction is mixed with 1µl loading buffer (see *Materials*) and loaded on to either an agarose or polyacrylamide gel. Agarose gels allow for the efficient separation of large DNA fragments at a relatively low resolution of ~20bp – depending on the percentage of agarose. Polyacrylamide gels, on the other hand, have a far higher resolution, allowing for the separation of DNA fragments differing in size of 5bp. Both types of gel are run at room temperature in the presence of 1x TBE running buffer and stained in EtBr to allow visualisation of DNA. EtBr is a polycyclic fluorescent dye that binds to double-stranded DNA molecules by intercalating a planar group between the stacked base pairs of the nucleic acid. EtBr can also bind to secondary structure in single-stranded RNA molecules: regions of local base pairing offer the stacked base pairs necessary for the dye molecules to intercalate. When excited by ultra violet (UV) light (at or near 546nm), the dye-nucleic acid complex exhibits an increased (about 20-fold) fluorescent yield at an emission wavelength of 590nm. Agarose gels are stained with EtBr prior to DNA loading and electrophoresis, and polyacrylamide gels are soaked in EtBr after electrophoresis. Markers are also loaded in separate lanes on the DNA gels to allow for determination of DNA band sizes. The agarose gels are typically run for between 30min and 2h at 50 to 80V depending on the size of the electrophoresis chamber used and the percentage

agarose present in the gel. The DNA bands are then photographed in the presence of UV light using Kodak Polaroid film.

Rat, mouse or human samples are genotyped at least twice to allow for inefficiencies in the digest that may lead to misanalysis. Furthermore, all digests are performed with control reactions containing the known polymorphism expected to lead to either absence of, or complete, cleavage. All RFLP analyses including the polymorphisms, primer pairs and restriction enzymes used in this study are listed in section 2.1.10.4.

2.2.1.6 Radioactive labelling

The Forward reaction was used for end labelling dsDNA and annealed oligonucleotides used in EMSA experiments, and were performed using fill-in end labelling. The oligonucleotides were annealed as described below in the EMSA. 1.5µl of the oligonucleotides were added together with 2µl 10x Klenow buffer, 4µl dATG, dGTT, dTTP (5mM), 9-6.5µl H₂O, 2.5-5µl ³²P-dCT and 1µl Klenow enzyme. This was incubated at room temperature for 30min, after which 4µl dCTP (5mM) was added and the reaction incubated again at room temperature for a further 5min. A Biospin column was used to clean up any free label. A working stock of 20,000cpm/µl was used for all reactions described.

The Exchange reaction was used for end labelling ssDNA oligonucleotides and was performed using the 5' termini labelling Forward Reaction. The DNA needs to be dephosphorylated for this procedure, which is the case for ordered oligonucleotides that are supplied dephosphorylated. dsDNA was firstly dephosphorylated by CIAP. This 5'hydroxyl terminus, lacking a phosphate group, is then rephosphorylated by transferring the γ-phosphate using T4 polynucleotide kinase (PNK). Efficiency depends on the first residue and experimental design ensures this was usually a G, which is most efficient, followed by A or T, and C, which is the least efficient. The reaction comprises 20pM DNA, 2µl Reaction buffer A, 5µl (γ³²P)ATP, 11µl H₂O and 1µl T4 PNK, which was incubated for 1h at 37°C. The reaction was terminated by addition of 1µl 0.5M EDTA(pH8.0), after which the unincorporated free radionucleotide is removed using a Biospin column. A working stock of 20,000cpm/µl was used for all reactions described.

2.2.2 RNA analysis

2.2.2.1 RNA extraction

AVP is expressed in only a small population of the neurons that make up the hypothalamus (for review see Burbach et al., 2001). Therefore, in order to obtain AVP mRNA, only the

Materials and Methods

hypothalamic tissue expressing AVP can be used for RNA extraction. Rats were decapitated and the brains removed. A 2mm lateral slice is taken containing the hypothalamus, and from this the PVN and SON were dissected out under the guidance of the group of Professor Landgraf. The PVN/SON samples were kept on ice for up to 10min, until the extraction procedure was initiated. The acidic phenol method, developed by Chomczynski (Chomczynski and Sacchi, 1987) was used for the extraction procedure. Commercially available kits employing spin columns (Qiagen) were tested, though the acidic phenol kit proved to be the most efficient for the type and size of material used in this study.

The frozen brain tissue was crushed with a plastic mortar in a 1.5ml Eppendorf tube. To this was added solution D containing β -mecaptoethanol, which breaks down di-sulphide bridges, and the potent protein denaturant guanidium thiocyanate which denatures RNases present in the sample. The sample was then combined with 2M NaOAc (pH4), acidic phenol and chlorophorm/isoamyl and vortexed. This causes the partitioning of proteins, lipids, and importantly, DNA into the phenol layer. DNA shows a pH-dependent partitioning while RNA does not – when the aqueous phase of phenol is above pH7.5 DNA partitions with RNA into the aqueous layer. When low pH4 is used DNA partitions to the phenol layer, leaving only the RNA in the aqueous phase. The sample was centrifuged to aid partitioning of the phenol layer, and the upper phase removed and added to cold isopropanol to precipitate the RNA. This was centrifuged again, and the pellet dissolved in solution D to dissociate any further proteins carried with the RNA in the sample. Again the RNA was precipitated with cold isopropanol and then washed in 70% ethanol to remove salt. The RNA pellet was further dissolved in warm proteinase K buffer and digested with 1 μ l proteinase K (10mg/ml) at 55°C for 30min to enzymatically remove any residual RNases still present in the sample. The sample was then mixed with equal volume of phenol/chloroform/isoamyl to denature and remove the previously added proteinase K, and the upper layer mixed with 1/10 3M NaOAc (pH5.5) and 2.5x ethanol to precipitate the RNA which was again washed in 70% ethanol. The final pellet was dissolved in between 20-50 μ l DEPC water.

Quantity and quality of the RNA samples were determined using spectrophotometry (OD260nm) and MOPS/formamide denaturing agarose-gel electrophoresis and EtBr staining were performed to check the integrity and size distribution of total RNA. The respective ribosomal bands, from all samples used in this study, appeared as sharp bands on the stained gel, and the intensity of the 28S ribosomal RNA (rRNA) band was approximately twice that of the 18S rRNA band.

2.2.2.2 Riboprobe

To generate the CBF-A riboprobe, used in the *in situ*-hybridisation experiments, the plasmid pBSK-CBF-A, containing the full length CBF-A cDNA cloned into the SmaI site (refer to section 2.2.3.2), was digested with BamHI and religated to contain only the 326bp N-terminal sequence of the CBF-A cDNA. To generate antisense probe, the plasmid was linearized with EcoRV, and for sense probe the plasmid was linearized with XbaI. The template DNA was then purified with a phenol/chloroform extraction and transcribed and labelled with ³⁵S-UTP in a 30µl reaction mixture containing 20U of either T7 (sense probe) or T3 (antisense probe) RNA polymerase, 1x reaction buffer, 0.5M DTT, 10mM each of ATP, GTP, and CTP, 10µM ³⁵S-thio-rUTP (12.5mCi/mM), 1.5 µg of linearized template DNA and 40U of recombinant RNasin RNase inhibitor. The reaction was incubated at 37°C for 3h after which the reactions were stopped by addition of 2U RNase-free DNase I. Unincorporated nucleotides were removed using the RNeasy kit following the *clean up* protocol.

2.2.2.3 *In situ*-hybridisation analysis

In situ-hybridisation was performed according to a protocol outlined by Cota et al., 2003. Slide-mounted frozen brain sections were fixed for 10min in ice-cold 4% paraformaldehyde/PBS, rinsed in 1x PBS, suspended in 0.1 M triethanolamine at pH 8.0 and acetylated by addition of 0.25% acetic anhydride over 10min. Both the antisense and the control sense probes were applied to the slide-mounted sections in a volume of 100µl hybridisation buffer/section, containing 4–5×10⁶ cpm of ³⁵S per section. Hybridisation buffer consisted of 50% formamide, 20mM Tris-HCl pH8.0, 0.3M NaCl, 5mM EDTA pH8.0, 10% dextran sulphate, 0.02% Ficoll 400, 0.02% polyvinylpyrrolidone, 0.02% BSA, 0.5mg/ml tRNA, 0.2mg/ml fragmented herring sperm DNA and 200mM DTT (Marsicano and Lutz, 1999). In control experiments slides were pretreated with RNase A prior to hybridisation. All sections were incubated for 20h in a humid environment at 55°C, and then rinsed in 2× SSC, washed in a standard series of washes, and dehydrated in a graded series of ethanols. The resulting slides were exposed to X-ray film for 8 days.

The slides were further dipped and the nuclei counterstained in Toluidine Blue. Kodak NTB2 was used for dipping. This was heated to 42°C and mixed with an equal volume of water. The slides were dipped, in a dark room for 4sec and dried at RT for 30min. They were then packed into light-tight black boxes with sufficient desiccant (silica gel capsules) at 4°C and exposed for 4 weeks. The slides were developed in Kodak D19 developer for 3min, rinsed in water for 30sec and fixed in Kodak fixer for 3min. The slides were then

counterstained in 1% toluidine Blue for 3min and dehydrated in a graded series of ethanols. The sections were then embedded in Roti-Histokitt (2 drops) followed by a cover slip.

2.2.2.4 Allele-specific transcription *in vivo*

RNA was extracted from the PVN of the hypothalamus of F1 animals, heterozygous for the two AVP promoter alleles, using the acidic phenol method (see above). Oxytocin and AVP heterogeneous RNA (hnRNA) was reverse transcribed and amplified using gene-specific primers in combination with the OneStep RT-PCR kit from Qiagen. The Qiagen OneStep RT-PCR enzyme mix contains enzymes for both reverse transcription and PCR amplification in the same tube. Omniscript reverse transcriptase is specially designed for reverse transcription of RNA amounts greater than 50ng, and Sensiscript reverse transcriptase is optimised for use with very small amounts of RNA (<50ng). This special enzyme combination provides highly efficient and sensitive reverse transcription of any RNA quantity from 1pg to 2µg. HotStarTaq DNA Polymerase provides hot-start PCR for highly specific amplification. During reverse transcription, HotStarTaq DNA Polymerase is completely inactive and does not interfere with the reverse-transcriptase reaction. After reverse transcription by Omniscript and Sensiscript reverse transcriptases, reactions are heated to 95°C for 15min to activate HotStarTaq DNA Polymerase and to simultaneously inactivate the reverse transcriptases. This hot-start procedure using HotStarTaq DNA Polymerase eliminates extension from non-specifically annealed primers and primer-dimers in the first cycle ensuring highly specific and reproducible PCR.

The design of gene-specific primers for the reverse transcription of the oxytocin and AVP genes was important. The primers were designed to be 18–30 nucleotides in length with a G/C content of 40–60%. The primers were designed with similar T_m values not lower than the reverse-transcription reaction temperature (e.g. 50°C). Furthermore, the primers were designed to avoid; (i) complementarity's of two or more bases at the 3' end to reduce primer-dimer formation, (ii) mismatches between the 3' end of the primer, (iii) runs of 3 or more G or C nucleotides at the 3' end, (iv) a 3'- end T, (v) complementary sequences within a primer sequence and between the primers of a primer pair.

It is usually suggested that primers should be designed so that one half of the primer hybridises to the 3' end of one exon and the other half to the 5' end of the adjacent exon. Primers will anneal to cDNA synthesized from spliced mRNAs, but not to genomic DNA. Thus, amplification of contaminating DNA is eliminated. Alternatively, RT-PCR primers should be designed to flank a region that contains at least one intron. Products amplified from cDNA (no introns) will be smaller than those amplified from genomic DNA (containing

Materials and Methods

introns). Size difference in products is used to detect the presence of contaminating DNA. However, our study required the analysis of heterogenous prespliced mRNA (hnRNA) and, therefore, primers were designed to specifically anneal to sequences in intronic regions. Control reactions were used with each RT reaction to test for the presence of contaminating DNA in the reagents. Therefore, contaminating DNA in the RT-reaction from the sample was checked for by performing deoxyribonuclease I digestion of the RNA sample prior to reverse transcription. Briefly, 1µg of RNA was digested in a reaction volume of 10µl containing 10x reaction buffer with MgCl₂ and 1U deoxyribonuclease I and incubated 37°C for 30min. The reaction is stopped by the addition of 1µl 25mM EDTA and heating at 65°C for 10min to destroy the deoxyribonuclease.

Primer pairs were designed to anneal to the RNA from oxytocin and the prespliced hnRNA from AVP (figure 5). The forward primer for oxytocin (ATC TCG GAC TGA ACA CCA ACG C) locates to the 5' untranslated region 2bp 5' to the start codon and 20bp 5' to the polymorphism. The gene-specific primer (CTG TGC ACA ATC CAT ATC GGG AC) locates to the first intron 28bp 5' to the intronI/ExonII splice junction. This gives an expected cDNA product of 343bp. The forward primer (CCG ACA TGG AGC TGA GAC) and the gene-specific primer (TGA GCC TAG TGA CTG GAT TCC C) for AVP derived from sequences in exon I, 2bp 5' to the exon I/intron I junction and the first intron.

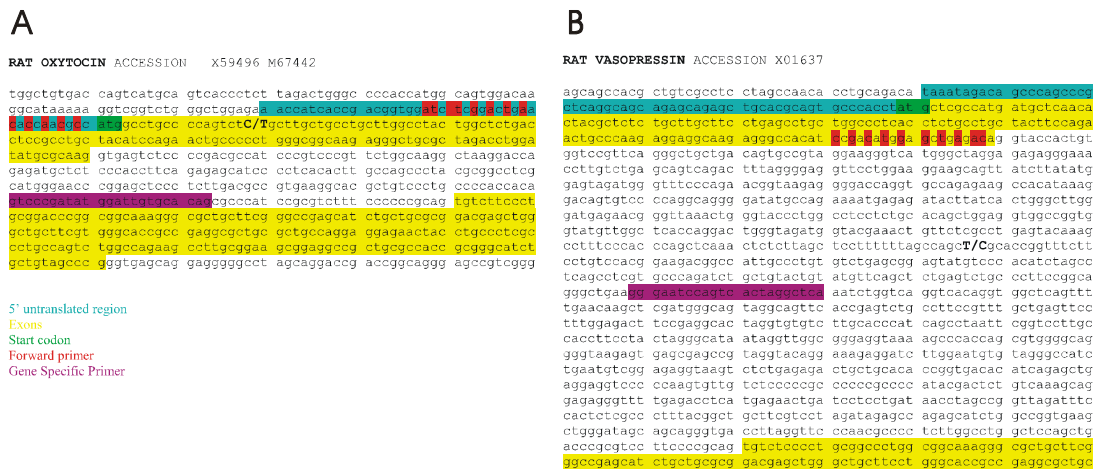


Figure 5. Sequence of oxytocin and AVP gene polymorphisms used in the *in vivo* transcription assay. (A) Oxytocin hnRNA was reverse transcribed using the gene-specific primer (GSP) in intron I, resulting in a 354bp cDNA representative of newly synthesised hnRNA. The C(+18)T polymorphism, located in the first exon, was further amplified from cDNA using the same GSP in conjunction with a forward primer complementary to sequences in the oxytocin RNA 5' untranslated region to provide a 343bp PCR product containing the polymorphism. Sequencing was performed using the forward primer as the sequencing primer. (B) AVP hnRNA was reverse transcribed using the gene-specific primer (GSP) in intron I, resulting in a 770bp cDNA representative of the hnRNA. The T(+549)C polymorphism, located in the first exon, was further amplified from the cDNA using the same GSP in conjunction with a forward primer complementary to sequences in exon I of the AVP RNA providing a 600bp PCR product containing the polymorphism. Sequencing was performed using the sequencing primer located 59bp upstream of the polymorphism.

Materials and Methods

PCR was performed under the following conditions: cDNA synthesis at 50°C for 30min for the reverse transcription, 94°C 15min to destroy the reverse transcriptase and activate the polymerase, amplification for 20 cycles with 94°C 30sec, 55°C 30sec, 68°C for 30sec. A further 20 cycles of PCR was performed on 1µl of the previous reaction using a nested primer and Pfu polymerase (NEB). Products were purified and cloned into the EcoRV site of the vector pBSKII (Stratagene). Following transformation into DH5α bacteria DNA was isolated from single colonies (Nucleospin miniprep kit, Macherey-Nagel) and sequenced to track the allele from which the RNA was transcribed. Every reaction included one negative control in every round of RT-PCR that lacked the template RNA in order to detect possible contamination of the reaction components.

2.2.3 Plasmids

2.2.3.1 Standard and parent plasmids

pBSKII is a high copy number ColE1-based phagemid with a large and versatile polylinker in two orientations to allow for the cloning of a wide variety of products. T3 and T7 promoters flanking the polylinker allow for *in vitro* transcription of RNA. The plasmid contains a gene for Ampicillin-resistance in *E. coli* to allow for selection of transformed bacteria. The plasmid further allows for the identification of recombinant clones containing inserts in the polylinker located in the β-gal gene, whose activity is destroyed in case inserts are incorporated.

pGEX-2-Tk vectors allow the construction of GST fusion proteins by inserting a cDNA inframe into the multiple cloning site. Expression is under the control of the tac promoter, which is induced by the lactose analogue isopropyl-β-d-thiogalactopyranoside (IPTG). The vector is also engineered with an internal lacIq gene coding for a repressor protein that binds to the operator region of the tac promoter, preventing expression until induction by IPTG, thus maintaining tight control over expression of the insert.

pRK8-PKA contains the catalytic subunit of PKA derived from rat under the control of the CMV promoter (Spengler et al., 1993).

pRK7-FLAG vector was created by cloning the oligonucleotides AGCTTCTCGAGATGGACT ATAAGGACGATGACGATAAGG and AGAGCTCTACCT GATATTCCTGCTACTGCTATTCCTAG into the HindIII and BamHI digested pRK7 vector. These oligonucleotides encode for the short hydrophilic 8 amino acid (aa) peptide Asp-Tyr-Lys-Asp-Asp-Asp-Asp-Lys. This epitope is likely to be located on the surface of a fusion protein due to its hydrophilic nature and, therefore, accessible to antibodies. The small

size means it has less chance of interfering with the fusion protein's function and transportation.

pGL2-Basic vector contains the coding region for firefly luciferase, but lacks eukaryotic promoter and enhancer sequences, allowing the cloning of putative regulatory sequences. Therefore, expression of luciferase activity in cells transfected with this plasmid depends on insertion and proper orientation of a functional promoter upstream from the luciferase gene. The vector also contains a high copy number prokaryotic origin of replication for maintenance in *E. coli*, and an ampicillin-resistance gene for selection.

2.2.3.2 cDNA constructs

pRSKII-CBF-A, which was used for the preparation of the riboprobe, contains CBF-A that was released from pSR-CBF-A-N (Kamada et al., 1992) using *Tth111I* and *SacI*, after which the ends were blunted by T4 DNA polymerase and cloned into the *SmaI* site of pBSKII.

2.2.3.3 Expression vectors

pCMV-YY1 contained the full length YY1 cDNA comprising 16bp of untranslated 5' sequence and 28bp untranslated 3' sequence. This was cloned into the *BamHI* site of pCMV-NEO-BAM3 under the control of the CMV promoter.

pRK7-CBF-A expression vector was made by cloning the mouse cDNA for CBF-A (a kind gift from Akira Inoue (Osaka, Japan) and Shinji Kamada (La Jolla, USA)) into the pRK7 vector downstream the CMV promoter.

pRK8-PKA_c expression vector contains the catalytic subunit of PKA derived from rat under the control of the CMV promoter (Spengler et al., 1993).

2.2.3.4 Recombinant protein constructs

pGST-2Tk-CBF-A was made by releasing CBF-A from pBSKII, by a partial *BamHI* and *EcoRI* digest, and inserting into pGEX-2TK digested with *BamHI* and *EcoRI*.

FLAG-CBF-A was obtained by ligating the CBF-A fragment, which was released from pBSKII-CBF-A by a partial *BamHI* digest and *EcoRI* digest, into the *BamHI* and *EcoRI* sites of pRK7-FLAG.

GST-CBF-A deletion constructs were a kind gift from Drs. Leandersson and Aranburu (Lund). These constructs contain deletions of either, or both, of the RNA-Binding-Domains (RBDs) (Bemark et al., 1998).

2.2.3.5 Reporter constructs

pGL2-AVP proximal vector contains the proximal AVP promoter. Fragments of the rat AVP gene were generated by PCR from genomic DNA purified from either a HAB or LAB animal. AVP promoter fragments were inserted into the polylinker site of pGL2. A proximal promoter fragment of 1146bp containing sequence -860bp (775bp after digestion) to +282bp relative to the start codon, was amplified (forward primer, ACA TCC ACT TCC CT CCT GC; reverse primer, CGT TCT GGG AAA CCC ATC TA). Pfu polymerase (NEB) was used in a 50µl PCR reaction (50ng DNA, 2mM MgSO₄, 0.2mM each dNTP, 2.5U Taq, 1x High fidelity PCR buffer). Amplification of the proximal promoter was performed using 15 cycles of 94°C 40sec, 58°C 40sec, 72°C 40sec, followed by 20 cycles of 94°C 40sec, 54°C 40sec and 68°C 2min, ending with 20min of 68°C. The PCR products were purified using Qiagen spin columns and the proximal promoter fragment was digested with KpnI and SmaI to give 931bp. Following separation by agarose gel electrophoresis, the proximal promoter fragments, from the HAB and LAB animals, were cloned into the pBSKII vector digested with KpnI and EcoRV. Recombinant plasmids were completely sequenced and inserts were released using KpnI and SmaI and then inserted into the pGL2 vector digested with KpnI and SmaI.

pGL2-AVPdistal vector contained the distal AVP promoter. To include additional upstream sequences genomic DNA was amplified (forward primer, GTA CCC CAT CCA CAC AGA CC; reverse primer, ATA TAA GAT AAC TGC TTC CTT C) to give a product of 3119bp harbouring 2797bp upstream from the AVP start codon. This distal promoter was amplified using the conditions of an initial 18 cycles 94°C 40sec, 59°C 40sec, 68°C 2min, then 12 cycles 94°C 40sec 56°C 40sec 68°C 3min, ending with 20min at 68°C. Both PCR products were purified using Qiagen spin columns and the distal promoter was digested by KpnI and HincII giving a 2950bp product. Following separation by agarose gel electrophoresis, the distal promoter fragments, from the HAB and LAB animals, were cloned into the pBSKII vector digested with KpnI and EcoRV. Recombinant plasmids were completely sequenced and inserts were released using KpnI and SmaI and then inserted into the pGL2 vector digested with KpnI and SmaI.

pGL2-CAR_G vectors were developed containing various copies of the CAR_G elements from either the HAB and LAB alleles. These were generated by serially cloning oligonucleotides containing the CAR_G box (LAB sense, ctc tag aga gct ccc act gtC CTT ATT AGG aag agg cag ct; LAB antisense, gcc tct tCC TAA TAA GGa cag tgg gag ctc tct aga ggt ac; HAB sense, ctc tag aga gct ccc act gtC CTT ATT GGG aag agg cag ct; HAB antisense, gcc tct tcC CAA TAA GGa cag tgg gag ctc tct aga ggt ac) into the KpnI and SacI site of

Materials and Methods

either of the following described pGL2 variants (figure 6). The oligonucleotides were annealed giving overhanging ends complementary to the digested ends of DNA products produced by the restriction enzymes KpnI and SacI. The LAB or HAB sense and antisense oligonucleotides (0.2µg) were mixed together, denatured at 85°C for 10min and then allowed to slowly cool to 37°C for efficient annealing. The oligonucleotides were then phosphorylated in the presence of 2U PNK, 250mM DTT, 50mM ATP and 10x PNK buffer in a reaction mixture of 50µl. This was incubated at 37°C for 30min and placed on ice.

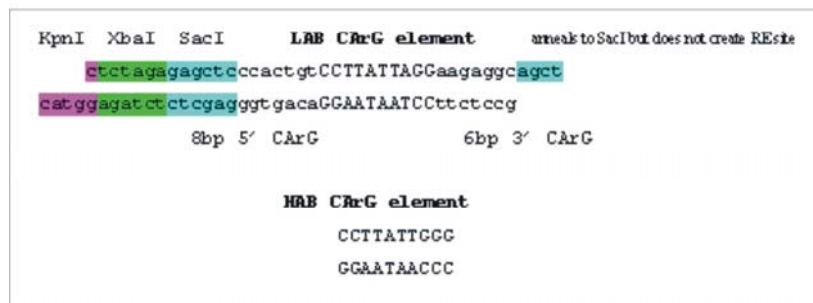


Figure 6. Sequence of the CARg cassette used for ligation into reporter plasmids. The LAB and HAB CARg elements were included with 8bp 5' and 6bp 3' of the rat AVP sequence. The 5' end of the annealed oligonucleotides is complementary to the KpnI enzyme site, while the 3' end contains sequence complementary enough to anneal to a SacI digested 'sticky' end DNA, without restoring the SacI site. This ensures correct orientation of the cassette in the vector. The XbaI site allows identification of recombinant clones using an enzyme digest of miniprep DNA, while the SacI site allows for further insertions of multiple copies of the cassette.

pGL2-SV40-CARg involves the CARg elements cloned into the pGL2-SV40 vector which contains the entire simian virus (SV40) late and early promoter sequence; this functions as a highly active transcription initiation element (Benoist and Chambon, 1981). The pGL2- SV40 vector was digested with the enzymes KpnI and SacI, and dephosphorylated by adding 1U of calf intestinal alkaline phosphatase (CIAP) removing the possibility of the small 6bp fragment, lying between the two sites, re-ligating. The vector was then phenol/chloroform purified and precipitated in the presence of Na-Acetate. This digested vector was then ligated with the phosphorylated and annealed oligonucleotides in the presence of ATP and T4 DNA kinase. This results in the CARg element being placed 375bp upstream of the SV40 early and late promoter start codon of the luciferase gene. Successfully ligated pGL2-SV40-CARg vector was identified by an XbaI digest on miniprep DNA from 10 selected clones of each ligation. The presence of an XbaI site in the cloned oligonucleotide results in a detectible 445bp fragment due to another XbaI site contained in the parent vector. Sequencing data confirmed the presence and integrity of positive clones from the digest results (figure 7).

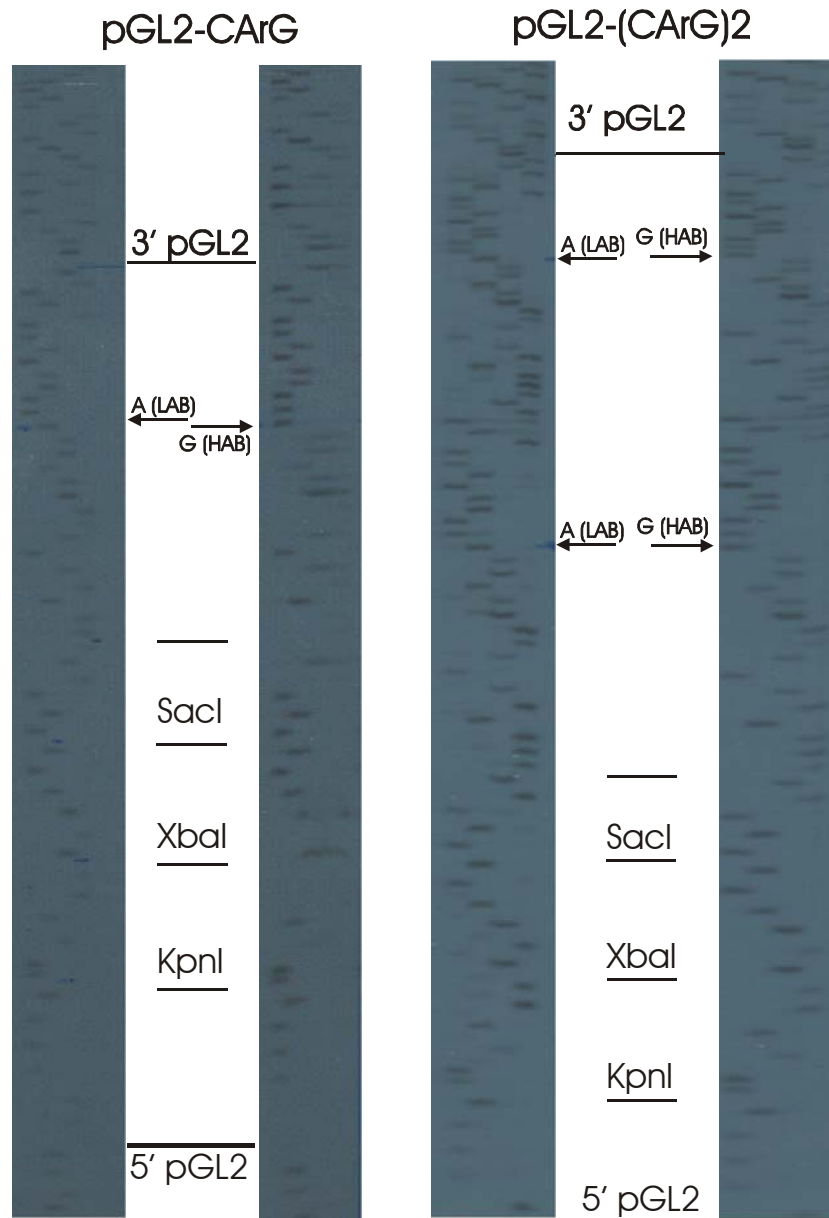


Figure 7. Sequences of the CARG ligated pGL2 vector – pGL2-CArG, pGL2-(CArG)2. Sequences were read from a sequencing primer located 5' to the insertion site and luciferase gene. Lane order of the nucleotides is G, A, T and C. Further note the HAB and LAB polymorphic CARG sequences.

pGL2-SV40-(CArG)2/ pGL2-SV40-(CArG)3 vectors were obtained by further cloning of the CARG elements adjacent to the first copy. This was achieved by digesting the pGL2-SV40-CArG vector with KpnI and SacI. This produces one small fragment of 8bp containing the XbaI site, which is discarded in the subsequent dephosphorylation and phenol/chloroform step. The annealed and phosphorylated oligonucleotides are then ligated with this digested vector, as described above. Bearing in mind that the previous XbaI site was lost in the previous digestion, inserts were again confirmed by an XbaI digest, where only positive clones produce any fragment, which, nonetheless, was 474bp long. pGL2-SV40-

(CArG)₃ containing three copies of the CArG element was further constructed by repeating the procedure above starting with a KpnI/SacI digest of pGL2-SV40-(CArG)₂ instead of pGL2-SV40-CArG.

pGL2-SV40early vector is derived from the pGL2SV40 vector which contains the intact SV40 promoter. The SV40 promoter is composed of two parts; the upstream ‘late’ enhancer and the downstream ‘early’ enhancer (figure 8). Since we wished to create a weakly active promoter we deleted the late enhancer by an SphI digest, of which two sites are found in the early/late promoter and a further site upstream in the vector (see below).

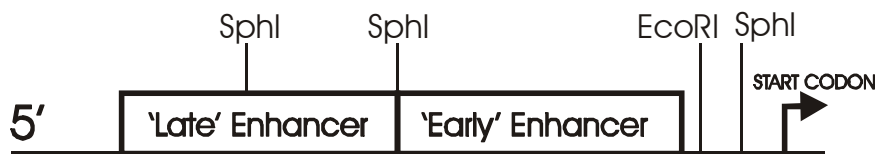


Figure 8. Schematic diagram of the simian virus (SV40) promoter. The promoter is divided into two regions constituting the proximal Early enhancer and the distally located Late enhancer. Three SphI restriction sites are contained by the vector, one situated in the late enhancer, the other mapping to the late/early enhancer boundary, and a third upstream of the start codon before the SV40 promoter sequence begins. An EcoRI sequence also locates close in the vicinity of the third mentioned SphI site.

The larger fragment, containing the early enhancer was purified on an agarose gel and the overhanging ends created by the SphI sites were blunted by T4 polynucleotide kinase to create sites compatible with other blunt ended restriction fragments such as HincII. This fragment was then further digested with EcoRI and then cloned into a pBSKII vector digested with HincII and EcoRI.

pGL2-SV40early-CArG vector consisted of a series of either one, two or three CArG elements inserted into the pGL2-SV40early vector. This was performed by cutting out the CArG elements from the pGL2-SV40-(CArG)_{1,2} or 3 by DraIII and XhoI, lying either side of the elements and cloning them into the pGL2-SV40early vector digested by DraIII and XhoI. All LAB and HAB CArG constructs were verified by XbaI digests, as before.

The minimal promoter plasmid pGL2-TATA vector contains solely the TATA element derived from E1B (Hoffmann et al., 2003).

pGL2-TATA-(CArG)_{1, 2} or 3 contained CArG elements cloned in series in front of a TATA element. CArG elements were ligated into the pGL2-TATA vector digested with DraIII and XhoI, as described above.

2.2.4 Cell culture and transfection experiments

2.2.4.1 Cell cultures

Saos-2, human osteosarcoma-like cells, (ATTC HTB-85) were established from the primary osteogenic sarcoma of an 11-year-old Caucasian female by J. Fogh and G. Trempe in 1977 (Fogh et al., 1977), and are epithelial in morphology. In this study, they were grown in Dulbecco's Modified Eagle Medium (DMEM) supplemented with 10% foetal calf serum (FCS).

Lu-165, human small cell lung cancer cell line (a kind gift from Dr. T Terasaki, Tokyo, Japan), was established from a 50-year-old small cell lung cancer patient presenting with a syndrome of inappropriate anti-diuretic hormone secretion and the cells consequently produce a high quantity of anti-diuretic hormone (ADH, 2.8 µg protein) (Terasaki et al., 1994). The cells grow as multicellular suspended aggregates and retain their small cell carcinoma morphology. In this study, the cells were grown in RPMI1640 with L-Glutamine and 10% iron supplemented FCS. The cells grew very slowly and changes in media, including Optimum, and DMEM failed to speed up growth.

Neuro2a is a mouse neuroblastoma cell line established by R.J. Klebe and F.H. Ruddle in 1969 (Klebe RJ, 1969) from a spontaneous tumour of a strain A albino mouse (ATCC No. CCL-131) and are neuronal in morphology. The cell line does not express AVP but do produce large quantities of microtubular protein which is believed to play a role in a contractile system which is responsible for axoplasmic flow in nerve cells. They were grown in DMEM supplemented with 10% FCS.

HeLa cells are derived from a cervical epithelial adenocarcinoma of Henrietta Lacks, a 31 year old woman from Baltimore, USA, who died of cervical cancer in 1951 and established by F.W. Scherer (Scherer, 1954) (ATCC No. CCL-2). The cells retain an epithelia morphology and in this study were grown in DMEM supplemented with 10% FCS.

3T3 cell line was established by G. Todaro and H. Green in 1962 (Todaro, 1963) from disaggregated Swiss mouse embryos (ATCC No. CCL-92). They consist of fibroblast cells of mesodermal origin that make the structural fibres and ground substance of connective tissues. They are characterized by an abundant and branched cytoplasm surrounding an elliptical, speckled nucleus having one or two nucleoli. These cells were again grown in DMEM supplemented with 10% FCS.

2.2.4.2 Transfection

Saos-2 cells were transfected by electroporation. Cells were seeded 12h before transfection. They were harvested by trypsinisation and resuspended in Electroporation buffer (EP) 1x (50mM K₂HPO₄, 20mM CH₃KO₂, 20mM KOH) to obtain a concentration of 2x10⁷ cells/ml. 1x10⁶ cells in 50µl of this was added to a 100µl mixture containing 1µg of AVP-luciferase vector, 0.2µg pRK7-β-gal expression vector, 4µl MgSO₄, 20µl EP5X, 3µg pGEM4 filling DNA, and water. This was incubated at room temperature for 10min, placed in a cuvette and then electroporated using a BTX 600 electroporator (290V, 500µF, 360Ω). After pulse delivery the cells were immediately transferred to 24-well culture dishes containing 1ml of DMEM+10% FCS and incubated overnight at 37°C 5% CO₂.

Neuro2a cells were transfected using lipofectamine reagent. Cells (2x10⁵) were seeded onto 24-well tissue culture dishes in 0.5ml DMEM+10%FCS and grown until 50-80% confluence. The medium prior to transfection is removed and the cells rinsed with 200µl of DMEM without FCS. For each well 2µl of lipofectamine reagent was mixed with 1µg of AVP-luciferase vector and 1µg pRK7-β-gal which was mixed in 50µl of serum free medium and incubated for 40min to allow complexes to form, after which a further 150µl of serum free DMEM was added. These complexes were added to the rinsed cells and incubated for 5h. After this 200µl of DMEM+20%FCS was added, and cells incubated overnight at 37°C.

Lu-165 cells were transfected using electroporation, as previously described (Coulson et al., 1999a). Briefly, 2x10⁵ cells were seeded onto 24-well tissue culture dishes in 0.5ml DMEM+10%FCS and grown until 50-80% confluence. The medium prior to transfection was removed and the cells rinsed with 200µl of DMEM without FCS. For each well 2µl of lipofectamine reagent was mixed with 1µg of AVP-luciferase vector and 1µg pRK7-β-gal which was mixed in 50µl of serum free medium and incubated for 40min to allow complexes to form, after which a further 150µl of serum free DMEM was added. The reaction was added to the rinsed cells and incubated for 5h, after which 200µl of DMEM+20% FCS was added. Cells were incubated overnight at 37°C/5% CO₂, and luciferase activity measured about 18h later.

2.2.4.3 Luciferase assay

To measure promoter activity cells were washed twice with PBS and then thoroughly lysed in 100µl lysis buffer (75mM Tris-HCl, 10mM MgCl₂, 1% Triton X-100, 2mM ATP, 1mM DTT). Aliquots were measured in a LKB luminometer for 20sec.

As an internal control of transfection efficiency, the luciferase readings were standardised on β -gal activity from a cotransfected β -gal expression vector (pRK7- β -gal) (Hoffmann et al., 2003). The β -gal activity in the extracts was measured as described previously (Spengler et al., 1993). The luciferase measurements were divided by the β -gal values.

2.2.5 Protein preparation

2.2.5.1 Nuclear cell extracts

Cells were transfected with an expression vector for either YY1 or CBF-A, 3 separate transfections were pooled together and grown for 24h at 37°C in a 6 well plate. The cells were washed with 1x PBS, and were then scrapped into solution in 1ml 1x PBS and centrifuged at 4,000rpm at RT for 5min. 100 μ l buffer (10mM Hepes pH7.9, 10mM KCl, 0.1mM EDTA, 0.1mM EGTA, 1mM DTT, 0.5mM PMSF) was added and gently mixed, and the cells incubated on ice for 15min to swell. To disrupt the cytoplasmic membrane 5 μ l of 10% IGEPAL was added for 10min. The sample was then centrifuged and the soluble supernatant containing the cytoplasmic extract discarded. The pellet was then resuspended in 50 μ l buffer (20mM Hepes pH7.9, 0.4mM NaCl₂, 1mM EDTA, 1mM EGTA, 1mM DTT, 0.5mM PMSF) containing 1 μ l protease inhibitor and shaken for 60min at 4°C to disrupt the nuclear membrane. This mixture was then centrifuged 14,000rpm, 4°C for 5min in a benchtop centrifuge and the aqueous solution containing the nuclear extract was removed. All nuclear extracts were either used immediately or stored at -80°C until use.

2.2.5.2 Recombinant proteins

Recombinant CBF-A-GST fusion proteins were used for EMSA. Following transformation of pGEX-2TK-CBF-A into DH5 α bacteria single colonies were grown at 37°C in 50ml 2YT (0.16% tryptone, 0.1% yeast extract, 0.1% NaCl) overnight, to which a further 450ml 2YT is added and grown for 3h until an OD600 of 0.5-1.0 was reached, after which, they were incubated with a final concentration of 1mM IPTG for a further 2h at 30°C. The GST-CBF-A protein was purified using glutathione-sepharose beads (Hoffmann et al., 2003). Eluted CBF-A was shown to be at least 95% pure as judged by Coomassie blue staining. Concentration of CBF-A was determined using Bradford assays and aliquots were stored at -80°C until usage. The recombinant proteins of the deletion constructs were produced as described above and again judged to be at least 95% pure from Coomassie blue staining.

Materials and Methods

For EMSA experiments CBF-A was incubated with 20,000cpm of dsDNA end labelled oligonucleotides (LAB CArG sense, gta tcc cca ctg tCC TTA TTA GGa aga ggc aaa; LAB CArG antisense, gta ttt gcc tct tCC TAA TAA GGa cag tgg gga; HAB CArG sense, gta tcc cca ctg tCC TTA TTG GGa aga ggc aaa; HAB CArG antisense, gta ttt gcc tct tCC CAA TAA GGa cag tgg gga).

2.2.5.3 Protein concentration and purity

Bradford assays were used to determine the concentration of all proteins used in this study. The assay is based on the observation that the absorbance maximum for an acidic solution of Coomassie Brilliant Blue G-250 shifts from 465nm to 595nm when binding to protein occurs. Both hydrophobic and ionic interactions stabilize the anionic form of the dye, causing a visible colour change. The concentrated Assay buffer was first diluted 1:5 and standards were prepared containing a range of 20 to 200µg protein (BSA) to a standard volume. The samples were diluted (3µl in 200µl water) to an estimated concentration of 20 to 200 µg/ml. 800µl Bradford assay is added to each sample and protein standard, and the absorbance was measured at 590nm. Protein concentration of samples was deduced from the standard curve.

Coomassie blue staining was then further used to assess the purity and integrity of recombinant protein preparations. Protein samples were loaded on to an SDS-PAGE gel (see *Western blots*) with a size marker (refer to section 2.1.1) and run at 150V. The gel was then soaked in 0.2% Coomassie blue for 1h and destained in 40% methanol, 50% acetic acid solution over night. The gel was then blotted on to paper and dried. All proteins used in the study were of at least 95% purity.

2.2.5.4 EMSA

Electrophoretic mobility shift assays (EMSA) were used to determine the affinity of a protein for a particular DNA sequence. For EMSA experiments CBF-A or YY1 was incubated with 20,000cpm of double-stranded end labelled (see above) oligonucleotides. Sense and antisense oligonucleotides, 30bp long, contained the CArG element and an overhanging GTA for end labelling - LAB CArG sense, gta tcc cca ctg tCC TTA TTA GGa aga ggc aaa; LAB CArG antisense, gta ttt gcc tct tCC TAA TAA GGa cag tgg gga; HAB CArG sense, gta tcc cca ctg tCC TTA TTG GGa aga ggc aaa; HAB CArG antisense, gta ttt gcc tct tCC CAA TAA GGa cag tgg gga. The uppercase letters denote the polymorphic CArG element.

For the YY1 experiments a control oligonucleotide containing a previously reported YY1 binding site was used. This binding site was described in the Moloney Murine Leukemia Virus (MuLV) promoter, and was integrated into two 29-mer oligonucleotides which were

Materials and Methods

annealed together; MuLV sense, gta tgc ctt gca aaa tgg cgt tac tgc ag; MuLV antisense, gta ctg cag taa cgc cat ttt gca agg ca.

The oligonucleotides were annealed in a 20 μ l reaction containing 5 μ g/ μ l of each of the sense and antisense oligonucleotides and 4 μ l of annealing buffer (1.5M NaCl, 100mM TrisHCl). This was heated at 85°C for 10min to ensure DNA separation, and then allowed to cool slowly over 3-4h to room temperature to allow for efficient annealing of the sense to the antisense oligonucleotide. This mixture was then diluted to 50ng/ μ l for the labelling reaction (see above). A working stock of 20,000cpm/ μ l labelled oligonucleotide was used for all EMSA experiments. ssDNA oligonucleotides were labelled using the forward reaction (see above), and again a working stock of 20,000cpm was used. The binding reaction was then performed using a specific amount of protein in a volume of 20 μ l reaction buffer (5mM TrisHCl pH7.5, 25mM NaCl, 2.5% glycerol, 0.5mM EDTA, 0.25mM DTT, 0.5 μ g dl/dC). This was incubated on ice for 5min and then 20,000cpm of labelled oligonucleotide (either single stranded or double stranded) was added and the whole reaction was incubated for a further 25min at room temperature. 1 μ l of loading dye was added and the samples were loaded on a 5% polyacrylamide gel (non denaturing). This gel, which was pre-run for 30min at 4°C; 150V; 0.5x TBE, was run with the samples at 100V for around 1h at 4°C in 0.5x TBE.

2.2.5.5 Western blots

Transfected, or non-transfected cells of HeLa, 3T3, Saos-2, Lu-165 and Neuro2a were used for Western blots. Cells were seeded 24h before harvesting in 10cm plates. The cells were first washed twice with 5 ml 1x PBS. The cells were then scrapped with 0,15 to 0,5 ml T10E1, 1mM PMSF, 1mM DTT and protease inhibitor cocktail (1/1000). A G21 needle was used to break the cells by passing through ~20 times. An aliquot of 50 μ l was kept at this step for measuring protein concentration. To the remaining 450 μ l were added 150 μ l of 4x Lamli buffer (200mM Tris-HCl pH6.8, 8% SDS, 40% glycerol, 0.4% Bromophenol blue, 0.1% β -mercaptoethanol). A G21 needle was again used to break the released high molecular DNA. A 12% SDS-PAGE, gel was prepared. 20 μ g of protein is boiled for 5min in an equal volume of Lamli buffer to denature the protein. The gel was run on 150V at room temperature with a water flow for cooling. The proteins were transferred to Nitrocellulose film in a transfer chamber at 50V for 1-2h RT. The membrane was briefly stained with Ponceau red to check if the proteins have transferred from the gel to the membrane. Unspecific binding of the antibodies to the membrane was blocked by placing the membrane

in Blocking Buffer (10mM Tris, 0.5M NaCl, 0.1% tween, 5% non fat dried milk) which was incubated on a shaker at room temperature for 1h. The blocking solution was poured off and the membranes incubated with the primary antibody over night at 4°C. Membranes were then washed 5-6 times with TBS/0,1 % tween to remove unbound antibody and then incubated for 1h at RT with the second conjugated antibody. The membranes are washed as before. A 1:1 mix of the chemiluminescent reagent was prepared and added to the membrane. This was left for between 10sec to 5min, after which the membrane was dried slightly and wrapped in saran wrap. This is exposed to X-ray film for 30sec to check, adjusting exposure time-dependent on the strength of signals.

2.2.5.6 *In vitro* DNA unwinding assay

Between 1ng and 10ng of GST-CBF-A or GST protein were incubated with 20,000cpm of end labelled LAB probe for 30min at RT, as described for the EMSA experiments. Varying concentrations of S1 nuclease (Amersham) were added to the sample which was then incubated at either 4°C or room temperature for between 1min to 1h. The reaction was stopped by incubating for 1min at RT with 1µl proteinase K (100µg/ml) to cleave the S1 nuclease and the CBF-A binding to the DNA. An equal volume of formamide loading buffer (95% formamide, 2mM EDTA, 0.025 % Bromophenol blue and 0.025% Xylene cyanol) was added and the whole sample was boiled for 5min to destroy the protein/DNA complexes and denature the DNA. The samples were then placed immediately on ice for 1min, then heated at 72°C for 2min and separated on either a denaturing 5% polyacrylamide gel and exposed to X-ray film.

2.2.5.7 Antibody analysis

2.2.5.7.1 Antibodies

CBF-A anti-N-CBF-A antibody, raised in the rabbit towards the first 75aa of the N-terminal part of CBF-A, was a generous gift from Drs. Leandersson and Aranburu (Lund). The anti-N-CBF-A serum was purified using protein A Sepharose, and has an approximate concentration of 1.4 mg/ml dissolved in PBS + 0.1% sodium azide. CBF-A 266, 267 and 269 were a kind gift from Dr. Fry (Haifa) and had yet to be tested in Western blots or antibody shift experiments. YY1 was commercially acquired (refer to section 2.1.5.1). It was raised against an epitope corresponding to amino acids 1-414 representing full length YY1 of human origin. It has been previously shown to react with YY1 of mouse, rat and human origin by Western blotting, immunoprecipitation, and immunohistochemistry and was further recommended for

gel supershift applications. The anti-GST, anti-FLAG and anti-His antibodies were acquired commercially (refer to section 2.1.5.2).

For supershift experiments protein and DNA were initially incubated together, as described in EMSA. Various quantities of antibody were then added directly to the mixture which was subsequently loaded on to a polyacrylamide gel and electrophoresed, as in the EMSA experiments.

2.2.5.7.2 Immunohistochemistry

Double immunofluorescence-histochemistry staining was used to visualize CBF-A and AVP immunoreactivity simultaneously and was performed by Nicolas Singewald (Innsbruck, Austria) to a procedure previously described (Salchner and Singewald, 2002). Briefly, 50µm Vibratome sections were preincubated for 30min in immunobuffer containing 5% normal donkey serum (Jackson Immunoresearch, West Grove, USA) to block non-specific binding sites. After washing in immunobuffer, sections were incubated for 48h at room temperature in a polyclonal rabbit antibody to CBF-A (dilution 1:1000) and a polyclonal guinea pig antibody to AVP (GHC 8103, Peninsula, Belmont, USA; dilution 1:10,000) in immunobuffer containing 5% normal donkey serum. The anti-N-CBF-A antibody, raised in rabbit towards the first low conserved 75aa of the N-terminal part of CBF-A, was a generous gift from Drs. Leanderson and Aranburu (Lund). After rinsing in immunobuffer, sections were exposed for 2.5h at room temperature to the species-specific fluorophore-conjugated secondary antibodies (Cy2-conjugated donkey anti-rabbit IgG, dilution 1:100; Cy3-conjugated donkey anti-guineapig IgG, dilution 1:400; Jackson Immunoresearch, West Grove, USA, AMCA-conjugated donkey anti-guinea pig IgG, dilution 1:100; Jackson Immunoresearch, West Grove, USA) diluted in immunobuffer containing 1% normal donkey serum. Following rinsing in 50mM Tris-HCl (pH 7.4), sections were mounted onto slides and dried overnight. Mounted sections were cleared in 100% ethanol and Histoclear (National Diagnostics, Atlanta, USA) and coverslipped in Eukitt (Kindler, Freiburg, Germany). Appropriate negative controls were performed by omission of the primary antibodies. No staining was observed in the control sections. Slides were viewed with a fluorescence microscope equipped with adequate filter systems to observe the green Cy2 and red Cy3 fluorescence (figure 38A-D) and to observe the red, which was converted from green to facilitate visualization of double labeling, Cy2 and blue AMCA fluorescence (figure 38E).

For semiquantitative immunohistochemistry experiments and correlation analyses, 5 HAB, 5 NAB and 6 LAB animals were phenotyped on the elevated plus-maze and two days later sacrificed for AVP immunohistochemistry. The semiquantification analysis of AVP

immunohistochemistry was performed by means of image analysis using optical software (Optimas 5.2, Optimas Corporation, Germany).

2.2.6 Statistical analysis and computer software

The predicted transcription binding site analyses were performed using the online programs TESS (www.cbil.epenn.edu/tess/) (Schug and Overton, 1997) and MatInspector (www.genomatix.de) (Quandt et al., 1995). DNA aligns were performed using the DiAlign program from Genomatix (www.genomatix.de) (Morgenstern et al., 1996). Analysis of the mouse AVP signal peptide was performed using the freely available software SignalP (www.cbs.dtu.dk/services/SignalP/) (Nielsen et al., 1997), PredictProtein (www.embl-heidelberg.de/predictprotein/) (Rost, 1996) and transmembrane helix prediction (www.cbs.dtu.dk/services/TMHMM/). Prediction of phosphorylation sites was performed using NetPhos 2.0 (www.cbs.dtu.dk/services/NetPhos/) and phosphorylation site prediction (www.cbs.dtu.dk/databases/PhosphoBase/predict/predform.php). Intensity of protein bands in the EMSA gels were determined using the TotalLab program. Restriction enzyme cut site sequences were elucidated through the DNA strider program (Marck, 1988) and the freely available Webcutter 2 (www.firstmarket.com/cutter/cut2.html). Primers were designed according to previously stated guidelines (Innis and Gelfand, 1990). All statistical analyses were performed using the software from Microsoft Excel. Statistical calculations of the second F2 analysis of the HAB and LAB rats were performed by Professor Müller-Myhsok with the statistical software R.81. All diagrammatic figures were designed through CoralDraw 10 (Corel Corporation, Ottawa).

3 Results

The HAB and LAB rat lines have been bi-directionally inbred since 1985 (figure 9A). An inbred strain, by definition, is one that has been brother-sister mated for at least 20 generations (for review see Beck et al., 2000). Each generation of brother-sister mating increases the probability of attaining homozygosity at any given genetic locus, and by 20 generations ~97.5% of the loci should theoretically be homozygous (Nicholas, 1987). The major value of a selective inbreeding strategy emanates from the fact that this approach actively enriches for genetic information associated with a particular trait shifting the animal's phenotype from the population mean (Falconer and Mackay, 1996).

Although it might be assumed that both the HAB and LAB inbred lines are at least 97-98% homozygous, an initial uncertainty was the extent of intra-line homozygosity i.e. the extent to which the lines differ to each other at any given locus. For this reason the study began by principally investigating the degree of intra-line homozygosity by conducting a low resolution genome screen using simple sequence length polymorphic (SSLP) markers (Landgraf and Wigger, 2003). This experiment was based on the analysis of 145 markers representing around six locations on each of the rat's twenty chromosomes, with the exception of chromosome 3, where fourteen markers were analysed. Chromosome 3 received greater attention due to the finding of line strict differences in the AVP promoter locus on chromosome 3, which was at the time of this analysis under study in the candidate gene approach (see below). The same DNA samples from the 10 HAB and 10 LAB animals used in the candidate approaches were used in this low resolution genome scan.

Results from figure 9B evidenced seven areas, revealing strict line differences, locating to chromosomes 2, 3, 4, 5, 9, 12, 15. It was further obvious that a rather large number of SSLPs were informative - sixty-four of the 145 giving a percentage of 44.1%. However, while some chromosomes, such as chromosome 3 provided a greater number of informative markers, other chromosomes, such as 16 and 17 were completely devoid of informative markers. This mosaicism suggests that certain areas of the genome are more heterozygous between the lines, than others.

In relation to the major emphasis of this study, which more specifically concerns the AVP locus, it should be noted that chromosome 3, in which the gene localises, revealed a number of line-specific differences. It was already evident, from data performed in parallel to this experiment, that chromosome 3q21 shows a line-specific difference. However, of concern was the size of the region in which the haplotype block, containing the AVP locus, extended.

Results

This was of importance to determine, when considering the further association results, in being able to discern between a definite number of genes segregating together with the AVP locus, and thus, acting as positional candidates.

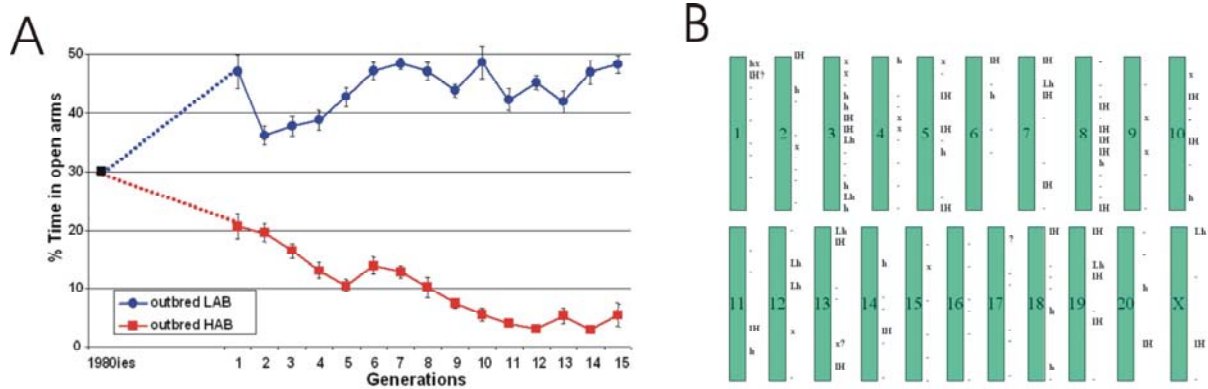


Figure 9. Inbreeding strategy of HAB and LAB rats. (A) Graph highlighting the divergence of the HAB and LAB lines in anxiety measured in percentage time spent on the open arm of the EMP (Landgraf and Wigger, 2002). (B) Screen of 145 markers across the HAB and LAB genomes (Landgraf and Wigger, 2003). - = homozygous, x = strict line difference, h = both lines are heterozygous, IH = LAB heterozygous, HAB homozygous, Lh = LAB homozygous, HAB heterozygous.

The results presented in figure 9B, revealed chromosome 3 to contain a number of strict line differences. The AVP gene, though not physically mapped, localises adjacent to the neighbouring oxytocin gene at 683.9 CentiRays (cR) in a radiation hybrid analysis. (Dutil et al., 2001). The two furthest homozygous markers spanning the area containing the AVP gene, before each region of heterozygosity, lie at ~500cR (D3Rat81) and 840cR (D3Rat63). This is compatible with the view that the region presenting with a strict line difference linked to the AVP locus, i.e. the area of linkage disequilibrium, is no greater than 340cR, which roughly translates to one third of the chromosome. One must also note, however, that the regions for which the markers are not informative do not necessarily infer chromosomal regions of homozygosity. This simply relates to the fact that markers did not differ at these specific alleles, and play no relevance to the fact that regions immediately adjacent to this area may show heterozygosity or strict line differences.

3.1 Candidate gene approach

A candidate gene approach was followed as part of a pathway analysis, focusing on the two ACTH stimulating genes involved in the HPA axis. This approach was also of initial importance for firstly, determining a frequency of polymorphisms between the lines in association with the previously mentioned genome screen, secondly as a basis for the

discovery of markers for future possible QTL analysis and thirdly, to determine if any candidate genes might contain possible deleterious mutations underlying the phenotype.

3.1.1 CRH

CRH is a 41 amino acid (aa) peptide derived by enzymatic cleavage from a 191aa preprohormone. The gene, localised on chromosome 2q24, encodes a cDNA of 1666 nucleotides comprising 2 exons and including 117 nucleotides of 5' untranslated sequences (Potter et al., 1991). A TATA and CAAT transcription initiation site were identified 22bp and 60bp upstream of the translation initiation site (Thompson et al., 1987) and DNA elements for cAMP responsiveness, glucocorticoid receptors and POU homeodomain proteins have been described in the region -221 to -278bp (Ramkumar and Adler, 1999).

The CRH gene and promoter sequence were also subjected to SSCP analysis as part of the candidate gene approach. Primers were designed to span the gene in overlapping 300bp segments from previously published sequence (M54987) (Thompson et al., 1987), covering 356bp upstream of the transcriptional initiation site and 222bp 3' downstream of the stop codon (figure 10).

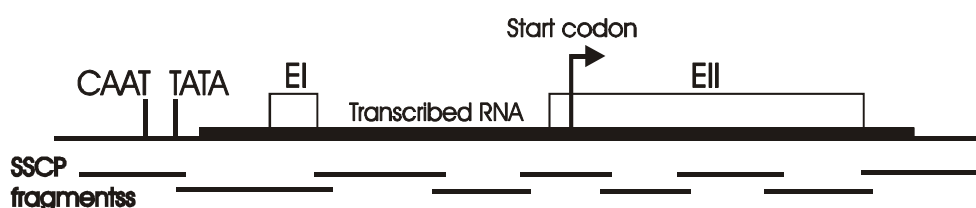


Figure 10. Diagrammatic scheme of the rat CRH gene demonstrating promoter, exons (E) and the regions investigated by SSCP analysis.

Results of the SSCP analysis lacked alternative band patterns suggesting an absence of polymorphisms in the CRH gene and proximal promoter region.

3.2 AVP

The AVP gene locates to chromosome 3 in the rat at position 3q35 or 3q41-q42 (figure 13A) (Khegai and Ivanov, 1994) encoding a 164aa precursor protein for AVP which includes the 9aa hormone, its carrier protein, neurophysin II (NP II), and a glycoprotein. The functional domains of the protein precursor are coded by 3 exons, the first of which encodes the hormone, the second most of the carrier protein, and the third the glycoprotein (figure 11). The transcriptional start site leads to a cDNA containing 33 nucleotides of 5' untranslated region, and 75 nucleotides of 3' untranslated region (Ivell and Richter, 1984).

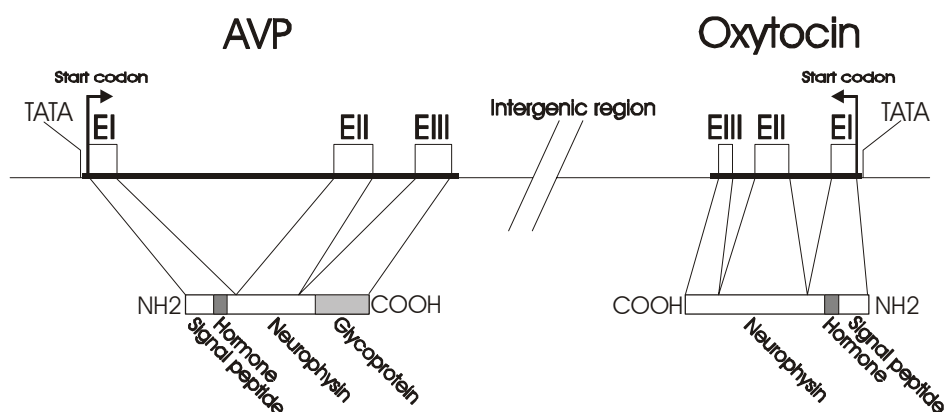


Figure 11. Schematic diagram of the rat AVP and oxytocin locus. The two genes locate 11kb apart (intergenic region) being transcribed towards each other from opposite strands of the DNA duplex.

3.2.1 AVP levels in the PVN correlate with anxiety-related behaviour

HAB, LAB and NAB Wistar rats were phenotyped for their behaviour and further subjected to immunohistochemistry to determine relative amounts of AVP in the parvocellular and magnocellular compartments of the PVN (figure 12A). In both subdivisions AVP peptide levels were significantly higher in the HAB animals when compared to either the LAB or NAB, which failed to differ (figure 12B). This data convincingly demonstrate that differences in AVP mRNA levels translate into peptide levels and confer a basal overexpression of AVP

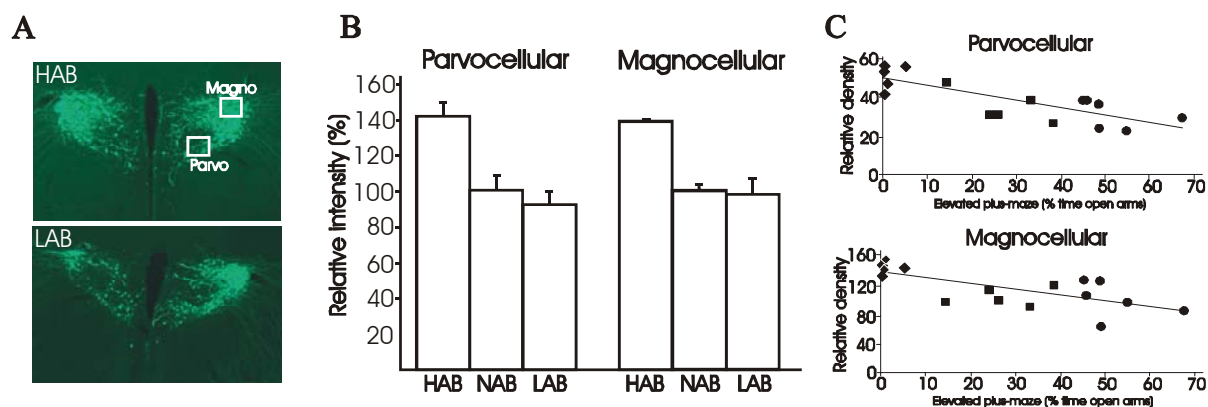


Figure 12. Correlation between AVP immunohistochemistry and anxiety-related behaviour. (A) Fluorescence-immunohistochemistry of AVP in rat PVN. The white squares denote the 80-100 μm^2 areas of magno- and parvocellular regions of the PVN, which was measured. (B) Percentage of AVP fluorescence-immunohistochemistry (relative grey density) performed, in parvocellular and magnocellular subdivisions of the PVN, in HAB (n=5) and LAB (n=6) compared to NAB (n=5). (C) Immunohistochemistry (relative grey density), in parvocellular and magnocellular subdivisions of the PVN, correlates significantly ($p < 0.001$) with anxiety-related behaviour (% time spent on the open arms of the elevated plus-maze) in HAB (n=5) (filled diamonds), NAB (n=5) (filled squares) and LAB (n=6) (filled circles) rats.

Results

in the HAB animals. Furthermore, in both the parvocellular and magnocellular subdivisions AVP peptide levels significantly correlate ($p < 0.001$) with anxiety-related behaviour (i.e. negatively with % time spent on the open arms of the elevated plus-maze as indicated in figure 7C) as measured by the EPM test, the paradigm on which the animals were originally selected. This, therefore, suggests that the AVP peptide content in the parvocellular and magnocellular neurons relates to HPA axis functioning in these animals.

This divergence in AVP gene expression between the HAB and LAB/NAB lines prompted us to analyse the AVP gene to address the question of whether the differential AVP regulation might be the result of a *cis*-regulatory effect stemming from promoter sequence differences between the lines.

3.2.2 Sequence analysis

The promoter of the AVP gene was subjected to SSCP analysis in a search for line-specific polymorphisms. This experiment evidenced a polymorphic region 341-678bp upstream of the start codon; 10 outbred Low Anxiety (LA) animals revealed an alternate pattern of bands when compared to 10 outbred High Anxiety (HA) animals (figure 13B). This confirms the presence of a strict line difference in this region of the AVP promoter. Further noticeable, in lanes 8 and 11 containing the HAB animals, are band patterns representative of both lanes suggesting heterozygosity. Considering these animals are the results of HAB and LAB inbred line crosses with outbred animals, the presence of the heterozygous sequences in the two HAB rats suggests that originally the outbred parents of these offspring contained the LAB allele. This is a tentative indication that the LAB allele represents the more common variant.

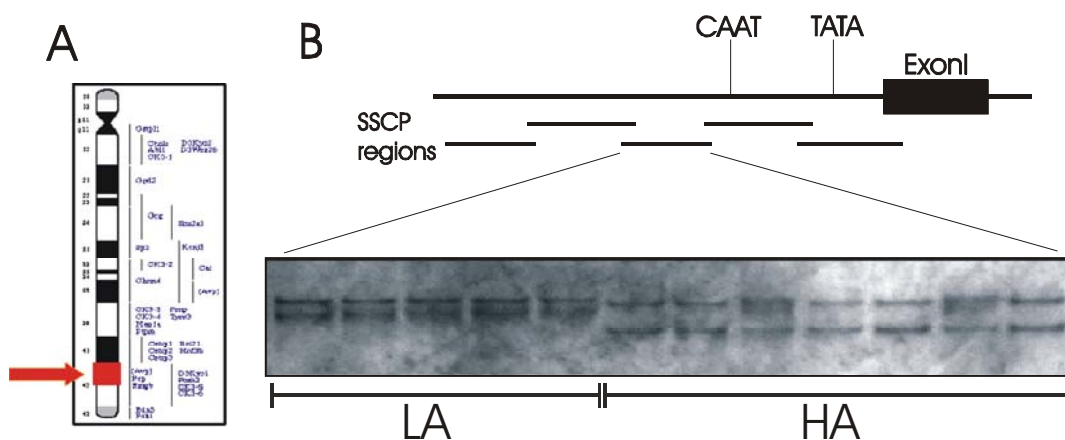


Figure 13. SSCP analysis of the rat AVP gene. (A) The rat AVP gene is located on chromosome 3 at either position 3q35 or 3q41-q42 (Khegai and Ivanov, 1994). (B) The proximal 700bp of the AVP promoter was subjected to SSCP analysis. The third PCR product, encompassing the region -341 to -678, revealed alternative band patterns specific between the two lines.

Results

The polymorphic allele was subsequently sequenced to determine the exact nature of the polymorphism(s), and from the results (figure 14) it became evident that a number of single nucleotide polymorphisms (SNPs) occur in this region between the HAB and LAB animals.

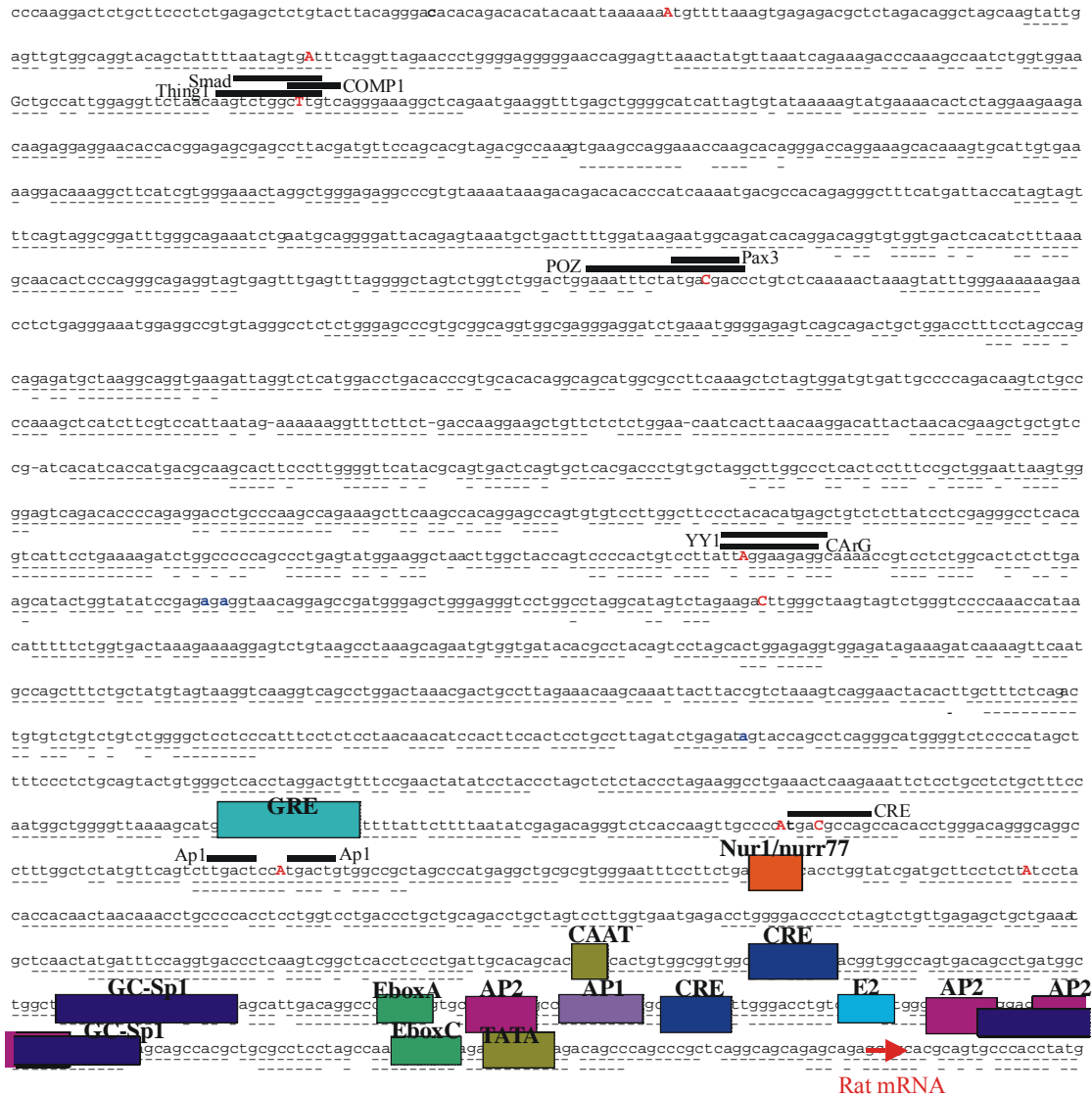


Figure 14. Rat AVP promoter (Acc. AF112362). Polymorphisms in the rat are in red capitals and single base pair differences or deletions to published sequence but found in both strains are in blue lower case characters or marked with a dash in the case of a deletion. Dashed lines under the sequence denote homologous bases; the upper line signifies the mouse (Acc. M88354) (Hara et al., 1990), and in the lower line the human (Acc. X62890, AL160414) (Bahnsen et al., 1992). Thick bold lines above the DNA sequence represent the various transcription factor elements mapping to the vicinity of the polymorphisms. Shaded boxes represent previously described AVP promoter elements.

When comparing the LAB and HAB sequences to published sequence of the AVP gene (AF112362) (Shapiro et al., 2000), it became apparent that the LAB line was identical to

Results

previously published nucleotides in all the SNPs A(-2640)C, A(-2565)T, T(-2453)C, C(-1958)A, A(-1276)G, C(-1161)T, A(-594)C, C(-590)T, A(-534)G, A(-455)C (and T(+549)C which is not included in figure 14) whilst the HAB line rats contained the divergent sequence. It is of importance at this point to retain caution in labelling these polymorphisms as mutations until actual frequencies can be confirmed in an outbred population. This would determine whether the alleles exist in the outbred population from which they originally derived, or if they occurred as spontaneous mutations in the inbred line. A mutation, by definition has to occur at a gene frequency of less than 0.1% in an outbred population (Lewin, 2000; Marez et al., 1997).

The coding region of the AVP gene was sequenced to determine if any non-synonymous differences occur leading to an abnormal AVP protein. Intronic regions of the AVP gene were also included in this experiment to allow for the possibility of polymorphisms spanning exon/intron slicing junctions or the presence of gross deletions/insertions effecting RNA splicing or transcriptional regulation (for review see Lewin, 2000). Results of the further sequencing confirmed that the coding region of the AVP gene was devoid of any polymorphisms, with the exception of a single SNP in intron I, involving the transition of a T for a C 549bp downstream from the start codon (figure 15A). The downstream region 3' to the AVP gene was also sequenced, acknowledging the possibility that DNA elements in this

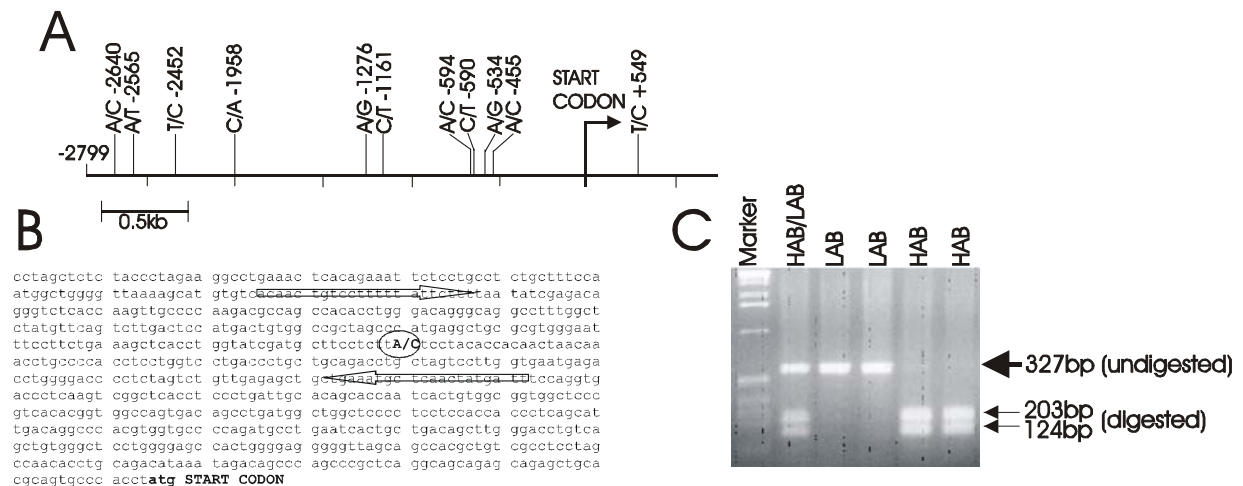


Figure 15. Rat AVP promoter polymorphisms. (A) Diagrammatic scheme of the rat distal AVP promoter region demonstrating the 2799bp distal promoter harbouring 10 SNPs. The T(+549)C polymorphism, located in intron I, was used in the allelic-specific transcription *in vivo* experiment (see figure 5) (B) Sequence of the A(-455)C polymorphism used in RFLP. Primer pairs A(-455)C-forward and reverse (refer to section 2.1.10.4) were used to amplify a 327bp DNA product. The restriction enzyme Eam11041 recognises the sequence CTCTTC and, therefore, only digests the HAB allele containing the C polymorphism. (C) Agarose gel of RFLP products digested with Eam11041 for the presence of the A(-455)C polymorphism. The HAB allele containing the C nucleotide is digested resulting in two products of 203bp and 124bp whilst the LAB allele, containing the A nucleotide, remains uncleaved.

Results

region exist which are important for AVP expression (Fields et al., 2003). Here, a further SNP was found 245bp 3' from the termination codon of the AVP gene.

Analysis of the sequence data using the online program webcutter (refer to section 2.2.6) allowed for the detection of polymorphisms affecting restriction enzyme sites (figure 15B). From this information restriction fragment length polymorphism (RFLP) assays were developed to genotype, both quickly and efficiently, animals from the HAB and LAB lines (figure 15C).

Genotyping of inbred rats from the HAB and LAB lines revealed a clear line difference for three of the SNPs in the promoter (A(-455)C, A(-534)G (figure 16) and T(-2455)C), the SNP in the first intron of the AVP gene [T(+549)C] and the C(+18)T transition in the first exon of the oxytocin gene, which is described below (refer to section 2.1.10.4). Therefore, all the polymorphisms segregate together, and the fact that the SNP in the oxytocin gene was also linked suggests the whole region segregates in linkage disequilibrium. Furthermore, the fact that genotyping revealed the presence of the HAB-specific allele in all breeding pairs comprising the HAB line suggests that the selective inbreeding inadvertently selected for the HAB allele.

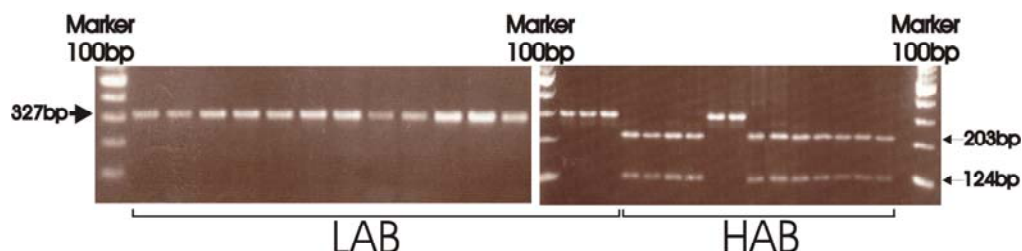


Figure 16. RFLP for A(-534)G in 29 animals representative of all LAB and HAB mating lines. The first 15 lanes deriving from inbred LAB animals are homozygous for the A allele, while the following 13 lanes, from the different mating pairs of the HAB line, are homozygous for the G allele, with the exception of two heterozygotes. The end lane contains the negative control PCR.

A number of the AVP SNPs occur in regions sharing homology with the mouse and human. DNA alignments reveal the conservation of the A allele from the A(-536)G transition in both the mouse and human and further confirm the homology of polymorphisms A(-457)C, C(-1163)T, A(-2589)T, A/C Intron I (not shown), and G(-245bp)A in the 3' sequence (not shown) in the mouse sequence (figure 14). It is of further interest to note the high degree of homology in the AVP promoter. The proximal promoter, comprising 1kb upstream of the start codon, shows 83% conservation in the mouse and 31% in the human, whilst the distal region of 2800bp upstream, still contains 68% conserved sequence in the mouse and 18% in the

human. This clearly demonstrates the importance of this area of the promoter, especially when considering the high degree of species-conservation in the tissue-specific expression of the AVP gene.

3.2.3 Sequence and genotyping of the adjacent oxytocin gene

The highly homologous AVP and oxytocin genes are closely linked, tail-to-tail, in the genome, being separated by an intergenic region (IGR) of 11kb in the rat (Schmitz et al., 1991), 3kb in the mouse (Ratty et al., 1996) and 10kb in the human (Gainer et al., 2001), they are transcribed towards each other from opposite strands of the DNA duplex (figure 11).

Sequencing analysis of the oxytocin gene was performed, firstly to determine if this gene might also segregate with the AVP gene. Secondly, it was of interest to clarify if the oxytocin gene contained similarly high numbers of SNPs as the AVP gene revealed. Thirdly, and importantly, we needed to discover a transcribed polymorphism, revealing line-specific segregation, in the HAB and LAB animals for use in *in vitro* transcription analysis (refer to section 3.2.6).

Sequencing of 2kb of the oxytocin promoter and the 700bp constituting the transcribed gene, revealed the presence of four SNPs (figure 17A). One SNP involved the transition of a C for a T in the first exon of the oxytocin gene, 18bp downstream of the start codon, whilst the other three SNPs involved base pair transitions and transversions 298bp, 734bp and 761bp upstream of the start codon in the promoter. Of particular interest was the C(+18)T transition in the first exon in codon position 3 encoding a synonymous mutation affecting the amino acid leucine at position 6, allowing employment of the *in vivo* transcription analysis assay. Literature and database searches (refer to section 2.2.6) revealed that the three SNPs in the promoter were embedded in various transcription factor-binding sites. Of these, only the T(-298)C transition effected an element found in mammals, the CACCC (HS40) element, which as a major controller of the human alpha-globin gene (Jarman et al., 1991), is unlikely to be relevant. Therefore, we conclude that none of the SNPs are suggestive to play a regulatory role.

The C(+18)T transition, lying in Exon I, provided a restriction site for the BsmAI restriction enzyme (gtctc), where the sequence containing the C allele, found in the LAB animals and consensus sequence (Accession No. X59496) (Schmitz et al., 1991), will be cleaved. Therefore, digestion of PCR products (figure 17B) with BsmAI was used to genotype animals representative of all the breeding pairs in the HAB and LAB rat lines, to establish whether this allele segregated with the AVP promoter alleles. For this analysis the

Results

same 29 animals genotyped in the AVP study were again included. These experiments showed that the LAB animals were homozygous for the published nucleotide while the HAB animals contained the non-conserved T allele (figure 17C), confirming that the oxytocin gene is in direct linkage to the AVP gene in each of the two lines.

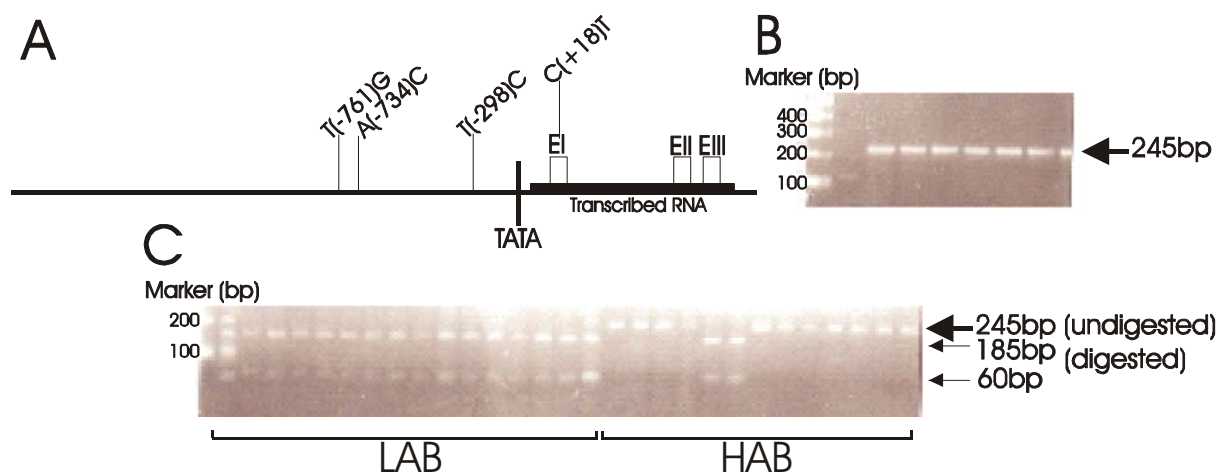


Figure 17. Rat oxytocin polymorphisms. (A) Diagrammatic scheme of the rat oxytocin gene demonstrating the 2kb region upstream and 0.7kb region downstream sequenced and the relative positions of the polymorphisms T(-761)G, A(-734)C and T(-298)C in the promoter region, and the C(+18)T in the first intron. (B) The 245bp PCR product spanning the exonic SNP C(+18)T polymorphism (refer to section 2.1.10.4). (C) Genotyping of the C(+18)T polymorphism by BsmAI digestion resulted in the detection of the C allele by the presence of two digested fragments of 185bp and 60bp.

3.2.4 Association of AVP gene and anxiety in EPM test

To address the question of an eventual contribution of the HAB-specific AVP allele to the anxious/depressive-like phenotype, a small scale, preliminary association study was performed. Sixty-six HAB/LAB F2 generation rats, the result of a cross-breeding between HAB and LAB lines, and 27 HAB/outbred F2 generation rats, resultant from a cross between a HAB rat and an outbred animal, were genotyped for both the Ksp632I and MaeIII polymorphisms and tested on the EPM test to measure their levels of anxiety-related behaviour.

When correlating the EPM test behaviour with AVP genotypes some associations were seen (figure 18). The latency to the first arm entry appeared to highlight a trend evident of a dosage effect of the AVP allele in association with anxiety-related behaviour; animals containing the HAB-derived AVP allele presented with longer durations to the initial entry into the open arm. This trend was evident in both the HAB/LAB and HAB/outbred crosses (figure 18A,C). Moreover, when latency to first open arm entry was compared amongst the

Results

male group of the HAB/LAB cross, the correlation between behaviour and genotypes become significant between the homozygous HAB and LAB allele groups ($p < 0.05$) (figure 18B).

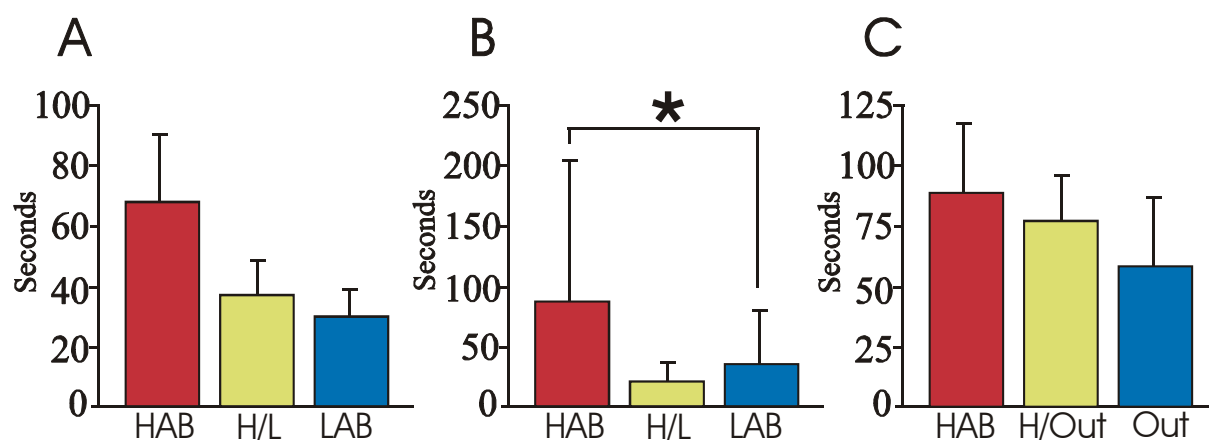


Figure 18. Preliminary association study of HAB/LAB-derived AVP promoter alleles and latency to first arm entry on the EPM test. (A) Latency to first arm entry in HAB/LAB F2 animals (16 homozygous for the HAB-specific polymorphisms, 26 heterozygous and 24 homozygous for the LAB sequence). (B) Latency to first arm entry in HAB/LAB F2 males (13 homozygous for the HAB allele, 15 heterozygous and 9 homozygous for the LAB allele cross). (C) Latency to first arm entry in HAB/outbred (Out) F2 animals involved 10 homozygous animals for the HAB allele (17 animals homozygous for the Out (LAB) allele and 15 heterozygous). *, Significantly different ($p < 0.05$).

Although the latency to first arm entry appears to suggest a trend other EPM test measurements performed in these animals did not associate as one might expect if the AVP allele was the single major determining factor in anxiety. The reasons for the lack of a clear significant association could depend on a number of reasons; firstly, the relatively small number of animals used in this study might have proved limiting to the statistical power. Secondly, the HAB/LAB mating or the HAB cross mating strategy might have somehow effected the behaviours of the animals i.e. if both animals represent clear isolated populations showing a distinct genetic makeup - in which the phenotype under study no longer presents as a continuum of variation - then a cross between these two genomes might result in a distinctly altered phenotype. Thirdly, the role of the AVP gene in controlling anxiety-related behaviour might, to some extent, depend on the contribution of other genetic loci, such as modifier loci, which would be separated from the AVP locus in this crossbreeding strategy. Fourthly, and not least, it appears feasible that the innate behaviour of the HAB line might result from a number of genes working in concert.

The issue of this association and the importance in quantifying the exact contribution of the AVP allele to anxiety was, therefore, readdressed in a larger study incorporating a greater number of animals and employing a more extensive battery of behavioural tests. The experiment was performed by mating HAB and LAB parents and crossing the F1 offspring to

Results

give 228 male animals, which were subjected in the behavioural analyses. These animals were kept in group cages of between 3 and 5 and were behaviourally phenotyped on the EPM and FS tests from the age of 6 weeks. Subsequent to the phenotyping, tail DNA was taken and the animals genotyped for the AVP SNPs.

Evident from the results was a complete lack of association between any of the phenotypic markers and the AVP allele. However, upon closer inspection it became clear that some cages associated with far higher or lower levels of anxiety and depression-related behaviour than others (figure 19A). Furthermore, when taking into consideration the differences in home cage behaviour, and standardising for this, patterns began to emerge. This became particularly apparent for the latency to float index in the FS test in which a clear promoter allele dosage effect occurred in which the HAB allele associated with a shorter latency to floating (figure 19B). Multiple regression analyses can be used to test whether, based on linear combinations of interval, dichotomous, or dummy independent variables, that a set of independent variables explains a proportion of the variance in a dependent variable at a significant level. When performing a Multiple Rank based Regression analysis on the data in figure 19B, a highly significant correlation emerged whereby the HAB allele associated with the shorter times to float, and the LAB homozygotes presenting with the longest durations ($p < 0.005$) (all multiple regression analyses were performed by Dr. Müller-Myhsok (Munich)).

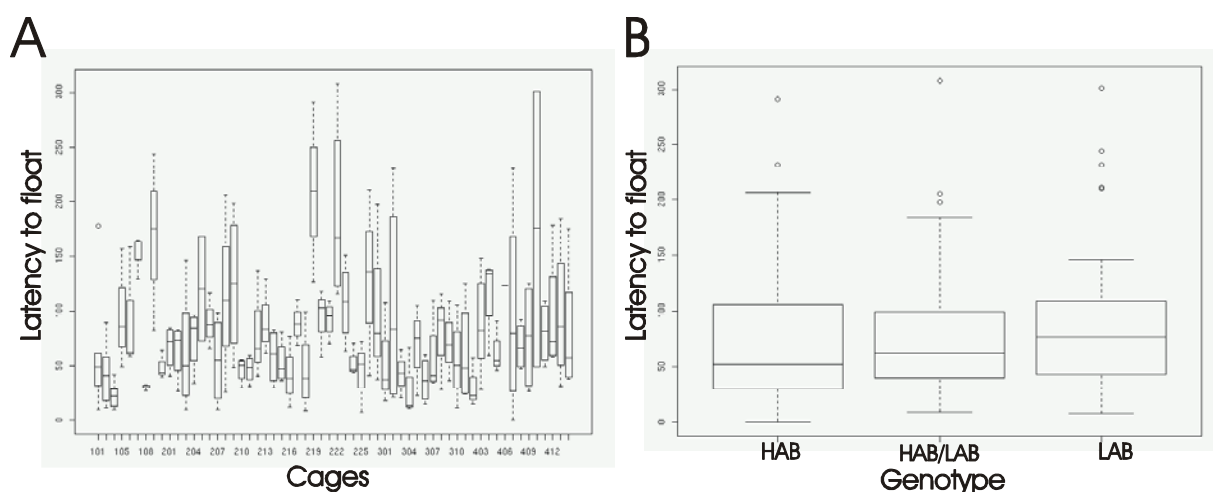


Figure 19. Large-scale association study on 228 F2 animals resultant from a cross between a HAB and LAB. (A) Graph of the average latency to float (seconds) in the FS test in each cage of multiply housed animals (B) Graph of latency to float between the HAB, heterozygote and LAB animals when home cage behaviour is standardized.

Results

The fact that the AVP allele did not associate with any further behavioural correlates, such as the EPM test, does raise some doubt as to the actual influence of the AVP gene on all aspects of the HAB behaviour, especially when considering that it was in the EPM test, and not the FS test, that these animals were originally selected. However, the observation that behavioural indices can fragment under F2 generation breeding has previously been reported (Henderson et al., 2004). And considering that the FS test has been well documented as a strong predictor for HPA axis dysregulation (Solberg et al., 2003) serves to suggest that this behavioural facet might have been the most robust marker of the HAB phenotype, aiding its survival during the F2 mating strategy.

3.2.5 Genotyping HAB AVP allele in an outbred population

The possibility of whether the LAB animals represent the common wild type allele, and HAB animals a less frequent allele needed to be investigated. To clarify this issue we tested for the presence of four SNPs spanning the first intron to the distal promoter of the AVP gene [T(+549)C, A(-455)C, A(-534)G, T(-2455)C] by RFLP analysis in 100 outbred Wistar rats, purchased from Charles River (Sulzfeld, Germany), as exemplified in figure 20A. Firstly, the four SNPs spanning the gene segregated together, reaffirming our original conclusion that the SNPs represent one allele and are in complete linkage. Secondly, the fact that all four polymorphisms were indeed present in the outbred animals confirms that non of these SNPs

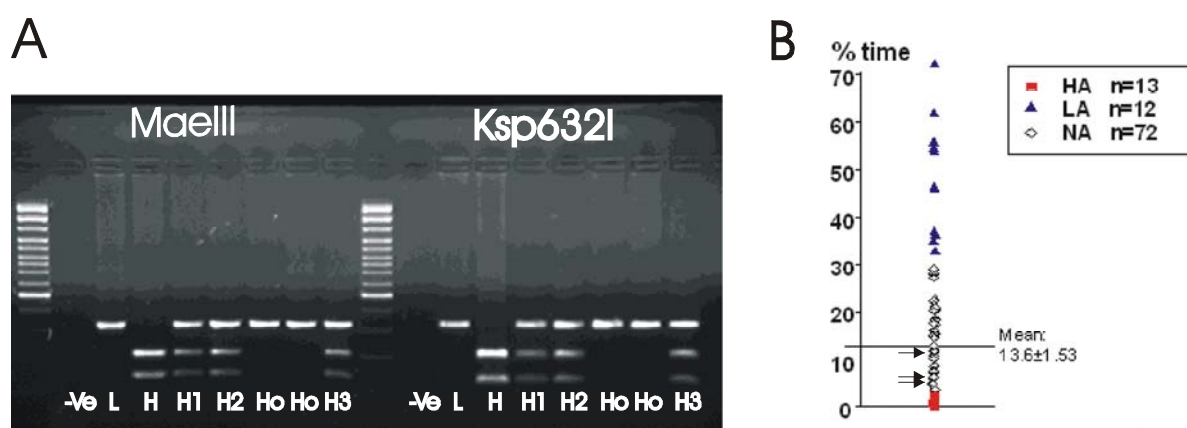


Figure 20. RFLP analysis for the HAB-specific AVP allele in an outbred rat population. (A) RFLP results of two polymorphisms, A(-455)C digested with Eam11041 and A(-534)G digested with MaeIII, in the AVP promoter which were screened in 100 animals. The -ve PCR controls, containing no DNA are included with two +ve controls for digestion efficiency of LAB (L) and HAB (H) DNA. Three animals (H1, H2, H3) were heterozygotes, whilst the remaining 97 were homozygotes (Ho). (B) EPM test data of the % time spent on the open arms in 100 outbred rats demonstrating those animals showing low (LA) and high (HA) anxiety-related behaviour. The three animals heterozygous for the HAB-specific polymorphisms (denoted by arrows) spent less than the mean time of 13.6 ± 1.53 on the open arm instead spending an average of 7.8%.

Results

represent mutations which occurred during the inbreeding. This which would be highly unlikely anyway accepting that the approximate mutation frequency of any given base in the genome per generation is less than 1×10^{-9} (Lewin, 2000); this would require the passage of a far greater number of generations in the HAB and LAB lines since their divergence. Thirdly, the fact that, of the 100 animals examined, three were found to be heterozygous indicates an allelic frequency of 1.5% for the HAB allele in the outbred population.

Overall, the results of the outbred genotypes are compatible with the view that bi-directional inbreeding selected for the HAB allele, which in turn, might critically contribute to increased anxiety in this line. This was further supported by the fact that indeed, all three heterozygous rats showed a 2-fold higher anxiety-related behaviour on the EPM test than the population mean (7.2% average for SNP containing animals vs. $13.6\% \pm 1.5\%$ average time spent on the open arm of the EPM for NA animals, figure 20B).

To pursue further the issue of AVP in relation to anxiety and depression, and to gain insight into the molecular mechanism underlying the behaviour in our rat lines, we decided to focus our further investigations on AVP as a candidate gene for HPA dysregulation and the associated phenotype in the HAB rat line.

3.2.6 *In vivo* transcription analysis

The above findings raised the question of whether the observed differences between HAB and LAB alleles could confer the differential transcriptional activities, evident in the previously described *in situ*-hybridisation studies (Wigger et al., 2004). This issue became of particular importance when considering that the oxytocin locus, located 10kb centromeric to the AVP locus, revealed additional SNPs. Previously published *in situ*-hybridisation analysis of AVP and oxytocin gene expression in the PVN of HAB and LAB animals evidenced clear differences only in case of the AVP gene, with AVP mRNA levels being about 2-fold higher expressed in HAB compared to LAB animals (figure 1B). In agreement, *in silico* analysis failed to evidence an eventual regulatory role for SNPs present in the oxytocin gene. The two closely linked AVP and oxytocin genes form part of a locus that is subject to precise differential cell-specific and physiological regulation, where the peptide products, both of which are expressed in hypothalamic neurones, function in the maintenance of distinct physiological systems, which in turn, respond to distinct regulatory cues. This was the rationale behind taking the oxytocin gene as a control in testing for AVP overexpression in the PVN; we postulated that only SNPs in the AVP gene fulfil a regulatory role in conferring higher gene expression, in contrast to the non-differentially regulated oxytocin gene.

Results

To obtain further experimental evidence for this concept we aimed to study the transcriptional activity of HAB and LAB alleles *in vivo*. We queried whether AVP overexpression in the PVN may be due to regulation in *cis*, caused by the polymorphisms in the regulatory region of the AVP gene or, alternatively, due to regulation in *trans* resulting from different cellular environments in the PVN of the HAB and LAB respectively (figure 21A).

To discern between these possibilities we devised a strategy that envisaged both promoter alleles within the same cellular environment, allowing for the standardisation of variations, in both, non-cell autonomous, i.e. synaptic input, and cell autonomous, i.e. cellular composition, traits between the HAB and LAB line animals. This is the case for a heterozygote animal derived from crossing homozygous HAB and LAB lines. As schematically shown in figure 21B, the representation of polymorphisms transcribed by the coding part of the gene is a result of the strength of the respective promoter allele, which in turn is critically dependent on the presence of regulatory polymorphisms in the promoter. Therefore, by extracting RNA from the PVN of a heterozygote animal and cloning the reverse-transcribed specific cDNA it is possible to determine the frequency of plasmid clones containing either transcribed polymorphism.

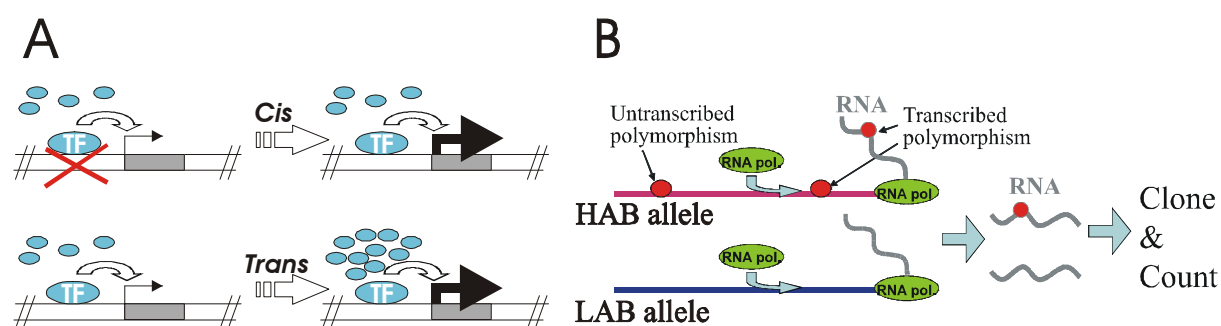


Figure 21. *In vivo* transcription analysis outline. (A) Scheme of *cis* and *trans* gene regulation. *Cis*-regulation refers to the promoter element working *in cis*, independent of cellular composition, to control expression levels. *Trans* regulation, alternatively, describes the process of where a promoter is entirely controlled by activities of cellular transcription factors (TF) independent of any sequence differences in the promoter of the gene in question. Therefore, a similar increase in gene expression might be caused, for instance, by either a stronger binding of TF to the promoter, or a higher level and/or higher activity of intercellular TF. (B) Scheme of the allele-specific transcription method. A heterozygote animal contains a promoter allele from both the HAB and LAB lines expressed in the same PVN neurons. A transcribed polymorphism localised on the same allele as a putative regulatory polymorphism in the promoter, can be used to track the promoter allele from which the mRNA was transcribed. RNA extracted from the PVN is used in RT-PCR and subcloning. Sequencing of the resulting products yields a precise measure of the efficiency by which either allele was transcribed *in vivo*.

This method allows one to track precisely which RNA species is more prevalent *in vivo* and, consequently, which promoter is more transcriptionally active.

Results

The PVN of two male F1 heterozygote rats were used for AVP and oxytocin studies and a further two female heterozygotes were used for AVP expression. In addition, the SON of four more heterozygotes were included for AVP expression as a second control as *in situ*-hybridisation and immunohistochemistry data suggest that AVP overexpression does not occur in this population of neurons. Over one hundred, randomly picked, plasmid clones harbouring the respective cDNA from each animal were sequenced to determine the allelic origin (figure 22A). The frequencies of the allelic cDNAs are included in figure 22B.

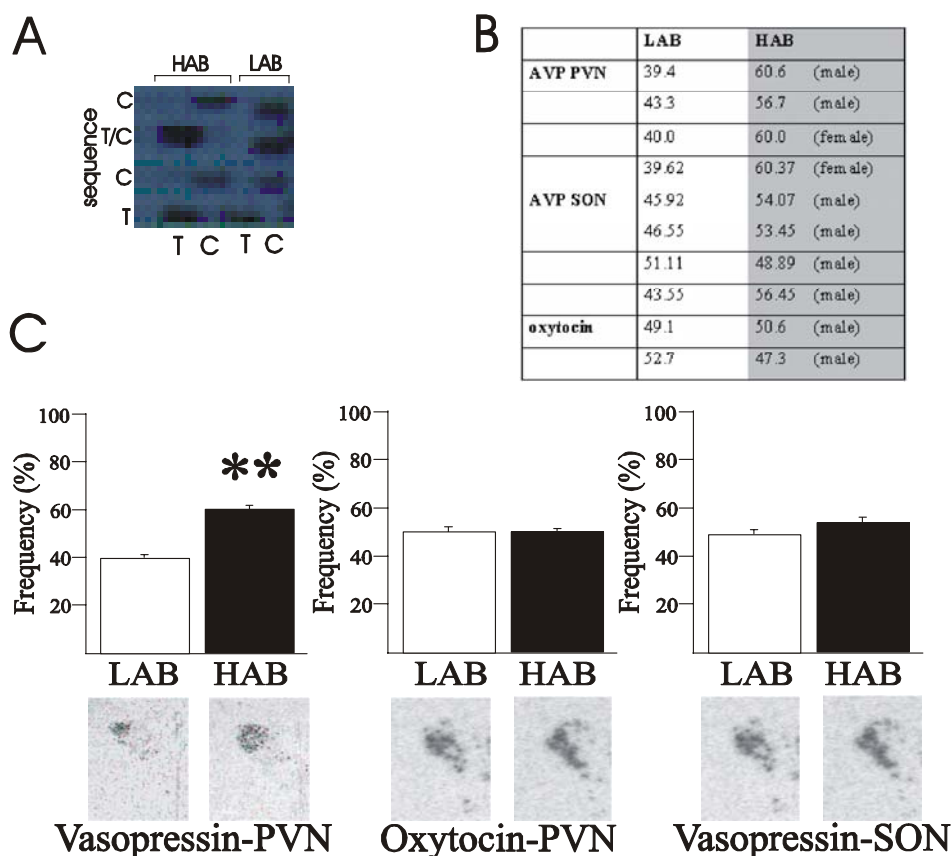


Figure 22. *In vivo* transcription analysis of AVP and oxytocin. (A) Autoradiogram of allele-specific transcript sequence demonstrating the CT-tracking. (B) Table of results from the *in vivo* expression analysis for AVP and oxytocin. (C) Allelic transcription rate for AVP and oxytocin in the PVN and SON. Values are given in percentage of 100 clones sequenced. *In situ*-hybridisation data of the AVP and oxytocin mRNA are also included. **, Significantly different ($p < 0.005$).

The allelic transcription rate for AVP in the PVN in each experiment evidenced a 60:40 ratio in favour of the HAB allele. When the results were combined in a Student's *t*-test a significantly ($p < 0.005$) distinct difference between the two lines was obtained with the HAB AVP promoter revealing a 50% increase in activity over the LAB promoter allele (figure 22C). Included in figure 22 are the *in situ*-hybridisation data from the HAB and LAB PVN tissues further demonstrating this higher level of AVP mRNA in the HAB animal, which correlates

Results

well with the higher activity of the AVP promoter. In contrast, the allele-specific transcription rate for oxytocin in the PVN revealed a 50-50% ratio, in agreement with the *in situ*-hybridisation data demonstrating a lack of difference between the HAB and LAB lines. Furthermore, no significant differences between the LAB and HAB alleles resulted from the SON studies confirming the previously published finding of AVP overexpression being specific only to the PVN and not the SON.

Concluding, the differences in the expression of AVP *in vivo* are, largely, due to differences in the *cis*-regulation of the AVP promoter allele, which further prompted us to study exactly which SNP(s) could be key to this differential expression.

3.2.7 Transcription factor element analysis

Having established that the HAB-specific allele confers higher transcriptional activity *in vivo* we further asked whether any of the SNPs in the promoter region exerts a regulatory role underlying the enhanced expression of AVP mRNA and secretion (Keck et al., 2002). We addressed this issue by first analysing each SNP in order to identify those which were embedded in putative DNA binding sites by scanning transcription factor databases (refer to section 2.2.6). We were particularly interested in *cis*-regulatory sequences important to expression, such as protein binding sites. Secondly, we asked whether the nucleotide differences between the HAB and LAB allele might affect the function of such DNA binding sites, altering the binding or activity of candidate proteins. Thirdly, we correlated these findings with a detailed survey of the literature regarding the expression of regulatory factors in the PVN. Questioning the relevance of any candidate protein to AVP expression *in vivo*, it is obviously imperative that the protein is expressed in the same cells as AVP. Based on these criteria, the particular SNPs highlighted in table 1 appeared to be of potential interest.

Table 1. SNPs embedded in putative consensus DNA-binding sites. Additionally, only those DNA binding sites are listed where the respective transcription factor (TF) is known to be expressed in the PVN.

SNP	AVP sequence	TF	Element	Expression	Reference
A/G -1276	gtccttattAggaagagg	YY1	CCWTNTTNNNW	Brain	Shrivastava and Calame, 1994
		CBF-A	CC(A/T)6GG	PVN	Treisman, 1987
A/C -596,	ccccAtgaCgccagcca	CREB,	TGACGM YMR	Ubiquitous	Angel et al., 1987
C/T -592		CREM,		Ubiquitous	Masquillier and Sassone-Corsi, 1992
		ATF-2		Ubiquitous	Hai and Curran, 1991

Of further consideration in evaluating the possible importance of any candidate regulatory protein was the relevance of the prospective transcription factor in regulation of the HPA-axis

and behaviour. For this, literature searches were used to evaluate if a candidate transcription factor regulates genes involved in anxiety and if the transcription factor, or gene, responds to changes in neurotransmission or drug treatment.

3.2.8 C(-592)T and cAMP responsive element

The polymorphism involving the transition of a C to a T, 590bp upstream of the AVP start codon, located in an imperfect cAMP responsive element (CRE) site (Angel et al., 1987; Masquilier and Sassone-Corsi, 1992) (table 2). This sequence, though not conforming at one position (position 6) to the palindromic structure usually found in such elements, might further be disrupted by the HAB sequence polymorphism at position 4 adjacent to the symmetry axis.

Table 2. Comparison of the consensus cAMP responsive element (CRE) with the LAB and HAB SNP 590bp upstream of the start codon of the AVP gene. The CRE comprises two palindromic half sites of the TGAC sequence. The LAB allele contains one mismatch to this consensus, whilst the HAB allele differs at a further nucleotide.

Nucleotide position	1234 5678
consensus seq.	TGAC GTCA
LAB seq.	ccaTGAC-GCCAgcc
HAB seq.	cccTGAT-GCCAgcc

With respect to the putative CRE, present in the LAB animal, our *in vitro* studies failed to evidence any difference in basal or in cAMP-dependent AVP promoter activity related to this SNP (refer to section 3.2.11.1). This finding was not unexpected since the AVP promoter contains at least two additional CREs, at positions -220bp and -116bp (Iwasaki et al., 1997), which suggests that this putative distal CRE site does not contribute to CRE-dependent expression of the AVP promoter. In further support of this view a recent genome-wide survey suggested that functional CREs preferentially locate more proximal to the transcriptional initiation site (Conkright et al., 2003).

3.2.9 A(-1276)G and YY1

The A to a G transition 1276bp upstream from the AVP start codon is predicted to disrupt a CArG element in the HAB promoter (figure 23A). This theory was supported by the view of Richard Treisman (London), the leading expert in the field of CArG elements, who suggested that such a change in the HAB would effect DNA binding of SRF by 5-10 fold (personal communication).

Results

The CArG element is characterised by the sequence of two Cs followed by a motif of six Ts or As and two Gs i.e. C, A repeat G (Minty and Kedes, 1986) (figure 23B). This *cis*- regulatory element, also known as a serum response element (SRE), is bound by serum response factor (SRF) (Treisman, 1987) and CArG binding factor A (CBF-A) (Kamada and Miwa, 1992). The consensus site for YY1 (Shrivastava and Calame, 1994) also matches the

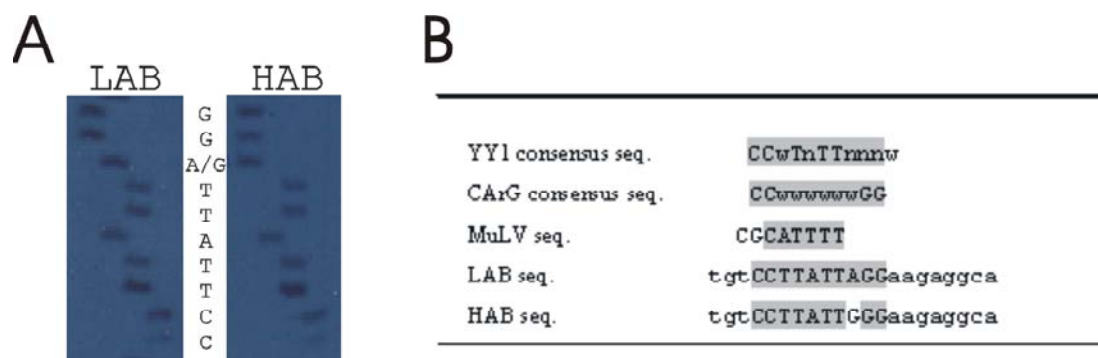


Figure 23. Nucleotide sequence of LAB and HAB CArG boxes in the AVP promoter at the A(-1276)G polymorphism. (A) Sequence of the SNP located 1276bp from the start codon consisting of an adenine ‘A’ in the LAB sequence substituted for a guanine ‘G’ in the HAB. (B) Table demonstrating comparison of the YY1 consensus sequence with the YY1 binding site in the MuLV promoter, the LAB sequence and the HAB sequence at the A(-1276)G polymorphism. W = A or T.

sequence for the LAB allele, and disruption of the usually A/T rich sequence by the substitution of a G in the HAB allele could effect YY1 binding, a scenario found in the YY1 consensus polyA tract of the motor neuron gene (SMN1) (Martin et al., 2002). However, opinion on the authenticity of this sequence as a YY1 element varied among experts in the field of YY1 research; Dr. Ed Seto (Tampa) was confident that this sequence was not a YY1 site, whilst Dr. Wayne Vedeckis (New Orleans) and Dr. Amy Lee (Los Angeles) both suggested that it was possible, and certainly worth testing with an electrophoretic mobility shift assay (EMSA) (personal communications). Moreover, other molecular biology groups specialising on the AVP promoter, namely the group of Dr. Judy Coulson (Liverpool), were also working on YY1 as a TF in AVP expression (personal communication). Furthermore, YY1 has been extensively reported to bind to CArG elements competing with other transcription factors to mediate repression (Ellis et al., 2002;Galvagni et al., 1998;Itoh et al., 2001;L'Honore et al., 2003;Martin et al., 1997;Vincent et al., 1993).

3.2.9.1 EMSA experiments

YY1, a 414aa protein with a molecular weight of 44kDa, is a member of the GLI-Krüppel family containing four of the C2H2 type zinc finger domains (figure 24A) involved in

Results

repression and activation of DNA elements (Hariharan et al., 1991). According to its ambiguous transcriptional activities, which are influenced not only by the nature of the DNA element but also by the cellular background, the name ying-yang, i.e. YY, has been coined. YY1 shows an expression pattern involving a wide variety of tissues including the hypothalamus (Hurd et al., 1999). YY1 interacts and competes with a number of transcription factors, which further modulate repressing and activating activities in a wide variety of genes. Previous reported YY1 binding site disruptions have been described for spinal musculature atrophy at a polyA sequence in the SMN1 promoter (Martin et al., 2002), and in cystic fibrosis where the CFTR promoter polymorphism T(-102T)A leads to differential expression disrupting a YY1 site at a CA_nG box (Romey et al., 2000).

Due to the uncertainty of whether this sequence might serve as a binding site for YY1, electrophoretic mobility shift assay (EMSA) experiments were conducted using nuclear extracts from Saos-2 cells transfected with the YY1 expression vector pCMV-YY1, and comparing the binding of the YY1 protein to the AVP promoter element with a known YY1 binding site (figure 24B) derived from the Moloney murine leukemia virus (MuLV) gene. The long terminal repeat of MuLV gene contains the upstream conserved region (UCR), CGCCATTTT, which has been well documented to bind to YY1 mediating negative regulation (Flanagan et al., 1992).

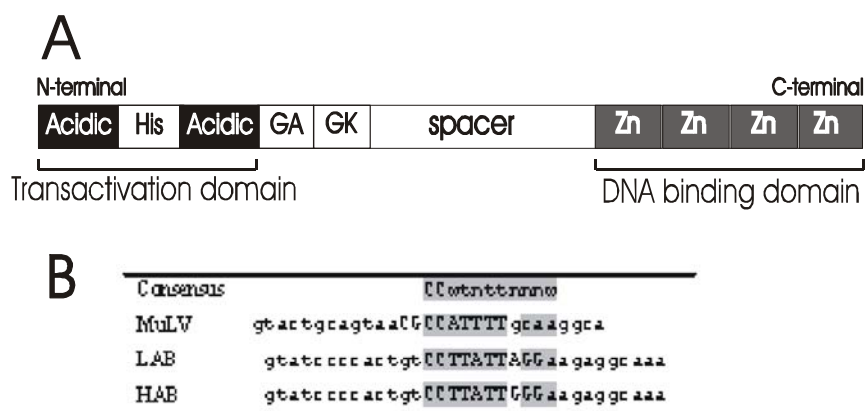


Figure 24. YY1 protein and binding element. (A) Schematic structure of the YY1 protein. The transactivation domain is contained in the acidic N-terminus whilst the DNA-binding domain maps to the C-terminal zinc-fingers. H; histidine, G; glycine, K; lysine, Zn; zinc-fingers. (B) Sequence alignments of the YY1 consensus sequence with the YY1 binding site in the MuLV promoter, the LAB sequence and the HAB sequence at the -1276bp polymorphism. W = A or T.

The results of the EMSA experiments in figure 25 substantiates previous evidence for YY1 binding, as expected, to the MuLV element with high specificity. This further confirms that the mouse YY1 protein, when produced in human osteosarcoma cells, retains the ability

Results

to bind its consensus DNA. The mouse and human YY1 proteins are 98.8% homologous (Hariharan et al., 1991). The specificity of the protein/DNA structure was further confirmed in an antibody shift assay, where the protein/DNA complex was retarded ('shifted') during gel electrophoresis upon addition of YY1 antibody (figure 25A). The YY1 antibody, though raised against full length protein of human origin is also specific for mouse and rat (refer to section 2.1.5.1). Moreover, nuclear extracts from mock-transfected Saos-2 cells failed to form a complex with this YY1 site further attaining to the authenticity of the observed complexes (data not shown).

The ability of the putative DNA element in the AVP promoter to function as a YY1 binding site was then tested. Equal amounts of HAB, LAB and MuLV oligonucleotides were mixed with equal volumes of YY1 protein in order to determine the specificity of the AVP elements by comparing these AVP elements to a highly specific YY1 binding site. As evident in figure 25B, YY1 from non-transfected nuclear extracts of HeLa, Saos-2 and 3T3 cells binds the MuLV sequence up to 20-fold more than either the LAB or HAB elements.

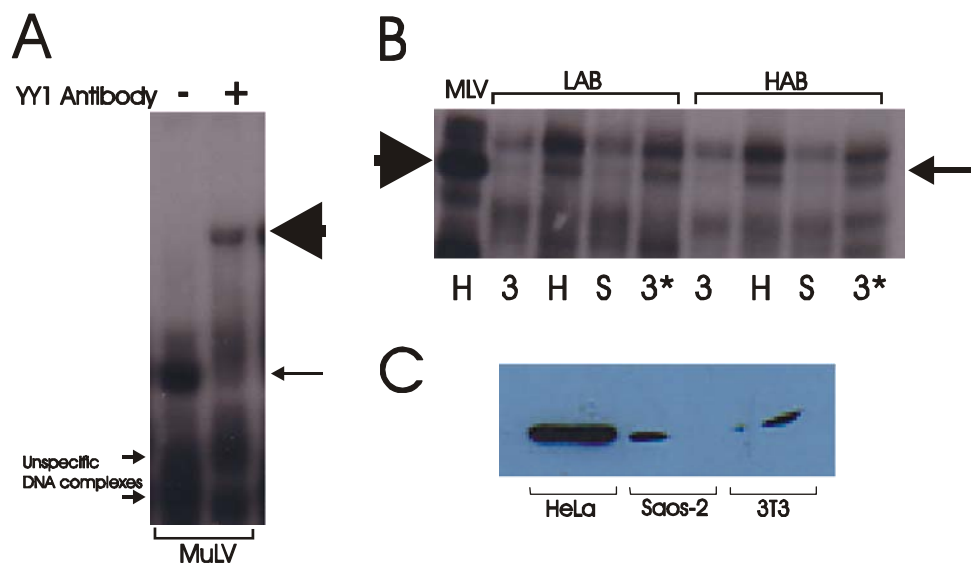


Figure 25. EMSA experiments using YY1. (A) Consensus MuLV binding site oligonucleotide incubated with 1 μ g nuclear extracts of YY1 transfected Saos-2 cells. In the absence of antibody YY1 binds as one single, high intensity, band (thin arrow). Addition of the YY1 antibody causes an almost complete supershift of this band (thick arrow), attesting to specificity of this band as YY1 bound DNA. **(B)** EMSA experiment comparing the MuLV element with the HAB and LAB AVP elements for binding of YY1. 5 μ g nuclear extracts of HeLa (H) cells, Saos-2 (S) cells and 3T3 (3) cells with (*), or without transfected YY1 expression vector, were incubated with the elements. A protein/DNA band clearly forms in the MuLV probe (thick arrow). Furthermore, YY1 can be seen to bind with similar efficiency to the LAB and HAB elements in the transfected cells, but at 20-fold less efficiency (thin arrow). **(C)** Western blot of 5 μ g of nuclear extracts from Saos-2, HeLa and 3T3 cells incubated with YY1 antibody. An abundance of native YY1 protein is evident in HeLa cells and, to a lesser degree, in both the Saos-2 and 3T3 cells. Results of all gels are representative of at least three independent experiments.

This suggests that the AVP element functions as a very weak YY1 binding site which does not, however, discriminate between HAB- and LAB-derived oligonucleotide probes.

3.2.9.2 YY1 and AVP promoter expression

Having established that YY1 weakly binds to the AVP promoter, it remained to be clarified whether YY1 regulates AVP expression *in vitro*, and if this might discriminate between the promoter alleles. Cotransfection experiments were conducted with either the HAB or LAB distal and proximal AVP promoter sequences cloned upstream of the firefly (*Photinus pyralis*) luciferase reporter gene and a β -galactosidase (β -gal) expression vector, used to standardise luciferase rates on transfection efficiency.

These experiments evidenced no significant expression differences when comparing the distal and proximal AVP promoter alleles (which are presented later in figure 33). However, it remained to be determined if these cell lines actually contain native YY1 protein. To test this, Western blots of non-transfected nuclear extracts were incubated with a YY1 antibody, and from the results it became evident that Saos-2 cells, HeLa cells and 3T3 cells all contain YY1 protein (figure 25C). The highest concentrations of YY1 were found in HeLa cells followed by Saos-2 and 3T3 cells, which contained a quarter of the amount. Therefore, the lack of line-specific luciferase expression differences in the promoter constructs transfected in the Saos-2 cells suggests that YY1 is actually not differentially regulating the LAB and HAB promoters.

However, the regulatory role of YY1 in AVP expression still needed to be determined because in addition to the weak polymorphic YY1 element at -1276bp, two further YY1 consensus binding sites exist in the AVP promoter, present only in the distal construct and absent from the proximal one (figure 26A). Therefore, the HAB and LAB distal and proximal promoter constructs were cotransfected with a YY1 expression vector, with the idea that differences in AVP-luciferase expression between the distal and proximal promoter constructs reflects the presence or absence of these YY1 sites. The expression experiments revealed that YY1 negatively regulated the AVP promoter (figure 26B). A gradual dose-dependant decrease in expression upon increased cotransfection of the YY1 expression vector occurred at 0.1 μ g, producing a 20% decrease of expression in both the distal and proximal promoter constructs. The pGL2 vector alone containing no AVP promoter construct was not repressed by increasing concentrations of YY1 (data not shown). However, it became evident that there was no significant difference, between the proximal and the distal promoter constructs, strongly suggesting that the predicted YY1 elements are not functional.

Results

Possible regulatory differences between the LAB and HAB AVP promoters by YY1 was still further explored because YY1 appeared to slightly repress the LAB constructs when compared with the HAB. Therefore, we conducted triple transfection experiments with the pRK8-PKAc-rat expression vector containing the catalytic subunit of cAMP-dependent protein kinase A (PKA) (Spengler et al., 1993) in addition to the YY1 expression and AVP reporter vectors. Protein kinases regulate a myriad genes involved in cellular processes during growth and development and form an integral part of the machinery activated in response to stress. The idea of the triple transfection was of two-fold; firstly to achieve a higher activated expression status of the promoter, in which a repressing factor might have a greater effect and secondly, to explore previous studies suggesting that YY1 can be activated by phosphorylation (Becker et al., 1994; Patten et al., 2000), indeed, the protein appears to contain a number of putative phosphorylation sites when analysed with phosphorylation site predicting programs (refer to section 2.2.6). Interestingly, when YY1 and PKA were cotransfected together with the promoter constructs of the AVP-luciferase vector,

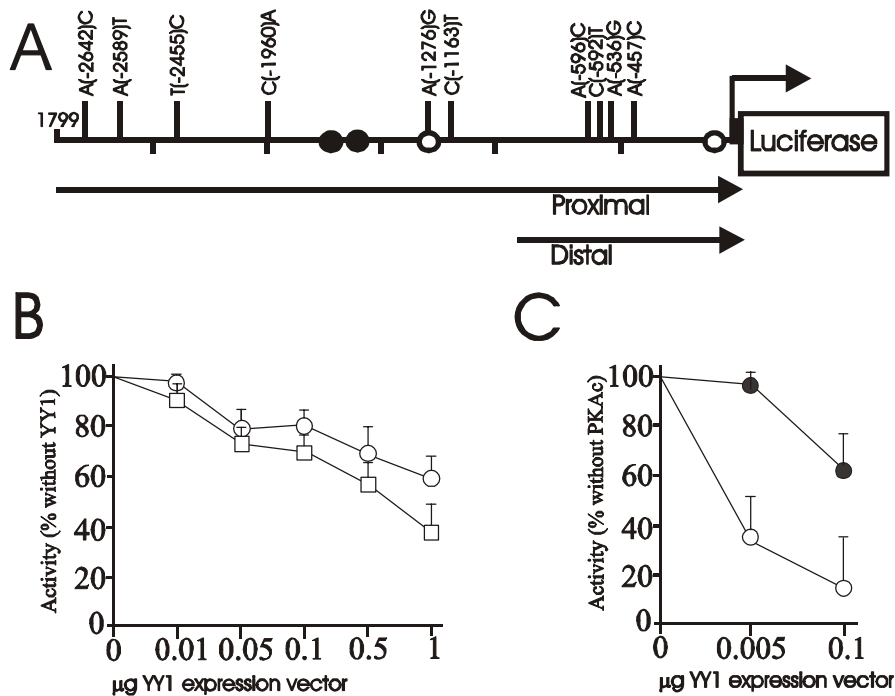


Figure 26. Activity of distal and proximal promoter AVP promoter constructs. (A) Schematic diagram demonstrating the rat AVP constructs used in the expression analysis. The distal promoter construct contains all 10 polymorphisms in the promoter, while the proximal construct contains only the four closest polymorphisms to the start codon (A/C -594, C/T -590, A/G -534, A/C -455). The filled and empty circles represent consensus and the weak polymorphic consensus YY1 binding sites respectively. (B) Luciferase expression of distal (empty circles) and proximal promoter (empty squares) AVP-luciferase constructs in Saos-2 cells cotransfected with YY1 in a dose dependent manner. (C) Gene expression of the distal and proximal LAB (empty circles) and HAB (filled circles) promoter AVP-luciferase vectors co-expressed with a fixed amount of 0.01mg PKA in Saos-2 cells cotransfected with YY1 in a dose dependent manner. Results of B and C are means of three independent experiments \pm SD.

YY1 caused a more pronounced decrease in expression in the distal construct than the proximal, with about a 75% reduction in expression (figure 26C). This, therefore, suggests that YY1 might preferentially repress induced AVP promoter activity – such as under PKA – due to binding to the distal consensus YY1 elements.

3.2.10 A(-1276)G and CArG box binding factor A (CBF-A)

CArG box binding factor A (CBF-A) is a ubiquitously expressed transcription factor specific found in the mouse and the rat. The CBF-A gene encodes a 1,573 nucleotide mRNA giving rise to a 285aa protein which is alternatively spliced at exon 7 resulting in a variant 47aa shorter (Dean et al., 2002). Both isoforms are found in the nucleus of cells whilst the spliced form further locates to the cytoplasm (Dean et al., 2002). CBF-A is also subject to posttranslational modifications leading to various phosphorylated forms including two phosphorylation sites at amino acid positions 90-97 and 259-274 according to matrix-assisted laser desorption/ionization time-of-flight mass spectrometry (MALDI-TOF-MS) predictions. (Umar et al., 2003). The close homologues of CBF-A in the human, AUF1 (Dean et al., 2002) and hnRNPA/B (Cvekl et al., 1995), are subject to many forms of posttranslational modification involving sumoylation (Vassileva and Matunis, 2004) - the conserved sumoylation sequence is found in CBF-A at lysine 207 within the consensus sumoylation target sequence ØKXE, Ø being a hydrophobic residue and X any residue (Verger et al., 2003) - methylation (Wada et al., 2002), and ubiquitination (Laroia and Schneider, 2002). Indeed, CBF-A closely resembles members of the hnRNA binding proteins (hnRNP) and ssDNA binding proteins (ssDBP) families containing the highly homologous two imperfect repeats located in the central portion of the protein which form the RNA and DNA binding domains (RBD) (Weisman-Shomer et al., 2002) (figure 27A). The hydrophilic carboxy-terminus of the protein shares similarities to sequences involved in nuclear cytoplasmic shuttling of JKTBP (Kawamura et al., 2002), which perhaps relates to the dual role of CBF-A as both a transcription factor and mRNA binding protein.

Owing to the co-expression of CBF-A with AVP in the PVN (see below), and its differential expression *in vivo* and *in vitro* under drug administration and its importance in controlling genes involved in behaviour (see *Discussion*), we carried out further experiments to determine, in detail, if CBF-A binds to the CArG box, and if CBF-A differentiates between the CArG boxes from HAB and LAB alleles.

3.2.10.1 CBF-A binds to the AVP CArG element

Preliminary EMSA studies were performed with nuclear extracts of cells transfected with the CBF-A expression vector to determine if binding of CBF-A to the CArG element occurred. Results in figure 27B clearly evidenced that CBF-A bound to the CArG elements in a dose-dependent manner. Although whole cell extracts showed additional bands, as seen in the gel (figure 27B), these did not change in their intensities upon CBF-A cotransfection. Importantly, the antibody shift assays, in figures 27E+F, using recombinant CBF-A attests to the specificity of CArG box binding.

The EMSA experiment with nuclear extracts lacked the resolution to measure precisely CBF-A binding between LAB and HAB elements, due the presence of unrelated protein-DNA bands in the gel. Therefore, purified recombinant CBF-A was tested in EMSA. For this a mouse full-length CBF-A cDNA was expressed in *E.coli* as a GST-fusion protein. CBF-A was purified using glutathione-sepharose beads (see *Methods*) and judged to be 95% pure from Coomassie blue stained gels (figure 27C). The specificity of the recombinant protein was further verified using a GST antibody in immunoblots (figure 27D). The single band visualised demonstrates that intact full length CBF-A-GST fusion protein was purified.

Following incubation of GST-CBF-A with the CArG element two distinct protein-DNA complexes were observed under non-denaturing polyacrylamide gel electrophoresis (figure 27E). This was interesting as only one band associating to CBF-A was evident in the nuclear extract. Addition of increasing amounts of the GST antibody to the incubation reaction caused a supershift of both the major low mobility and the minor higher mobility complexes. In contrast, preincubation with control IgG or BSA failed to elicit a supershift attesting to the specificity of the observed DNA-protein complexes (data not shown). The formation of two complexes with GST-CBF-A fusion protein, a stronger with lower mobility and a weaker with somewhat higher mobility, has previously been reported and suggested to be a function of the GST part of the recombinant GST-CBF-A fusion protein (Bemark et al., 1998). This would explain the lack of similar bands in nuclear extract obtained from Saos-2 cells transfected with non-tagged CBF-A. In support of this new His-CBF-A and FLAG-CBF-A fusion proteins bound the CArG element as a single major DNA-protein complex, which was completely shifted by the respective antibodies, whereas this was not the case for additional weaker higher and lower mobility complexes, which appear thus unrelated to CBF-A.

Overall, the EMSA results demonstrate that CBF-A, produced in either eukaryote or prokaryote cells, binds with the same specificity to the AVP CArG element. Since eventual

Results

posttranscriptional modifications in eukaryotic systems appeared of no importance to CBF-A DNA-binding *in vitro*, bacterially produced CBF-A protein was used in the following studies.

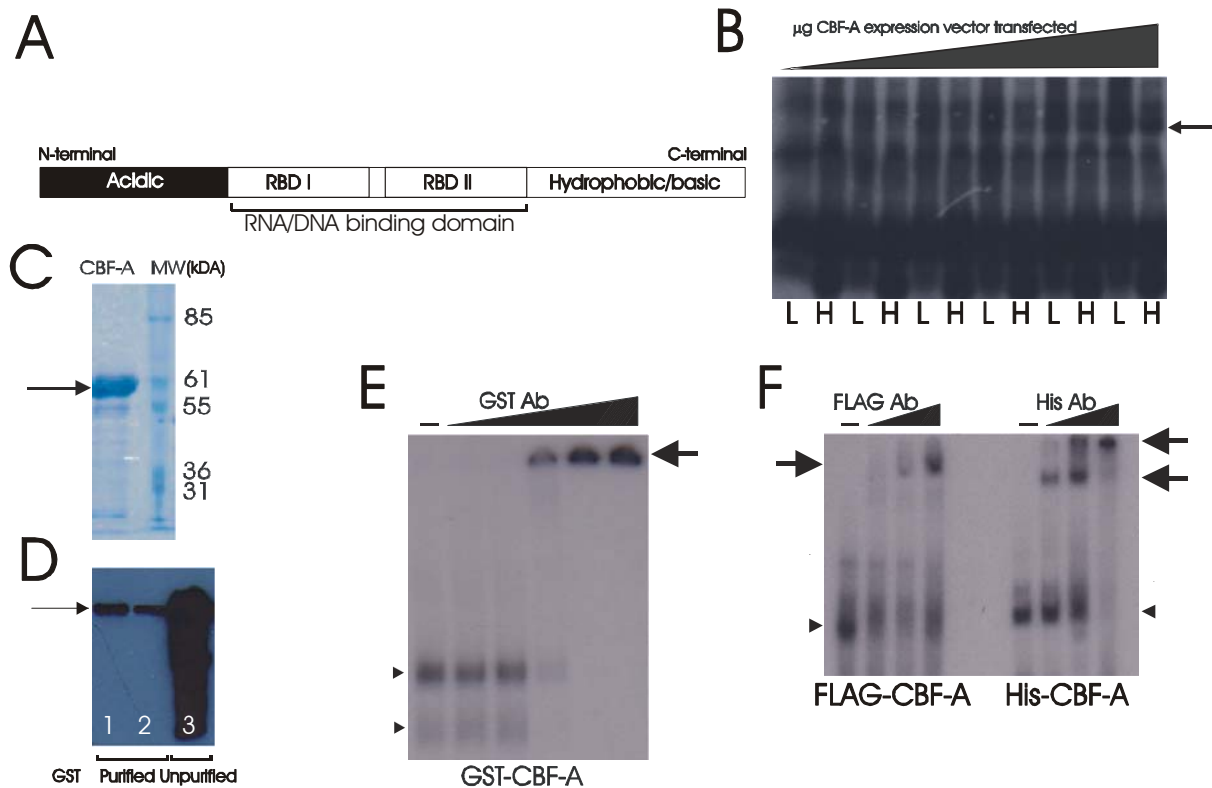


Figure 27. CBF-A binds to the AVP CARG element. (A) Schematic diagram of the structure of CBF-A. The two inverted repeats between 75 and 234aa form the RNA and DNA binding domain (RBD). (B) EMSA using nuclear extracts of Saos-2 cells transfected with increasing amounts of the PRK7-CBF-A expression vector and incubated with the double stranded CARG element from the LAB (L) and HAB (H) lines. A number of unspecific bands are evident, however, increasing concentrations of CBF-A result in the appearance of a specific band (arrow), which binds to the CARG element. Furthermore, the specific band appears to bind to the LAB allele with higher specificity. (C) Purified GST-CBF-A protein (arrow) migrates at a weight of about 60kDa and appears to be at least 95% pure, as judged by Coomassie blue staining. (D) An immunoblot using a GST antibody attests to the specificity and purification of the GST tag and antibody when comparing GST purified protein (lanes 1 and 2) with unpurified *E.coli* protein extract. (E) Recombinant GST-CBF-A binds specifically to the CARG element from the AVP promoter of the LAB line forming two complexes in an EMSA. The major low mobility and minor higher mobility complexes (thin arrows) are both supershifted with increasing concentrations of GST antibody (thick arrow). (F) Recombinant FLAG-CBF-A and His-CBF-A bind to the CARG element as a single major complex (thin arrow) and each is supershifted with increasing concentrations of FLAG and His antibody (thick arrows). Results of B-F are representative of at least three independent experiments.

The CBF-A antibody was tested for its affinity to bind the CBF-A fusion proteins, firstly as a control for the validity of the CBF-A part of the fusion protein, and secondly to test for the specificity of the CBF-A-specific antibody for further use in Western blots and immunohistochemistry. As evident in figure 28A, the antibody was unable to completely shift either the GST or the His tagged protein in the same way that the GST, His or CBF-A antibodies did.

Results

The inability of the antibody to elicit a complete shift of the recombinant-protein/DNA complexes might be caused by the N-terminus being inaccessible to the N-terminal-specific N-CBF-A antibody, which has been previously reported (Bemark et al., 1998). However, this low specificity might also be the result of the tagged domain of the fusion proteins interfering with the binding site of the antibody to the CBF-A protein. The third possibility might be that the antibody is simply inefficient, and to address this question further experiments were performed using an immunoblot with *E.coli* produced GST- and His-labelled CBF-A incubated with the CBF-A antibody. This procedure allows more efficient binding of the antibody to the membrane-bound protein, and subsequently, a more direct measure to test the relative efficiencies of each of the antibodies. The result in figure 28B demonstrate that N-CBF-A clearly recognises the recombinant proteins, binding to both GST and His-CBF-A.

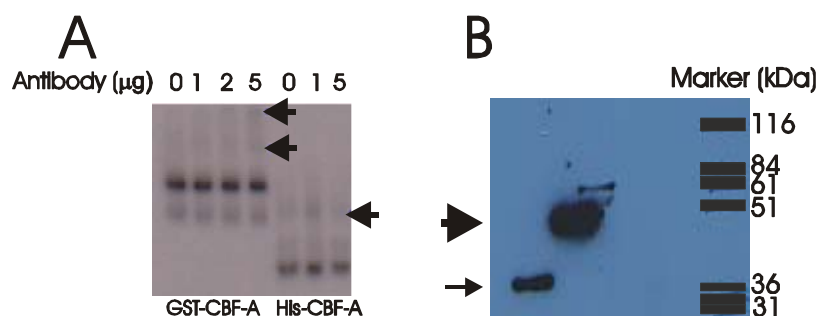


Figure 28. (A) Antibody shift analysis of recombinant GST- and His-CBF-A using increasing amounts of N-CBF-A antibody. The N-CBF-A antibody causes some shift of the GST-CBF-A resulting in two shifted bands (arrows) as well as a slight shift of His-CBF-A. (B) Immunoblot of GST- (thick arrow) and His-CBF-A protein (thin arrow) with the N-CBF-A antibody. The two gels are representative of at least three independent experiments.

3.2.10.2 CBF-A binds differentially to LAB and HAB polymorphisms

We next investigated whether CBF-A discriminates between binding to the HAB and LAB CA_rG elements in EMSA. Interestingly we observed, for different concentrations of CBF-A, a strikingly stronger binding of CBF-A to the CA_rG box derived from the LAB allele when compared to the HAB allele (figure 29A). We obtained similar results in three independent experiments making differences in the probe preparations – such as separation of labelled from unlabelled probe – an unlikely source for this differential CBF-A binding.

To substantiate our findings we carried out a competition assay in which identical concentrations of labelled LAB oligonucleotide were incubated with increasing concentrations of either unlabelled LAB or HAB oligonucleotide. In this experiment the LAB oligonucleotide was clearly more efficient than the HAB oligonucleotide to compete for

Results

CBF-A binding as evidenced by the rapidly decreasing radioactive DNA-protein complex (figure 29B).

In conclusion, CBF-A binds to the CARG element of the AVP promoter with high affinity and specificity and, importantly, the SNP A(-1276)G in the AVP promoter greatly reduces the binding of CBF-A by a degree of 4-5 fold.

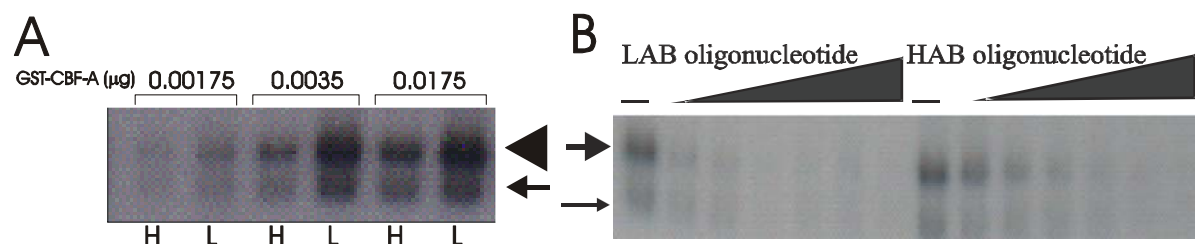


Figure 29. EMSA of CBF-A with HAB and LAB CARG boxes. (A) Increasing concentrations of GST-CBF-A were tested with double stranded CARG elements derived from either the HAB (H) or LAB (L) alleles. CBF-A clearly has a higher affinity for the LAB CARG box than for the HAB CARG sequence. (B) A fixed amount of labelled LAB CARG box was competed with increasing concentrations of either unlabelled LAB or HAB CARG elements. The unlabelled LAB oligonucleotide competes more efficiently than the unlabelled HAB oligonucleotide for CBF-A binding demonstrating that the CARG element from the LAB animal binds CBF-A more efficiently. Gels are representative of three independent experiments.

3.2.10.3 CBF-A binds ssDNA of the CARG element

In the EMSA experiments so far we used double-stranded DNA (dsDNA) as the probe, however, CBF-A has also been reported to bind to single-stranded DNA (ssDNA) with an even higher affinity (Kamada and Miwa, 1992) which might be important to its function in RNA metabolism and additionally to its function in transcriptional regulation (see below). To address this topic, and to obtain further insight into the consequences of CBF-A binding to the CARG-box element of the AVP promoter, we competed the LAB probe with increasing concentrations of dsDNA self-oligonucleotide or, alternatively, with increasing concentrations of ssDNA sense or antisense self-oligonucleotide. As demonstrated in figure 30A, the ssDNA probes were clearly more efficient for CBF-A binding in this assay than the dsDNA probe. Of further interest was the finding that, CBF-A bound to the antisense probe with higher affinity than the sense probe, revealing a further level of specificity in the recognition of the CARG element. This finding was corroborated by an EMSA experiment in figure 30B where the antisense probe clearly shows a greater specificity for CBF-A than the sense strand.

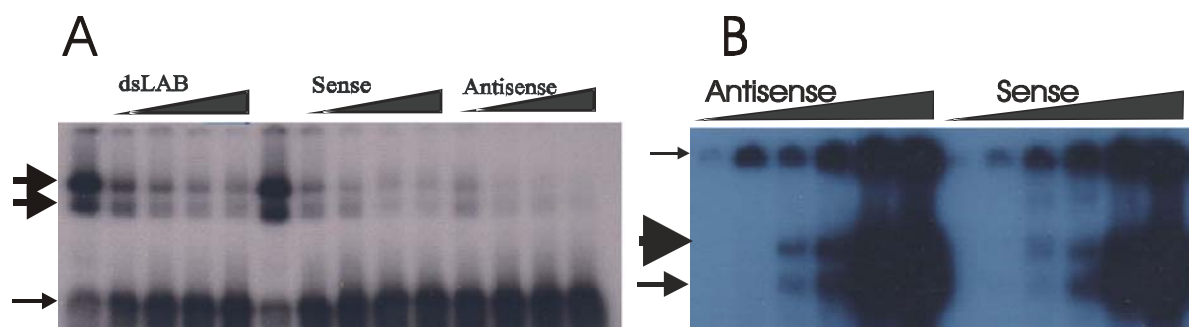


Figure 30. CBF-A binds to single stranded CARG element. (A) A fixed amount of labelled dsDNA LAB oligonucleotide is competed with increasing concentrations of unlabeled dsDNA of LAB CARG element (dsLAB), ssDNA of sense strand (sense) and ssDNA of the antisense strand (antisense) of the CARG element for GST-CBF-A binding. The ssDNA probes compete more efficiently for CBF-A DNA binding than the dsDNA element. Additionally, CBF-A DNA binding to the dsDNA CARG box is preferentially competed with the antisense ssDNA of the CARG element. Thick arrows denote probe bound by protein, and thin arrows free probe. (B) EMSA experiment using GST-CBF-A protein incubated with single stranded antisense and sense DNA of the LAB-specific CARG element. The ssDNA probes bind CBF-A forming a major high molecular weight band (thick arrow) and a minor band (medium arrow), similarly to the dsDNA probe. Thin arrow denotes protein trapped in wells of the gel. The results of A and B are representative of at least three independent experiments.

3.2.10.4 CBF-A causes local unwinding of dsDNA CARG element

In view of this high affinity of CBF-A for ssDNA, we examined further the possibility that CBF-A could induce or stabilize single-stranded regions within the AVP promoter CARG element. To test this hypothesis we devised an experiment utilising the specificity of S1 nuclease to preferentially digest ssDNA (figure 31A). CBF-A protein is firstly incubated with the dsDNA CARG element, after which S1 nuclease is added, which will cleave any ssDNA regions, induced by CBF-A binding, rapidly into mononucleotides. Therefore, in case CBF-A

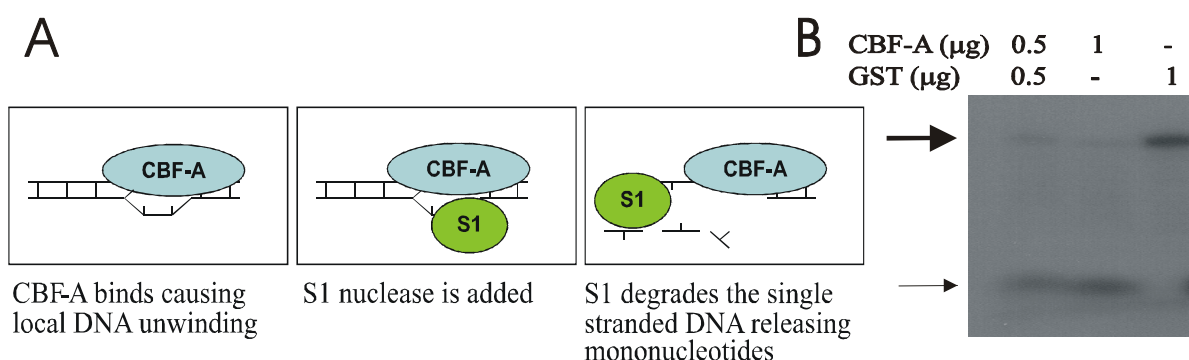


Figure 31. CBF-A causes DNA strand separation. (A) Scheme of the S1 nuclease assay for the detection of dsDNA melting. CBF-A binding to dsDNA is predicted to cause local strand separation and to confer increased sensitivity to S1 nuclease that cleaves the DNA into mononucleotides. (B) S1 nuclease assay for differing concentrations of CBF-A and GST with LAB CARG element. GST alone causes no cleavage of the dsDNA probe (thick arrow), whereas, increasing amounts of CBF-A cause dsDNA cleavage into mononucleotides (thin arrow). The results in B are representative of five independent experiments.

supports the formation of any ssDNA regions in the dsDNA CArG probe S1 nuclease cleavage will be enhanced, as evidenced by the appearance of mononucleotides at the expense of dsDNA. Different concentrations of CBF-A were supplemented with GST protein alone to keep total protein concentrations in each reaction constant. The results of the experiments in figure 26B clearly demonstrate an increase of S1 nuclease mediated degradation correlating with concentration of CBF-A and not GST. This data, therefore, suggests that CBF-A enhances melting of the dsDNA CArG box.

3.2.10.5 CBF-A RBD domains are important for unwinding

We further aimed to test to which extent this DNA melting is dependent on DNA binding of CBF-A by the RNA-Binding-Domains (RBD). For these experiments we used a series of CBF-A deletion constructs lacking either or both of the RBDs (figure 32A). Previous work has shown that the amino terminus and carboxy-terminal regions of the CBF-A protein have little or no effect on DNA binding, which in contrast critically depends to equal parts on both the central RBDs (Bemark et al., 1998).

The deletion constructs were expressed as GST-fusion proteins in *E.coli* and purified using glutathione-sepharose beads as previously described. All deletion constructs were judged to be, at least, 95% pure from Ponceau stained gels (figure 32B). To adjust the concentrations of the recombinant proteins, immunoblots were carried out with the GST-antibody (figure 32C).

EMSA experiments using similar adjusted amounts of the recombinant CBF-A deletion proteins support, in general, these findings in demonstrating that the presence of both of the RBD domains of CBF-A are crucial for the dsDNA binding. Specifically, however, our results reveal the second amino-terminal RBD of CBF-A appears to be of more importance in dsDNA binding (figure 32D). The deletion of the N-terminus results in a slight reduction in binding, and, moreover, the appearance of only one major band. The Δ RBD1 and Δ RBD2 proteins also produced only one band, migrating at the same molecular weight as the Δ N-terminus. This difference in the importance of the RBDs in DNA binding, in contrast to the previous work of Bemark (Bemark et al., 1998), might reflect the nature of the probes used as the previous study involved an A-T rich region (AATTTACTTC) of the SP6 promoter, in contrast to the CArG element (CCTTATTAGG) used here. The deletion proteins were further tested with ssDNA to gain more insight into the mechanism of DNA binding, if either the sense or antisense specificity is crucial for binding-specifically to the LAB CArG element than to the HAB, and if one of the RBDs might be of particular importance in sequence

Results

recognition of the ssDNA element. Therefore, EMSA experiments were conducted incubating the various CBF-A proteins with either the sense or antisense ssDNA elements from the LAB and HAB CARG elements. The results in figure 32E prove that the sequence of the LAB antisense CARG strand provides the highest specificity-binding site for full length CBF-A. Deletion of the N-terminus, although resulting in somewhat less binding, does not alter the specificity of the protein for the LAB antisense strand, in comparison to the deletion of RBD2 which results in a more variable binding between the four ssDNA sequences.

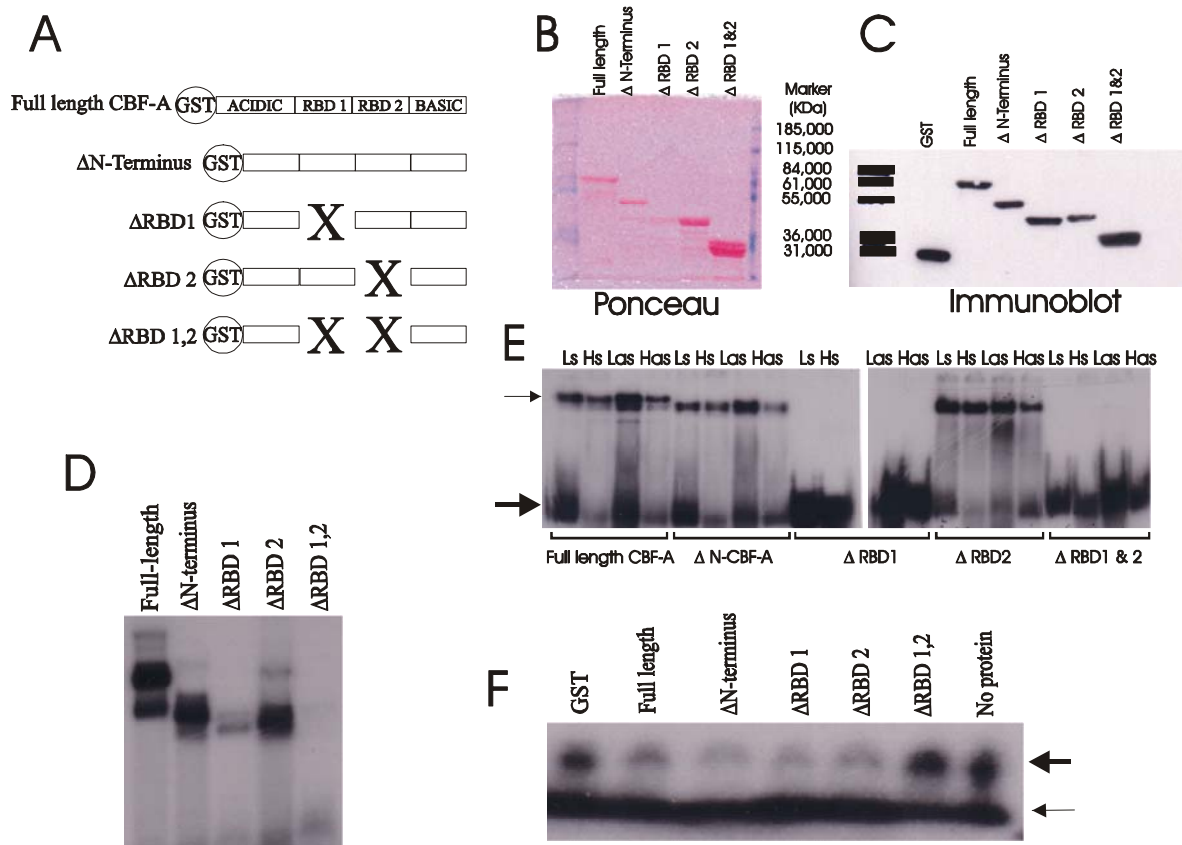


Figure 32. RNA binding domain (RBD) deletion mutants and CARG element binding. (A) Scheme of RNA binding domain (RBD) deletion mutants. The two RBDs, labelled RBD 1 and RBD 2, localize to the central part of CBF-A and are flanked by an acidic amino-terminal and a basic carboxy-terminal region. (B) A Ponceau stained gel of purified GST-CBF-A deletion constructs suggested the protein preparations to be of, at least, 95% purity. (C) An immunoblot verified the authenticity of the purified proteins concerning the size and reactivity with the GST antibody. GST protein alone migrates at a size of 25kDa, whilst the GST-CBF-A Δ 1 & 2 migrates at a slightly higher weight of 33kDa. The two proteins lacking either RBD 1 or 2 both run at 40kDa, while the Δ N-Terminus runs at 52kDa. The full length protein, as stated previously, migrates at a weight of 60kDa. (D) EMSA of RBD deletion mutants. The RBD motifs are crucial for dsDNA binding as evidenced by full-length CBF-A DNA binding compared to the Δ RBD 1,2 protein. Moreover the presence of the N-terminus RBD 1 is more important for DNA binding than the COOH-terminal RBD 2. (E) EMSA experiment comparing the HAB and LAB sense (Hs and Ls) and antisense ssDNA (Has and Las) for binding with the various CBF-A deletion constructs. The thick arrow indicates the free unlabelled probe while the thin arrow indicates the CBF-A/protein complex. (F) S1 nuclease assay of CBF-A RBD deletion mutants. The thick arrow indicates the dsDNA and the thin arrow denotes the degraded mononucleotides. The presence of either of the RBD motifs leads to S1 nuclease sensitivity. Moreover, the Δ RBD 1,2 protein which was unable to bind DNA conferred no such S1 nuclease mediated digestion. The autoradiograms of D-F are representative of at least three independent experiments.

The results of the S1 nuclease assay when conducted using the CBF-A deletion proteins, revealed that DNA binding strictly correlates with S1 nuclease sensitivity since the CBF-A protein containing a deletion of both RBDs is unable to enhance S1 mediated DNA digestion (figure 32F). The recombinant CBF-A proteins containing either of the RBD domains, however, both increased S1 nuclease sensitivity suggesting that despite reduced DNA-binding in the absence of the N-terminal RBD, the proteins were still able to efficiently promote S1 nuclease sensitivity.

3.2.11 Reporter assays

3.2.11.1 AVP promoter expression in cell culture transfection experiments

Reporter gene assays were used to delineate which regions of the AVP promoter were important for the differential expression seen in the allele-specific transcription *in vivo*, and if above differences in CBF-A binding translate into different transcriptional activities.

Reporter plasmids containing the proximal and distal AVP promoter sequences of the HAB and LAB rats were transfected into, the osteosarcoma cell line, Saos-2. Results were standardised against a cotransfected expression vector for β -galactosidase (β -gal). Firstly, it became evident after repeating this experiment a considerable number of times that the AVP gene promoters revealed no differences in expression between either alleles from the HAB and LAB lines (figure 33A). Secondly, this experiment confirmed that the construct containing the distal promoter exhibits a third of the activity of the proximal promoter. Therefore, the proximal promoter construct is considerably more active than the distal construct. This finding has been previously reported (Iwasaki et al., 1997), and suggests that the region lying between the constructs, 2.8kb-0.9kb upstream from the start codon, contains regulatory elements important for repression of the AVP gene.

The mouse neuronal cell line Neuro2a was transfected with the AVP promoter constructs, as described above. It was queried that a cell line more relevant to the rat AVP promoter, i.e. from a more closely related species, and consisting of neuronal cells, might contain specific factors which could highlight any differences between the polymorphic promoters. Again, however the cell lines produced no significant differences between the HAB and LAB sequences (figure 33B).

Finally, the AVP-expressing small cell lung cancer cell line (SCLC), Lu-165, was also transfected. It was argued that a cell line specifically expressing AVP might contain further factors, absent in the previous cell lines, important for the AVP-specific expression of this promoter construct, and these factors might finally highlight a differential expression effect

Results

between the LAB and HAB sequences. The Lu-165 cells, however, grew very slowly, and it became evident that a large number of cells needed to be transfected, which took many months to collect. Owing to the limiting factor of cell quantity, transfection efficiencies were low. In addition, the AVP promoter constructs revealed minimal levels of expression, on the borderline of detection (figure 33C), in contrast to the pGL2 vector, lacking the AVP promoter sequences, which showed a 4-fold increase of expression. Overall, no significant differences in expression levels arose between either the distal, proximal, HAB or LAB AVP promoter constructs in the Lu-165 cells.

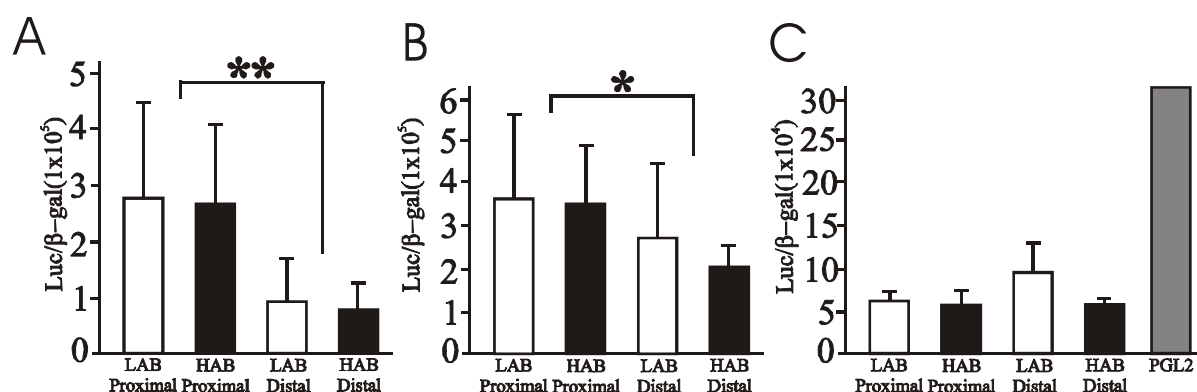


Figure 33. AVP promoter gene assays for HAB and LAB proximal and distal AVP promoter activity. (A) Saos-2 cells (B) Neuro2a cells (C) Lu-165 cells. ± SD. * p<0.05, ** p<0.005. All results were taken from three individual experiments.

3.2.11.2 PKA and AVP promoter expression

The previous luciferase expression experiments suggest that either the cells lines investigated lack the specific transcription factor important for enhanced AVP gene activity in HAB animals, which might be expressed only in the PVN, or that other factors in the cell lines, such as SRF in the Saos-2 and HeLa cells, might even mask the effect of the regulatory SNPs on AVP promoter expression under these experimental conditions.

Therefore, we considered that any possible differences between the HAB and LAB alleles might become unmasked under promoter activation. For this reason we co-expressed the proximal and distal LAB AVP promoter constructs with the pRK8-PKAc-rat expression vector. Results revealed, as expected and previously published (Iwasaki et al., 1997), that PKA induced activation of the AVP promoter dose-dependently (figure 34). It was further evident from these results that the distal promoter construct was more potently activated to give expression levels 2-3 fold higher than the proximal construct; the reverse as to what was seen in the non-stimulated transfections (figure 33A). This, therefore, suggests that a number

Results

of DNA elements activated by the PKA pathway, such as AP1, AP2, CREB etc. (for review see Tasken and Aandahl, 2004) locate to the promoter region between the distal and proximal constructs. However, when comparing the LAB and HAB constructs under PKA stimulation no significant differences emerged (data not shown).

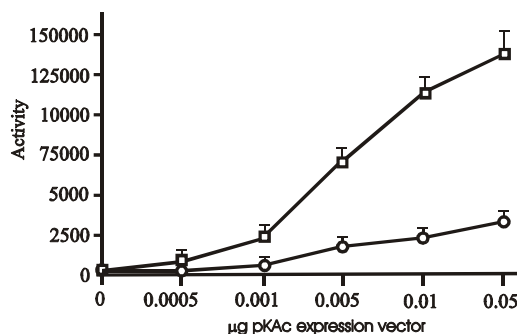


Figure 34. AVP promoter activity is activated by PKA. PKA-induced activation of LAB distal promoter construct in relation to the proximal promoter construct. Squares represent the distal promoter, circles the proximal. Values are expressed as the percentage increase of basal standardised luciferase values. Results are means of three independent experiments \pm SD.

Results of the PKA activation experiments failed to assign a functional role to any of the polymorphisms, not least the CArG element located in the distal promoter. Therefore, we next tested the presence of a single particular transcription factor in relation to the single polymorphism in the CArG element by overexpressing CBF-A.

3.2.11.3 Transcription control of AVP promoter by CBF-A

Cotransfecting an expression vector for CBF-A with the AVP-luciferase constructs revealed that increasing concentrations of CBF-A repressed promoter activity in both the Lu-165 (figure 35) and Saos-2 (data not shown) cell lines.

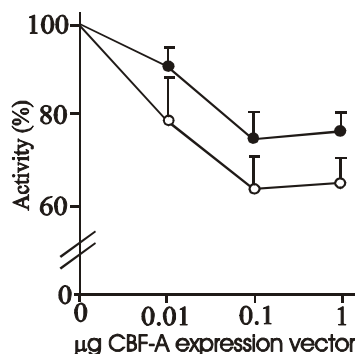


Figure 35. CBF-A differentially repressed LAB and HAB promoter activity. HAB (filled circles) and LAB (empty circles) distal promoters were cotransfected with an expression vector for CBF-A in Lu-165 cells. Both the HAB and the LAB promoter constructs are repressed with increasing concentrations of CBF-A. Importantly the LAB promoter, though not significantly different, is more efficiently repressed to a higher degree. Results are means of three independent experiments \pm SD.

Although non of the values reached statistical significance, dose-dependent differences were consistently measured in CBF-A mediated repression between the HAB and LAB constructs with the HAB AVP sequence being less prone to repression than the LAB construct at similar CBF-A concentrations.

3.2.11.4 AVP CArG element expression in cell culture transfection experiments

To clarify if this differential repression of the HAB and LAB constructs might be mediated by CBF-A through the polymorphic CArG element at position -1276 we created promoter constructs carrying only the CArG element, flanked by 8bp up- and downstream of the neighbouring AVP sequence, in front of a TATA element. Firstly, we wanted to determine if the CArG sequence behaves as a regulatory element in such a less complex system, secondly if the polymorphism might influence this function and, thirdly, if CBF-A confers transcriptional regulation through this element. The CArG element has been well documented as a potent activating sequence (Greco et al., 2002;Scott et al., 2002), with SRF being one of the major transcription factors to bind (Treisman, 1987). Expressing the LAB CArG element in osteosarcoma cells, which contain SRF (Bebien et al., 2003), indeed showed the element to function as a potent enhancer (figure 36A). Moreover, insertion of additional copies of the CArG element in the promoter increased the activity by double and triple the expression, in accordance with previous studies (Greco et al., 2002;Scott et al., 2002). When comparing the HAB and the LAB CArG elements, however, we observed that the LAB sequence conferred twice the activity of the HAB, demonstrating that the polymorphism affects the function of the CArG element (figure 36A). CBF-A has been reported to confer both repression (Kamada and Miwa, 1992) and activation (Mikheev et al., 2000) at the CArG element. Therefore, we next aimed to determine the role of CBF-A in relation to AVP promoter expression. When Saos-2 cells were cotransfected with a constant amount of an expression vector for CBF-A and the minimal CArG promoter plasmids, we measured that CBF-A repressed promoter activity, and this repression was closely related to the number of CArG elements present (figure 36B).

Next, we cotransfected increasing amounts of CBF-A with the minimal promoter construct encoding three copies of either the LAB or HAB line derived CArG boxes. We observed, at the highest doses of CBF-A, a striking 4-fold repression of the LAB line derived CArG box when compared to the HAB (figure 36C).

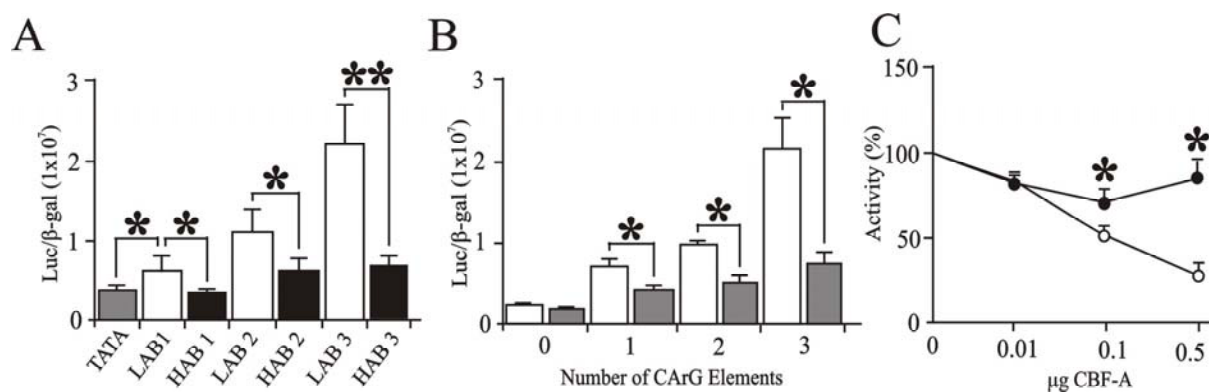


Figure 36. Minimal CARg element reporter constructs are differentially expressed. Constructs containing CARg elements derived from either the LAB or HAB AVP promoter were expressed in Saos-2 cells. (A) One, two or three copies of the CARg element from the LAB animal (black bars) conferred a potent transactivation, when compared to an empty TATA vector (shaded bar), which is impaired in the presence of A(-1276)G polymorphism derived from the HAB line (empty bars). (B) Constructs containing the CARg element of the LAB AVP promoter cloned in series, and cotransfected with a constant 0.1μg of CBF-A expression vector (shaded bars), were repressed by CBF-A. The most pronounced repression was evident when three copies of the CARg element were cotransfected with CBF-A. (C) CBF-A dose-dependent repression of the CARg element. Minimal reporter constructs containing 3 copies of either the HAB (filled circles) or LAB (empty circles) CARg elements were cotransfected with increasing amounts of an expression vector for CBF-A in Lu-165 cells. The CARg element from the LAB line is strongly repressed when compared to the HAB element. \pm SD. * $p < 0.05$, ** $p < 0.005$. All results were taken from three individual experiments.

The pGL2.TATA vector alone, containing no CARg elements in the entire plasmid sequence, was not repressed by increasing concentrations of CBF-A (data not shown) demonstrating that CBF-A dependent repression required the presence of the CARg box element. Together, these findings support the view that the A(-1276)G transition in the CARg element impairs CBF-A binding to the minimal HAB reporter construct which in turn relates to a weakened repression of the intact HAB AVP promoter by CBF-A.

3.2.12 CBF-A expression in the PVN

Collectively, our results so far support a role for CBF-A in repression of the AVP gene promoter *in vitro* and suggest a similar function for CBF-A *in vivo*. Therefore, we next addressed the issue of CBF-A expression in relation to AVP containing neurons in the PVN. A previous study reported that CBF-A messenger RNA is intensely expressed in the PVN of the hypothalamus (Rushlow et al., 1999). However, this finding needed further characterising which neurons of the PVN specifically express CBF-A, and in particular, if CBF-A is co-expressed with AVP in the parvocellular compartment.

3.2.12.1 Immunohistochemistry

A preliminary study conducted using mice brains supported the presence of CBF-A in the PVN. This experiment was performed with the N-CBF-A antibody on 3 separate mice (figure 37). Immunohistochemistry data show that CBF-A localises to a number of brain regions such as the hippocampus, dentate gyrus, habenula, thalamus and amygdala. More importantly in this context was the high expression of CBF-A in the PVN, observed in both the parvocellular and magnocellular sections where, approximately, 80% of the neurons in this region were CBF-A immunopositive.

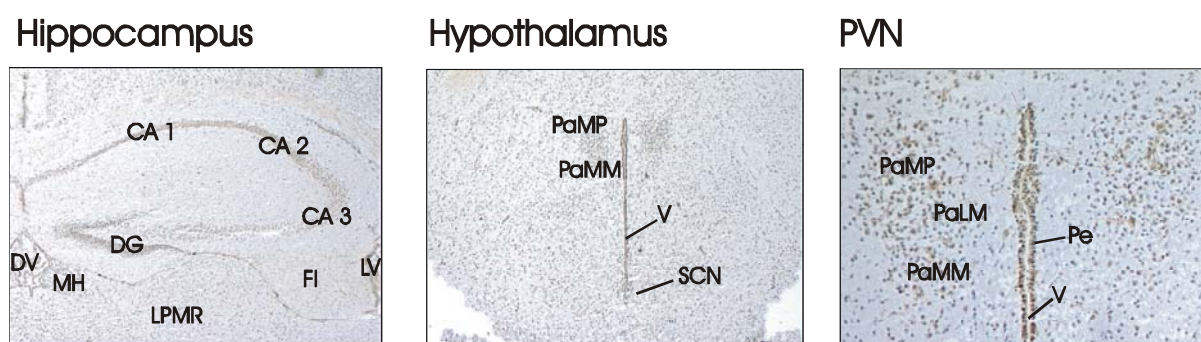


Figure 37. Immunohistochemistry of CBF-A expression in mouse hippocampus, hypothalamus and PVN. CBF-A shows neuron-specific labelling intensely localising to the PVN. CA1/2/3; field of hippocampus, DV; dorsal 3rd ventricle, FI; flocculus, DG; dentate gyrus, LPMR; lateral posterior thalamic nucleus, medial part, LV; lateral ventricle, MH; Medial habenular nucleus, PaLM; paraventricular hypothalamic nucleus, lateral magnocellular part, PaMM; paraventricular hypothalamic nucleus, medial magnocellular part, PaMP; paraventricular hypothalamic nucleus, medial parvocellular part, Pe; periventricular hypothalamic nucleus, SCN; suprachiasmatic nucleus, V; ventricle.

3.2.12.2 Double immunohistochemistry

To determine if CBF-A localised to the specific parvocellular AVP-producing neurons of the PVN double fluorescence-immunohistochemistry was performed for AVP and CBF-A. These double fluorescence-immunohistochemistry experiments for CBF-A and AVP expression in the PVN of the hypothalamus evidenced an intensive colocalisation of AVP and CBF-A in both the magnocellular and parvocellular regions (figure 38).

Interestingly, CBF-A localises to the lateral magnocellular subdivision of the PVN containing the magnocellular neurons, as well as the parvocellular neurons that make up the more medial parvocellular subdivision. Furthermore, it should be noticed that CBF-A also localises in the magnocellular neurons that make up the entire SON of the hypothalamus, as well as the SCN. It is within only the parvocellular PVN, where CRH is also synthesised, that

Results

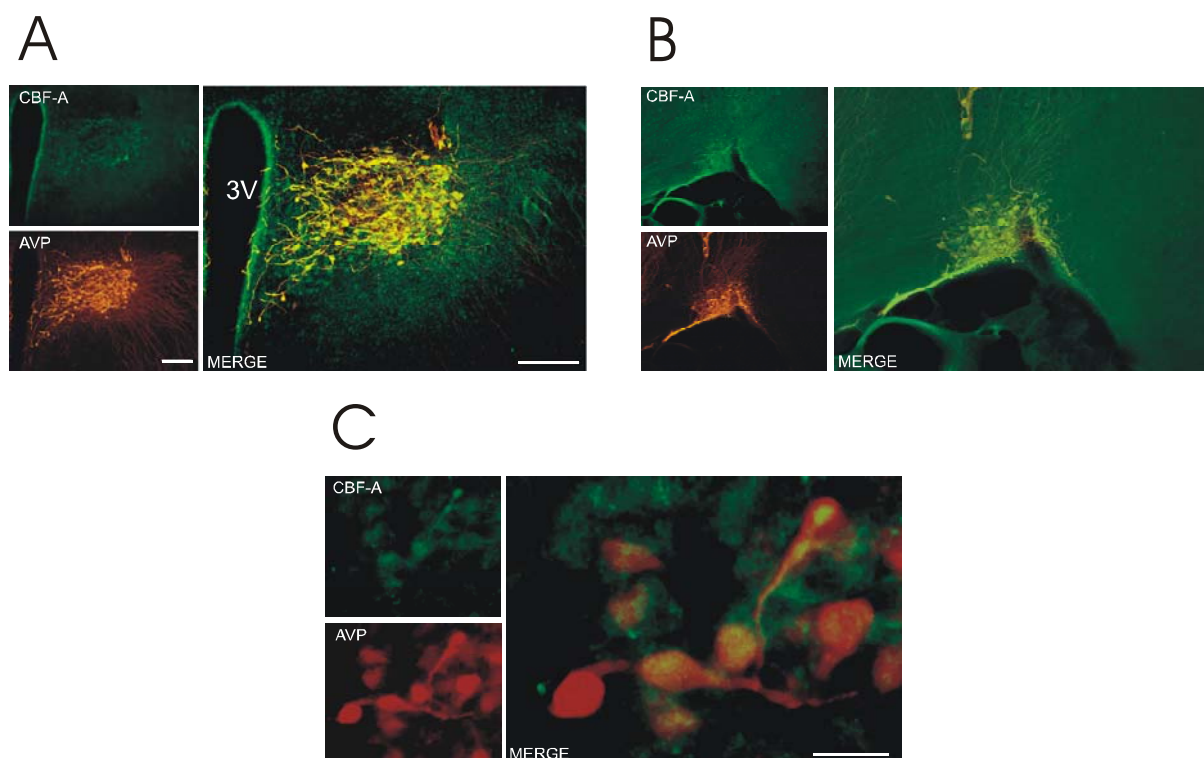


Figure 38. Double fluorescence-immunohistochemistry for CBF-A and AVP in rat hypothalamic neurons. (A) CBF-A and AVP expression broadly overlaps at the hypothalamic and cellular levels. Fluoro-immunohistochemistry for CBF-A (upper left) and AVP (lower left) expression in rat PVN. Merge of CBF-A and AVP fluoro-immunohistochemistry (right). Scale bar = 200µm. **(B)** CBF-A localises with the AVP expressing neurons of the SON. Fluoro-immunohistochemistry for CBF-A (upper left) and AVP (lower left) expression in rat SON. Merge of CBF-A and AVP fluoro-immunohistochemistry (right). **(C)** Cellular colocalisation of CBF-A and AVP. Fluoro-immunohistochemistry of CBF-A (upper left) and AVP (lower left) in neurons of the rat PVN. Merge of CBF-A and AVP fluoro-immunohistochemistry (right). Scale bar = 25µm.

AVP gene expression is suppressed by adrenal glucocorticoids as part of the negative-feedback loop and, therefore, regulated by stress as part of the HPA axis (Sawchenko, 1987). The magnocellular neuron-produced AVP, in both the PVN and SON, on the other hand, has a crucial role in osmoregulation, being released into the blood circulation upon physiological demand, such as a consequence of dehydration (Burbach et al., 1984; Sherman et al., 1988). These neurons are in contrast again to the dorsal-medial region of the SCN, the circadian generator of the mammalian brain (Weaver, 1998), where diurnal cues modulate AVP gene expression in these cells (Tominaga et al., 1992). Nerve signals here, from the SCN, cause the PVN to release pulses of CRH roughly once per hour, resulting in HPA axis activation and cortisol release. There are also direct links between the SCN and the adrenal gland itself (bypassing the HPA axis) through sympathetic nerve fibres, causing the adrenal gland to become more sensitive to ACTH stimulation during the morning, further adding to the circadian pattern of cortisol release throughout the day (Sage et al., 2002).

Results

The HAB and LAB rats differ in AVP content in only the PVN- magnocellular and parvocellular neurons - whilst SON and SCN AVP content are unchanged. The fact that CBF-A is present in those cells showing no AVP expression differences then suggests that another level of control, either pre- or post-translational, involving the CBF-A factor might be at work. This is a line of thought currently being followed up in drug response and CBF-A expression in the PVN of the HAB rats.

3.2.12.3 *In situ*-hybridisation

To exclude line-specific differences in CBF-A expression between the LAB and HAB - which would bias the importance of binding to the polymorphic CBF-A element - five non-stressed HAB and 5 non-stressed LAB animals were subjected to *in situ*-hybridisation with a riboprobe specific for CBF-A. Furthermore, 5 stressed HAB and LAB rats were included as a preliminary study in determining to which extent CBF-A might be altered under stressed states. The animals were exposed to the open arm of the EPM, the same stressor previously used to highlight the HAB and LAB AVP differences in rat PVN sections. Our *in situ*-hybridisation data revealed that no differences in CBF-A expression existed in the PVN between the HAB and LAB animals under basal or stressed conditions (figure 39). This finding rules out the possibility that differing levels of CBF-A between lines could underlie

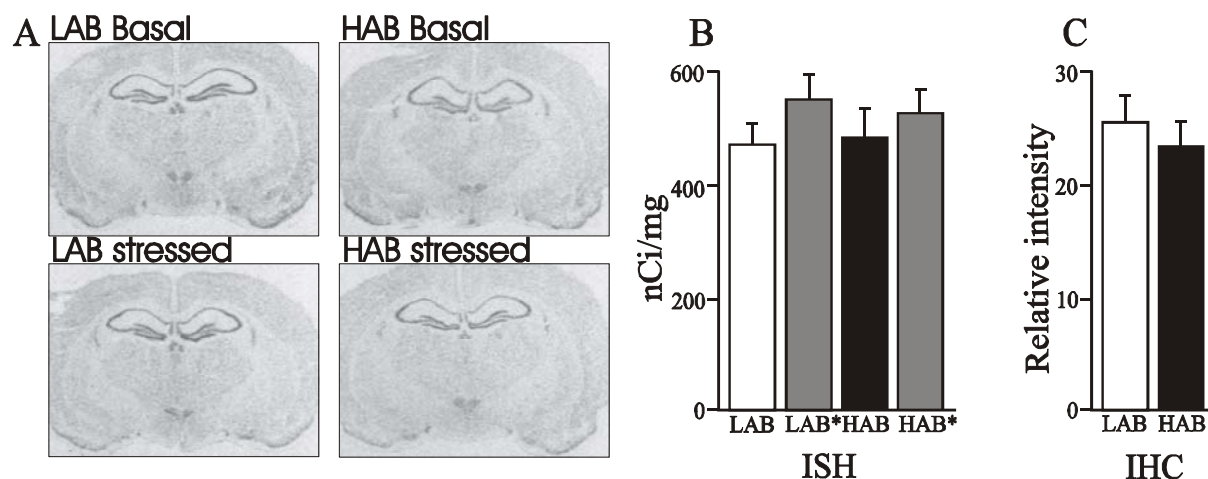


Figure 39. *In situ*-hybridisation and immunohistochemistry confirm similar CBF-A expression in the PVN between the HAB and LAB lines. (A) *In situ*-hybridisation for CBF-A in the rat brain (B) *In situ*-hybridisation for CBF-A in the PVN of five LAB and five HAB animals reveal similar CBF-A expression between the LAB and HAB lines under either basal or stressed conditions. (C) Immunohistochemistry for CBF-A in the PVN of five LAB and five HAB animals again reveal no significant differences in CBF-A expression between the lines.

the increased AVP expression present in the HAB AVP neurons. This result was further supported by immunohistochemistry stains for N-CBF-A (figure 39B). The trend for higher

levels of CBF-A in the PVN after stress exposure, however, seemed evident in both the HAB and LAB animals (figure 39A), compatible with the idea that CBF-A is responsive to stress.

3.2.13 Model for the polymorphic CArG element leading to differential AVP expression

Our data for rat AVP and CBF-A are summarised in the following model describing the differential regulation of the two AVP promoters by CBF-A (figure 40).

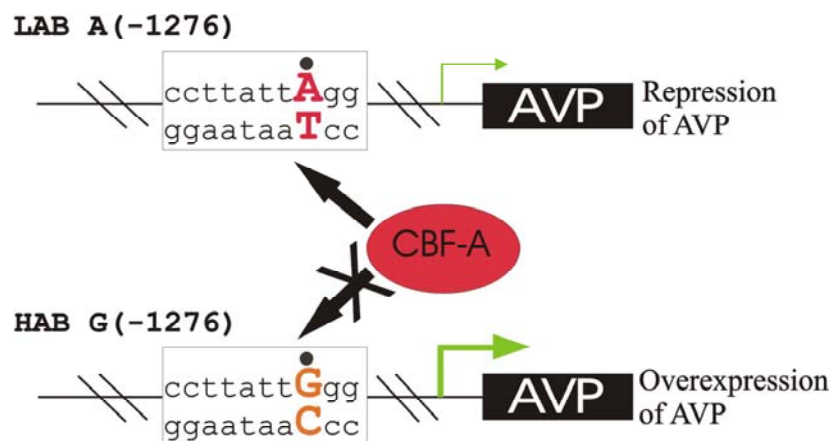


Figure 40. Model for derepression at the AVP promoter by the A(-1276)G polymorphism. The A(-1276)G polymorphism impairs binding of the transcriptional repressor CBF-A resulting in overexpression of AVP in magno- and parvocellular neurons of the PVN under non-stressed basal conditions.

SNP [A(-1276)G] conferred reduced binding of the transcriptional repressor CBF-A in the HAB allele, the consequent differential regulation of the AVP promoter resulting in an overexpression of AVP *in vitro* and *in vivo*. Furthermore, CBF-A is highly co-expressed in AVP-containing neurons of the PVN supporting an important role for regulation of AVP gene expression *in vivo*. The *in vivo* transcription analysis data lead us to conclude that the promoter region of the AVP gene plays a causal role in the differential AVP expression between the HAB and the LAB rats. *In vitro* analysis revealed an increased binding of CBF-A to the LAB-specific CArG sequence consequently resulting in “super” repression in the LAB-specific minimal construct sequence. This, we hypothesise, leads to the observed ~1.7-fold overexpression of AVP peptide in the parvocellular and magnocellular neurons of the PVN under non-stressed basal conditions. Taken together, our results demonstrate a role for an AVP gene polymorphism and CBF-A in elevated AVP expression in the PVN of HAB rats likely to contribute to their behavioural and neuroendocrine phenotype (Murgatroyd et al., 2004).

3.3 Genetic analysis of HAB and LAB mice lines

Ongoing studies in the laboratory of Professor Landgraf focus on HAB and LAB mice, developed from 1999 onwards by selective breeding for their response in the EPM test. The practicality of a QTL analyses was investigated by assessing a limited set of published markers. Alternatively, considering the absence of sufficient CD1-specific markers, outbreeding the HAB mice to another mouse strain, for which sufficient published markers exist, is required. In this case, marker analysis of different mouse strains serves to identify those most genetically divergent and, therefore, most informative in an outbreeding strategy. To address this question, sequencing analyses were conducted to determine to which extent SNPs from CD1 are informative for an intraline versus an interline cross.

3.3.1 Marker analysis of mouse chromosome 2

Polymorphic markers on chromosome 2 were selected from the Mouse Genome Database (MGD) to cover the complete length of chromosome 2. Fourteen of these regions were amplified and sequenced and compared to sequences of eight other common inbred and outbred mouse strains; Spre, DBA/2J, CAST/Ei, C3H/HeJ, BALB/cByJ, A/J, 129s1/SumJ and c57bl/6J. Each region, contained up to 15 SNPs, all of which were genotyped in two LAB and two HAB mice (figure 41).

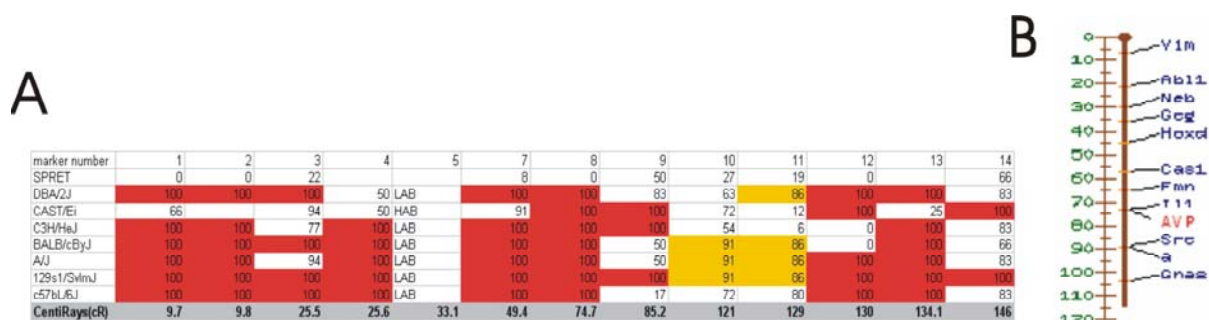


Figure 41. SNP screen of chromosome 2 in mice strains. (A) Table of the percentage of polymorphisms found at each of the 14 loci that are conserved in the CD1 mice. Also included are the chromosome locations of each locus in centimorgans (Cm). The data, demonstrate that the SPRET mouse strain is the most genetically removed from CD1, whilst 129s1/SvimJ is the most closely related at all loci. (B) The mouse AVP gene is located on chromosome 2 at location 73.2cM.

The data demonstrate that the CD1 mouse strain is genetically distinct from all of the other mice strains analysed and share no strain-specific polymorphisms. Furthermore, an SNP at the fifth locus lying at 33.1cM, revealed a line difference where the HAB animals contained an A and the LAB animals a T. Considering that the AVP locus also contains line differences

in SNPs (see below) one can speculate that a gene segment of, at least, 33.1cM to 73.2cM is differentially inherited between the HAB and LAB lines; this signifies half of chromosome 2.

3.3.2 AVP

The 5.5kb region of the mouse AVP gene, encompassing the three exons, two introns and 3kb of promoter, was entirely sequenced to determine if any HAB or LAB line-specific polymorphisms existed in this locus. The mouse AVP gene is situated on chromosome 2 at 73.2cM (Marini et al., 1993) (figure 41B) encoding a 168aa prepro-AVP protein highly homologous to the rat (figure 43).

Sequencing of the AVP gene resulted in numerous nucleotide line-differences. However, it quickly became evident that sequences between the HAB and LAB mice differed to those in the rat lines in a number of ways (figure 42). Firstly, the LAB and HAB mice contain AVP alleles divergent from each other and, in addition, from the published sequence (accession M88354) (Hara et al., 1990). Secondly, the alleles contain single nucleotide deletions. Thirdly, the LAB allele contains a sequence gap in the promoter comprising 12bp. Fourthly, both alleles show SNPs in the coding sequence. Together, these data support the idea that these sequences represent distinct alleles that diverged from a common sequence, perhaps some time ago. Lastly, the LAB allele contains an SNP resulting in a non-synonymous mutation in the signal peptide of the AVP protein.

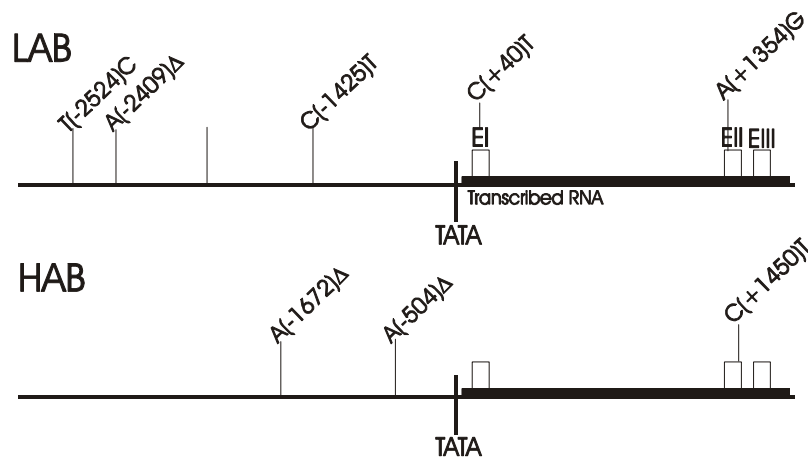


Figure 42. Scheme of the promoter, introns and exons (E) of the mouse AVP gene subjected to sequence analysis. Included are the LAB- and HAB-specific polymorphisms.

The HAB allele contains three SNPs in the 5.5kb of the AVP locus sequenced. One of the SNPs, the C to T transition [C(+1450)T]in exon 2, lies in the coding region of the AVP gene coding for a same-sense mutation at amino acid position 91 (serine) in the neurophysin

Results

part of the prepro-AVP protein. The other two SNPs involve deletions of As, the first 504bp upstream of the transcriptional start site A(-504) Δ , and the second further 5' at position 1672bp upstream A(-1672) Δ . The A(-504) Δ polymorphism seemed to effect no protein binding sites and matched no other DNA regulatory elements according to transcription element search programs (refer to section 2.2.6). The other polymorphism deleted specifically in the HAB line, again represented an A deletion, A(-1672) Δ . This deletion occurs in the spacer region of an imperfect palindromic element (TGACCTgatcAGGTCA) previously shown to bind nuclear receptor heterodimers and particularly the T3R-beta homodimers as evidenced from DNase I footprinting (Kurokawa et al., 1993). This could, therefore, suggest that the HAB allele lacks this element, which might function in controlling the AVP gene through nuclear receptor binding, although this remains to be experimentally tested.

The LAB allele also reveals a number of sequence differences to either the HAB allele and published sequence. These involved four SNPs, one single nucleotide deletion and a 12bp deletion. Two of the SNPs located in the translated sequence, one causing a synonymous mutation [A(+1354)G], and the other a non-synonymous mutation [C(+40)T]. The A(+1354)G transition occupied position 3 of the codon encoding Proline at amino acid position 59 in the neurophysin part of the AVP protein. The C(+40)T transition, importantly, lays in codon position 2 exchanging the third amino acid, Alanine, to a Valine during translation (figure 43).

The position of the third Alanine amino acid, located in the signal peptide, is evolutionary conserved in the rat (it is not conserved in the human) supporting the idea that this amino acid plays an important role in the functioning of the AVP precursor. AVP is synthesised by neurons of the hypothalamus as a pre-pro-hormone. Pro-AVP is generated by cleavage of the signal peptide from pre-pro-AVP during cotranslational translocation and is released into the lumen of the endoplasmic reticulum. It is subsequently transported within neurosecretory vesicles to the axon terminal in the neurohypophysis via the regulated secretory pathway yielding AVP, neurophysin II (NPII) and glycoprotein (for review see Burbach et al., 2001). Signal peptides are, therefore, important in targeting the protein for secretion, taking part in an array of protein-protein and protein-lipid interactions. Signal peptides are 22-23aa long and have a common structure: a short, positively charged amino-terminal region (n-region), a central hydrophobic region (h-region), and a more polar carboxy-terminal region (c-region) containing the site that is cleaved by the signal peptidase (figure 44A) (for review see von Heijne, 1998).

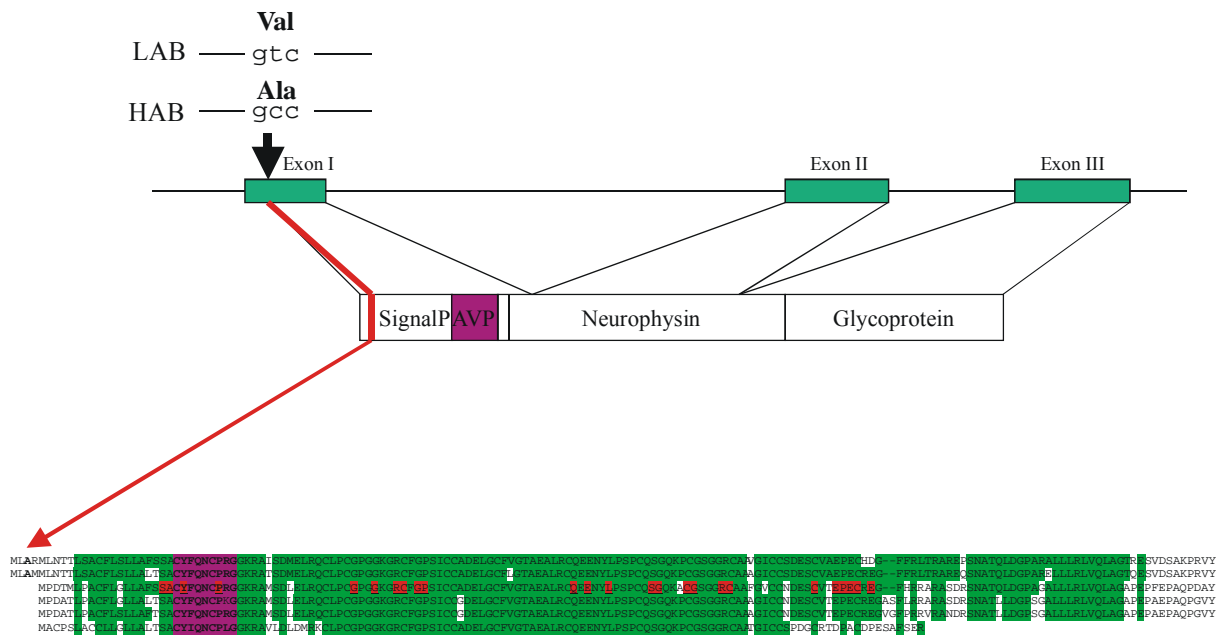


Figure 43. The arginine vasopressin-neurophysin II (AVP-NPII) gene consists of three exons. The first exon encodes the signal peptide, AVP and NH2-terminal region of neurophysin II (NPII); the second exon accounts for the central region of NPII and the third exon gives rise to the COOH-terminal region of NPII and glycoprotein. The polymorphism in the LAB animal causes an amino acid change in position 3 of the signal peptide resulting in an Alanine, which is also conserved in the rat, being substituted by a Valine. Protein alignments include the AVP protein sequences of the mouse, rat, human, pig, cow and mouse oxytocin.

As the signal peptide emerges from the ribosome, it is first recognized by a ribonucleoprotein complex, the signal recognition particle (SRP), at the highly variable h-region (Nagai et al., 2003). The signal peptide is then inserted in a lipid-exposed location at the ER translocon, at this point the signal peptide spans the membrane with its carboxy-terminal end facing the ER lumen. Although still associated with the translocon, it is also exposed to membrane lipids and its h-region has a helical conformation. The signal peptidase then skims the lumen surface of the membrane, looking for suitably exposed signal-peptide cleavage sites where the h-region serves to position the c-region near the lipid headgroups, within reach of the signal peptidase. This may also explain why signal peptidase does not cleave trans-membrane helices in integral membrane proteins, or signal peptides with artificially lengthened h-regions (Nilsson et al., 1994) or helix-breaking proline residues (Ryan and Edwards, 1995). Such helices generally extend across the lipid head-group region, so they do not present the required extended conformation, and naturally have to be hydrophobic in nature. Indeed, the degree of hydrophobicity of this region of the signal sequence is a major determinant of translocation efficiency (Bird et al., 1990; Ryan et al., 1993). Therefore, it is of some interest to note that the inactive hydrophobic amino acids A and V (also including Glycine (G), Leucine (L) and Isoleucine (I)) differ in their

hydrophobicity, where the LAB Valine is more hydrophobic than the Alanine amino acid present in the HAB (relative hydrophobicity V= 4.2, A= 1.8) (Kyte and Doolittle, 1982) (figure 44B).

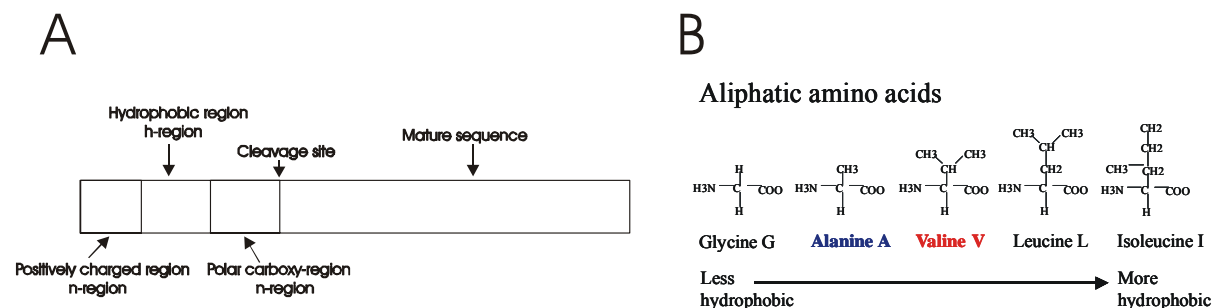


Figure 44. Signal peptides and aliphatic amino acids. (A) Schematic diagram of a signal peptide illustrating the conserved amino acid regions. (B) Comparing hydrophobicity of amino acids demonstrates that Valine is more hydrophobic than Alanine.

Using protein structure prediction programs of PROF (Rost and Sander, 1993) and PHD (Profile fed neural network systems from Heidelberg) (Rost et al., 1996) it became further evident that the A to V amino acid substitution would alter the helical h-region of the signal peptide, the LAB structure predicting a longer helical region extending further towards the n-region (figure 45). However, overall the difference in hydrophobicity at this position results in the HAB, wildtype, signal peptide containing a higher percentage of helical structure and a greater solvent accessibility.

One might speculate from this that the predicted helical h-domain in the LAB, for assigning the transmembrane helix, is altered to an extent that the peptide would situate differently across the ER lipid membrane compared to the wildtype prepro-AVP, with more amino acids in the LAB signal peptide locating outside the membrane. This alteration of the h-region might further effect interaction with the SRP system resulting in less efficient AVP peptide processing.

Further evidence for the role of this signal peptide difference in the impairment of AVP release was provided in the behaviour of the animals in which fluid intake and serum osmolarity was measured in relation to the DI hypothesis provided above. Firstly, the animals from the LAB line all show a robust 2-3-fold increase in water drinking than the HAB line. Secondly, the LAB animals when deprived of water, show a massive increase in osmolarity and die of dehydration after 2 days when compared to control animals. Thirdly, the LAB animals show a reduction in neuronal density in the PVN, which becomes further evident as

Results

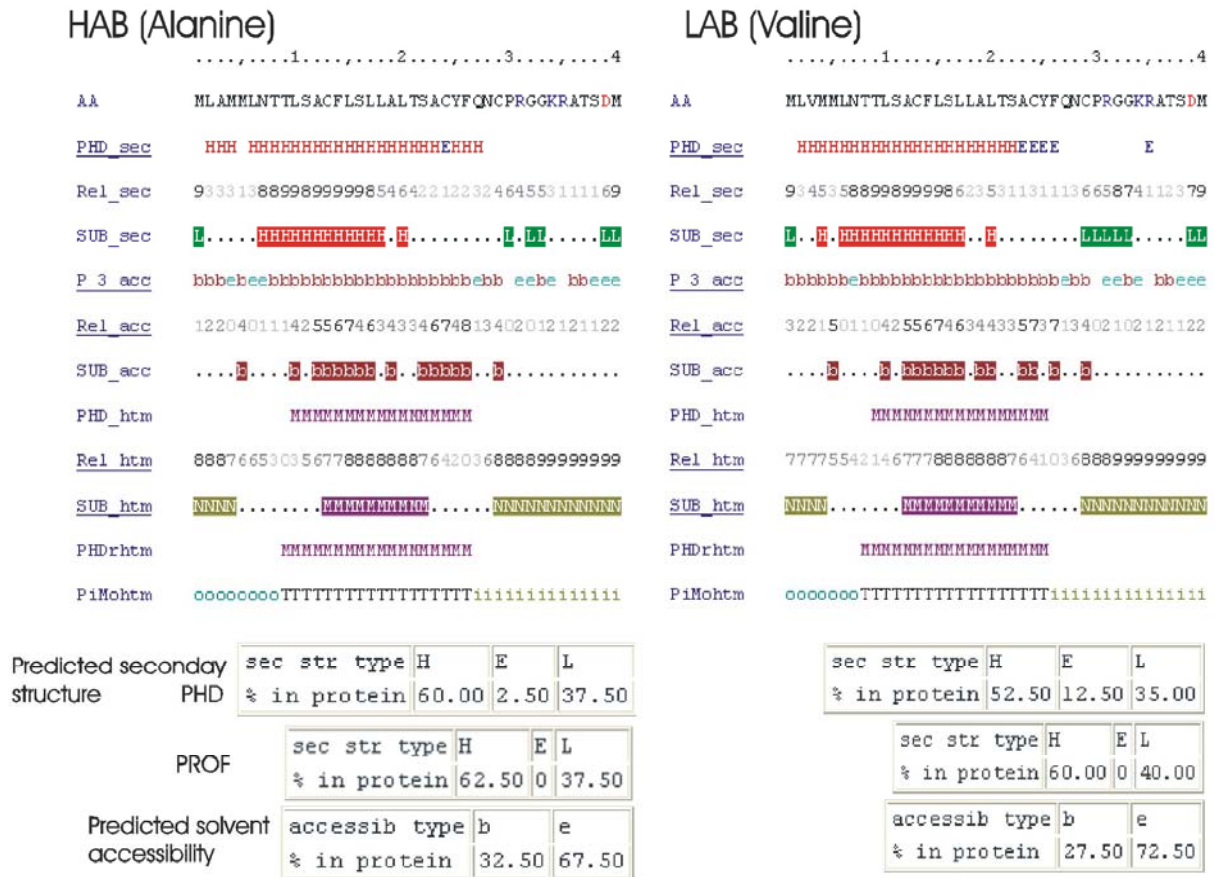


Figure 45. Comparison of the secondary structures of the LAB and HAB AVP signal peptides using the PHD (Profile network prediction Heidelberg) and PROF secondary structure prediction programs. PHD sec; predicted secondary structure H=helix, E=extended (sheet), blank=other (loop). Rel sec; reliability index for PHDsec prediction (0=low to 9=high). SUB-sec; subset of the PHDsec prediction, for all residues with an expected average accuracy > 82%. P 3 acc; PHD predicted relative solvent accessibility (acc) in 3 states: b = 0-9%, i = 9-36%, e = 36-100%. Rel acc; reliability index for PHDacc prediction (0=low to 9=high) SUB acc; subset of the PHDacc prediction, for all residues with an expected average correlation > 0.69. PHD acc; PHD predicted relative solvent accessibility (acc) in 10 states. PHDhtm; PHD predicted membrane helix: M=helical transmembrane region, blank=non-membrane, PHD = Profile network prediction Heidelberg. Rel htm; reliability index for PHDhtm prediction (0=low to 9=high). SUB htm; subset of the PHDhtm prediction, for all residues with an expected average accuracy > 98%. N: is non-membrane region. PHDrhtm; refined PHD prediction: M=helical transmembrane region, blank=non-membrane. PiMohtm; PHD prediction of membrane topology: T=helical transmembrane region, i=inside of membrane, o=outside of membrane. PT htm; 'probability' for assigning transmembrane helix. The tables demonstrate the predicted secondary structure using the PHD and PROF programs and the predicted solvent accessibility composition (core/surface) ratio of the two proteins; e=residues exposed with more than 16% of their surface, b=all other residues.

the animals age (Kessler et al., unpublished data). It is well known that progressive degeneration of AVP-producing cells might accelerate the pathogenesis of diabetes insipidus (DI) (for review see Maghnie, 2001). These three findings certainly support the diagnosis of DI.

Electrolyte abnormalities in DI are caused by the loss of urinary free water, which produces hyperosmolar dehydration, leading to hypernatremia, hyperchloremia, and prerenal

Results

azotaemia caused by diminished blood volume (for review see Verbalis, 2003). Azotaemia is characterised by a high level of urea or other nitrogen containing compounds in the blood caused by the inability of the kidney to excrete these compounds. Therefore, it is also of interest that an enhanced expression of the enzyme, glyoxalase I (GLO1), occurs in the LAB animals (Kroemer et al., unpublished data). GLO1 is part of the glyoxalase system present in the cytosol of cells catalysing the condensation of methylglyoxal and reduced glutathione to form S-lactoyl-glutathione; GLO2 converts the latter substance to D-lactic acid and reduced glutathione (for review see Thornalley, 2003). Remarkably, GLO1 deficiency leads to azotaemia (Miyata et al., 2001) highlighting the importance in the regulation of this enzyme in regard to osmolarity control.

Aside from the signal peptide mutation, the LAB allele contains a further number of polymorphisms in 2.5kb of the promoter sequence (table 3). The C(-1425)T transition results in a sequence containing a T allele in the HAB line forming a z-box element characterised by the consensus of ggaccct. This binds the little known transcription factor NF-Zz in lymphocytes (Tsang et al., 1990). Both alleles of the A(-2409) Δ form binding sites for different factors. The HAB allele containing the A forms a binding site for the sex-determining factor gene product (Trimmer et al., 1998), as well as matching an artificial sequence TGTGGT, which binds the acute myeloid leukaemia I (AML1) gene product in EMSA experiments (Meyers et al., 1993). The deletion of the A in the LAB line forms an N-box sequence (ctgtg) which has been shown by DNaseI footprinting to bind the bHLH factor HES1 (Ishibashi et al., 1994) conferring transcriptional inhibition. This allele further results in

Table 3. Polymorphisms in the mouse AVP promoter embedded in protein-binding DNA elements. Included are the relative transcription factors binding to the respective DNA elements and if they are specifically expressed in the hypothalamus.

Polymorphism	Allele	Element	Sequence	Transcription Factor	Expression in hypothalamus	Reference
C(-1425)T	T	z-box	ggaccct	RFX and NF-Y	Yes, ?	Tsang et al., 1990
A(-2409) Δ	A	CD3 γ gene enhancer	aacaag	sex determining factor	Yes	Trimmer et al., 1998
	A		tgttgt	AML1	?	Meyers et al., 1993
	Δ	N-box	ctgtg	HES1	Brain	Ishibashi et al., 1994
	Δ	thymidine kinase promoter	ccnennnct	Yi	?	Dou et al., 1991
T(2524)C	C	B-element	agccag	NF-1	Brain	Takiguchi and Mori, 1991
A-2183-2194	+		ccagagctacag	HNF1A, NF-1	Brain, brain	Courtois et al., 1987; Takiguchi and Mori, 1991
	Δ	F-element	tggctgg		no	Uzan et al., 1991

Results

a sequence identical to an element in the mouse thymidine kinase promoter which, by DNaseI footprinting and EMSA, has been shown to bind inducible proteins (Dou et al., 1991). A transition further 5' involving T(2524)C results in the formation of a B-element (agccccg) in the case of the HAB-specific C allele. This element, found in the rat type arginase promoter, binds the NF-1 controlling factor, evidenced by DNaseI footprinting (Takiguchi and Mori, 1991)

Of most interest in the LAB promoter was the 12bp deletion found between nucleotides -2183 to -2194, which was not present in either the HAB or published sequence. This sequence, ccagagctacag, does not match any mobile genetic elements (for review see Bennet et al., 2004), or neighbouring sequence – evident of a duplication or inversion - and one must conclude that it arose via a spontaneous deletion in a founder individual. The HAB allele and published sequence, with the extra 12bp, contains the consensus sequence for HNF1A (Courtois et al., 1987) and another NF-1 site (Takiguchi and Mori, 1991). The LAB allele deletion, on the other hand, results in a consensus F-element (tggctgg) which, by DNaseI analysis, binds transcription factors and controls the platelet glycoprotein IIb gene (Uzan et al., 1991).

3.4 Human AVP gene as a candidate gene for anxiety

The human AVP gene is located on chromosome 20 at position 20p1 (Rao et al., 1992) (figure 46A). The promoter and the 3' downstream region of the human AVP gene were sequenced to elucidate polymorphisms that might be of use in an association study in order to test whether the role of AVP as a culpability gene in rat and mice, in addition, extends to anxiety and depressive disorders in human patients. This was, naturally, the ultimate goal of these animal experiments.

3.4.1 Sequence analysis

The DNA from 15 humans was subjected to sequencing in regions of 1kb upstream of the AVP gene and 1kb downstream revealing a number of polymorphisms (figure 46B). These areas were chosen as it was believed that polymorphisms may be more prevalent in the non-transcribed than in the transcribed region, and it was assumed that a polymorphism upstream and downstream enables a more powerful statistical analysis in an association study. Furthermore, this study has focused on AVP promoter polymorphisms in the rat and mouse and, therefore, it was of interest to analyse the homologous region in the human.

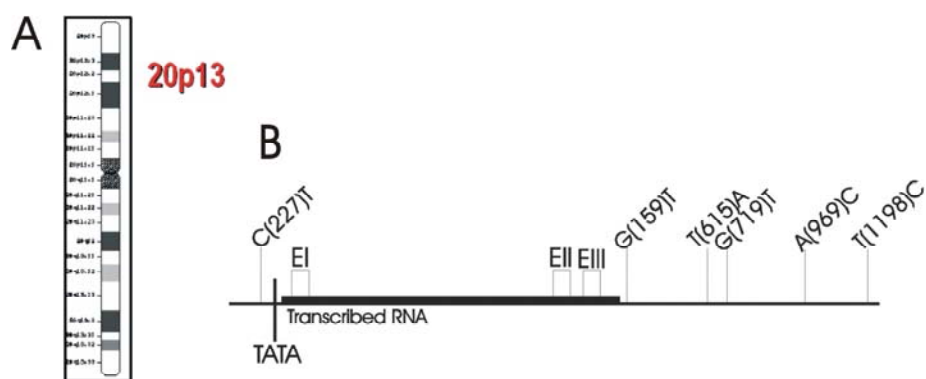


Figure 46. The human AVP gene and location of polymorphisms. (A) The AVP gene is located on chromosome 20 at position 20p1. (B) Schematic diagram of the human AVP locus highlighting the locations of SNPs discovered in the vicinity.

3.4.2 C(-229)T promoter SNP

The C(-229)T transition lies close to the TATA box of the human AVP gene. The polymorphism actually affects a number of very interesting putative protein binding sites. Firstly, the C allele results in the consensus sequence of an Sp1 binding site (Gustafson and Kedes, 1989), and furthermore would also be predicted to bind the histone H4 gene-specific transcription factor H4TF-1 (Stauffer et al., 1998). Both factors bind to the consensus sequence of GGGGGAGGGG, as evidenced by EMSA, methylation interface and DNaseI footprinting. Sp1 is an important transcription factor controlling a large number of genes in a variety of cell types (for review see Li et al., 2004). Moreover, the rat AVP gene has previously been reported to bind and be regulated by Sp1 at a GC-rich region in position -170bp (Grace et al., 1999) which is homologous to the human AVP promoter GC-rich region containing the C(-229)T polymorphism (figures 14 and 47A).

The C(-229)T polymorphism, therefore, represented a good candidate polymorphism for the regulation of AVP, as well as providing a marker for the AVP gene itself to be used in an association study. To test the feasibility of this marker in a patient-control association study 100 human DNA samples were analysed using an RFLP based approach (refer to section 2.1.10.4) (figure 47B). We calculated a gene frequency for this polymorphism of 75% T allele and 25% C allele. The common nature of the alleles, in addition to possible functional effects caused by disruption of an Sp1 element makes this SNP a good candidate for further association and functional genomic studies.

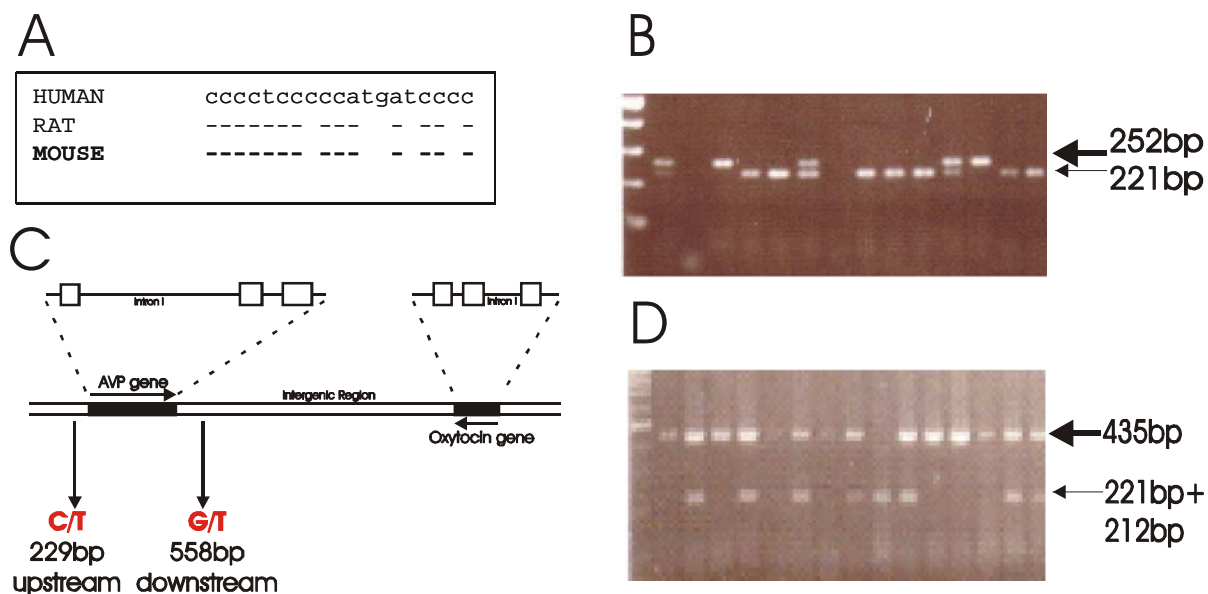


Figure 47. Human AVP polymorphisms. (A) Homology between the human, rat and mouse at the promoter GC rich region. Note that the C polymorphism, lying 229bp upstream from the start codon in the Sp1 element, is further conserved in both the rat and mouse. (B) Analysis of the C(-229)T polymorphism with the NlaIII RFLP in human controls and patients with affective disorders. The T polymorphism results in only two digested products of 252bp and 64bp, whereas the C polymorphism results in an extra digestion product leaving sizes of 221bp, 64bp and 31bp. The 64bp and 31bp fragments are not visible on the gel. (C) Schematic diagram of the 5' and 3' human AVP polymorphisms. (D) RFLP analysis of the G(-558)T polymorphism lying 3' of the AVP gene. Incubation with the MseI enzyme results in cleavage of the 435bp product into 223 and 212bp products only in the presence of the t allele.

3.4.3 G(-558)T downstream SNP

Sequencing of the region downstream of the human AVP gene revealed a number of SNPs (figure 46). As previously described, polymorphisms in the 3' region of the human AVP gene were required for inclusion in a prospective association study. The G(-558)T polymorphism, embedded in a MseI restriction site sequence, provided a suitable SNP for RFLP analysis (figure 47D) (refer to section 2.1.10.4). This second SNP downstream of the AVP gene was included for two reasons. Firstly to determine if the AVP gene represents a real candidate locus, in which a meta-analysis of the 5' C(-229)T transition combined with the 3' G(-558)T transversion (figure 47C) should provide greater statistical power and, secondly, to test the hypothesis that the 3' region of the AVP gene contains major control elements for AVP tissue-specific expression.

As evident from figure 47C, the G(-558)T transversion also makes an ideal SNP to study in association studies from its ease in RFLP studies using the MseI restriction enzyme and its relatively common alleles frequencies of 55% G and 45% T allele when tested in the same 100 human samples.

Results

It would, therefore be of interest to test these two polymorphisms in a case/control study and to further calculate to which extent the two polymorphisms are in linkage to each other. This is of importance in testing for disequilibrium, and subsequent relevance of these polymorphisms in an association study. However, this experiment is beyond the scope of this study.

4 Discussion

4.1 HAB rat

Previous work demonstrated a critical role of AVP gene overexpression in a HAB/LAB animal model of trait anxiety and comorbid depression, which was established by bi-directional breeding (for review see Wigger et al., 2004). This approach enriches for genetic information associated with a particular trait, which shifts the animals phenotype from the population mean (Falconer and Mackay, 1996). In an extension of this work we identified here a A(-1276)G transition within the AVP which plays a causal role in the differential AVP expression where this particular SNP results in a decrease in binding of the CBF-A leading to less efficient transcriptional repression of the AVP gene. This would, therefore, result in the observed overexpression of AVP in the magno- and parvocellular neurons of the PVN under non-stressed basal conditions. HAB animals have been well documented to show increased AVP mRNA expression, as well as elevated release of the neuropeptide in the PVN, which correlates with a hyperactive HPA axis. We now present direct evidence for line-specific differences in the sequence of the AVP promoter playing a direct role in this differential AVP expression. In the heterozygous rat PVN, the HAB AVP promoter shows a 50% increased activity compared to the LAB sequence, which lacks all of the HAB-specific SNPs. Evidently, this difference will enlarge under the homozygous condition present in the HAB animal and, in turn, correlates well with the differences seen in the AVP messenger RNA studies. The fact that the allele-specific transcription rate was measured *in vivo*, circumvents the limitations associated with the analysis of cell-specific genes in cultures and adds further relevance to these findings. Genotyping the promoter SNPs in outbred Wistar rats resulted in the finding that the HAB-specific allele occurs with a frequency of 1.5%, compatible with the common-disease-common variant hypothesis (Lohmueller et al., 2003), and supports the idea that trait selection leads to homozygosity at loci conferring trait anxiety/depression. Moreover, we observed that the LAB-specific AVP allele was identical to published sequences from outbred rats in accordance with normal levels of hypothalamic AVP gene expression (figure 40). Hence, LAB and HAB lines represent distinct disease entities, with AVP behaving as a vulnerability gene solely in the latter. The line-, neuropeptide- and site-specificity of AVP overexpression in the PVN of HAB animals is underlined by the findings that (i) the expression of oxytocin, the structurally and functionally related neuropeptide, did not differ between the lines, and (ii) AVP expression in the SON, in contrast to the PVN, did not

Discussion

differ between the lines. Further studies are necessary to identify the mechanism(s) responsible for this nucleus-specificity (see below).

We further provide preliminary evidence for the polymorphic AVP locus associating with anxiety. We observed that F2 animals from a HAB/LAB or HAB/outbred cross containing the HAB-specific polymorphic promoter sequence tended to present with longer durations until the initial exploratory entry onto the open arm of the EPM, reflecting a higher innate anxiety. The small number of animals involved in this preliminary study, we speculate, was the limiting factor underlying the reduced statistical power evident in these results. However, these results led us to repeat this experiment using a greater number of animals, which was performed in the autumn of 2003 with 238 male F2 animals. We observed that the latency to float in the FS test associated with the AVP allele. However, this association depended on a home cage effect, which might reflect the effects of group housing. Although, cages with higher numbers of animals were not on average more or less anxious (data not shown), the chance that group-housing could affect the AVP polymorphism in relation to the HPA axis is a real possibility. Indeed a study on nociceptin/orphanin FQ knockout mice, revealed the presence of increased anxiety only when the animals were group-housed (Ouagazzal et al., 2003). Furthermore, the anxiety in these gene knockout, group-housed, animals correlated with increased levels of basal and post-stressed plasma CORT, suggestive of an elevated HPA axis underlying genetic-environmental interactions. It is well accepted that environmental stressors, such as group housing has a role in the effect of behaviour (Hilakivi et al., 1989; Karolewicz and Paul, 2001; Rodgers and Cole, 1993; van Loo et al., 2001). Considering that the FS test is a robust predictive marker of HPA axis dysregulation (Will et al., 2003), it is feasible that this polymorphism might represent a real association which, however, responds to environmental effects; a situation well known in the clinic. Therefore, we plan to conduct this experiment again using singularly housed rats to corroborate the present results.

Of the 10 SNPs found in the distal promoter of the AVP gene, only two mapped to known consensus DNA binding sites. The C(-592)T transition embedded an imperfect putative CRE site, which locates further upstream to the TATA element than the optimal distance CREs usually require (Conkright et al., 2003) and seems, therefore, not to fulfil a regulatory role in agreement with previous studies. In fact, we observed no differences in the proximal promoters, which led us to conclude that both the SNP and the CRE element might play only a negligible role in expression. The CArG element, however, appears an attractive candidate, regarding differential regulation of the AVP gene. CArG boxes form the core of

Discussion

the serum response element (SRE), which is bound by the transcription factor SRF (Treisman, 1987), and SREs have been characterised in the promoter regions of a number of Immediate-Early-Genes (IEGs) such as c-fos (Gilman et al., 1986), FosB (Lazo et al., 1992), zif268 (Changelian et al., 1989), *cyr61* (Kim et al., 2003), *nurr77* (Williams and Lau, 1993) and *pip92* (Latinkic and Lau, 1994). IEG expression in the brain responds to a variety of stimuli including growth factors, stress, mechanical injury, seizures and ischemia, as well as numerous chemical agents and receptor agonists and antagonists (for review see Herdegen and Leah, 1998). Importantly, CBF-A binds equally well to the CA_rG element hereby possibly attenuating gene expression and has, therefore, been suggested to be involved in the refractory period observed for c-fos induction upon repeated stimulation (Rushlow et al., 1999). Interestingly, c-fos, as well as a number of the IEG genes, are expressed in the same tissues as AVP and are both strongly upregulated in response to stress (for review see Pirnik et al., 2004) - AVP expression occurs in step with IEG responses, contrasting to the rapid induction of CRH, which is in parallel to that of CREB phosphorylation, but preceding induction of c-fos (Kovacs and Sawchenko, 1996). This might suggest that these IEG genes and the AVP gene could share similar regulatory elements. We indeed provide evidence that the CA_rG element, which also controls c-fos, repressed the AVP promoter *in vitro* when CBF-A protein levels were increased in Saos-2 cells. SRF also binds the CA_rG box (Treisman, 1987) and is highly expressed in a large number of brain areas such as the forebrain, cortex, striatum, amygdala and hippocampus, and in some scattered neurons in the medulla and spinal cord, as well as peripheral non-neuronal tissue (Norman et al., 1988). Interestingly, SRF, though moderately expressed in the hypothalamus, (Herdegen et al., 1997; Stringer et al., 2002), is distinctly absent in the PVN (Blume et al., 1998, which was further supported by personal communication from Annegret Blume (Kiel)). Conversely, CBF-A reveals an intense expression in the PVN in this study, in addition to being widely expressed in many other areas of the brain including the olfactory bulb, hippocampus, cerebellum and hindbrain and additional tissues such as the spleen, lung and thymus (Rushlow et al., 1999). In the PVN, therefore, CBF-A seems to act independently of SRF possibly as a constitutive repressor or alternatively competing with an, as yet unknown, PVN-specific activating transcription factor operating at the CA_rG box. It should also be further noted that our immunohistochemistry experiments also revealed CBF-A expression in the SON (figure 38C). This raises the issue of why AVP expression does not differ in this nucleus despite the presence of CBF-A, and lead us to propose that a further level of control, perhaps involving posttranslational modification of CBF-A, is at work in the SON of the hypothalamus. Indeed, different alternatively spliced

Discussion

isoforms of CBF-A exist, in addition to post-translational modifications involving either differential phosphorylation or glycosylation (Bemark et al., 1998), all of which can be regulated in response to certain cellular signals (Umar et al., 2003;Cok et al., 2004). This might explain the differential activity of CBF-A irrelevant of its similar expression/concentration in the PVN and SON, as measured by *in situ*-hybridization and immunohistochemistry (data not shown).

We explored the possible mechanism by which CBF-A mediates repression. Key to these experiments was our observation that CBF-A preferentially binds ssDNA. Therefore, the high affinity binding of CBF-A to the specific ssDNA appears to be the driving force for local DNA strand separation at this element. CBF-A is closely related to members of the heteronuclear RNA binding proteins (hnRNP) and ssDNA binding proteins (ssDBF) containing the characteristic conserved RNA binding domains (RBD) allowing interaction with RNA (Weisman-Shomer et al., 2002). However, its additional role in DNA-binding and transcriptional regulation has also been increasingly recognised and well documented (Kamada and Miwa, 1992). Members of the hnRNP and ssDBF protein families, which bind ssDNA, have been thoroughly investigated as being implicated in transcriptional regulation of a wide variety of genes, including growth related genes such as thymidine kinase (Hsieh et al., 1998), EGF receptor (Chen et al., 1993) and Growth hormone receptor (Schwartzbauer et al., 1998), and IEGs such as Egr (Taira and Baraban, 1997), c-Myc (Michelotti et al., 1996b), c-fos (Sadakata et al., 2000) and Src (Ritchie et al., 2003) at a diverse range of elements in promoter regions such as CT rich regions (Michelotti et al., 1996b), hormone response elements (Chen et al., 1998;Chen et al., 2003), CREs (Sadakata et al., 2000) and repeat regions. Specifically, hnRNP K (Michelotti et al., 1996a), FUSE binding protein (Michelotti et al., 1996b), Msy-1 (Schwartzbauer et al., 1998) ERDBP-1 (Chen et al., 1993), puralpha (Sadakata et al., 2000), and cold shock domain proteins (Coles et al., 2002) have been demonstrated to induce or stabilize single-stranded regions. These alterations in DNA conformation and topology may underlie gene expression by affecting the DNA binding activities of transactivating factors operating through *cis*-regulatory elements located within or next to these structures. This would provide an efficient mechanism for the regulation of genes showing very low basal activity which can be induced by up to 100-fold very quickly in response to a stimulus, i.e. c-fos. A number of these hnRNP and ssDBF proteins are differentially regulated under various signals. It could, therefore, be envisaged that these ssDNA binding proteins keep the gene promoter in a repressed conformation which may be relieved by specific signals allowing activating factors to bind. This mechanism could then

Discussion

apply to CBF-A pointing to a role in regulating repression of the AVP gene by governing the binding of dsDNA-dependent activators in the PVN to the CArG element or adjacent sequences.

It is well established that the ssDBF protein families have preferences for A/T rich regions, which appears evident in this study when substituting a G for an A. The stoichiometry of the DNA helix differs considerably dependent on sequence. Studies on the A/T composition of CArG elements have highlighted the importance of the precise sequence order on the nucleotides to DNA topology. On average more local bending occurs at T-A steps (8.21°), which display a positive role bending towards the major groove, than at an A-T step (5.71°) that displays a negative role bending slightly towards the minor groove of the DNA helix. Sequences of A-tracts containing at least four consecutive As or Ts are relatively straight and rigid, while addition of an A-T causes the sequence to become more bent displaying more variable deformations of minor groove, width, cup twist and buckle (for review see Mack et al., 2001). This explains why proteins usually choose pyrimidine-purine steps as the locus for bending and involve A/T tracts near that locus, and this might further explain the preference for ssDNA binding proteins for this site. In view of this, the A/T rich regions of the CArG elements might be crucial to the binding of ssDNA binding proteins.

AVP overexpression and over release at the PVN level is likely to contribute to the anxious and depressive-like phenotype of HAB rats. Accordingly, periferal administration of the V1-receptor antagonist $d(\text{CH}_2)_5\text{Tyr}(\text{Me})\text{AVP}$ induced a shift towards reduced depression and anxiety-related behaviour. Similar antidepressant effects were triggered by paroxetine, probably via normalisation of AVP expression (Wigger et al., 2004). In addition to its behavioural effects, paroxetine, as well as the peripherally administered V1 receptor antagonist, have been shown to normalise the pathological outcome of the DEX/CRH test in the HAB animals (Keck et al., 2002;Keck et al., 2003). In this context it is of interest to note the growing literature linking AVP expression to affective disorders (see below and for review see Scott and Dinan, 2002;Millan, 2003). Thus, our finding that the SNP in position 1276 of the AVP gene promoter underlies AVP overexpression in the PVN of HAB rats, makes this SNP a potential target for further studies aimed at improving diagnostic and therapeutic tools. Interestingly, CBF-A may represent a “drugable” target. Cells treated with nerve growth factor cause upregulation of CBF-A which correlates with downregulation of c-fos and zif268 attesting to the important role CBF-A plays in response to neuronal signals (Rushlow et al., 1999). In addition, the dopamine D1 agonist SKF-82958 effects CBF-A and resulting c-fos expression (Rushlow et al., 2000). Furthermore, acute injections of the

neuroleptic fluphenazine or clozapine also cause an upregulation of CBF-A increase in the brain (Rushlow, 1997). These findings provide tentative evidence that CBF-A might be regulated by, or play some role in the efficacy to, certain psychiatric drugs.

Condensing, we provide a mechanism underlying the overexpression of genes involved in an altered anxiety-like phenotype of a rat model. Furthermore, elucidating this mechanism provides the opportunity to study candidate proteins important in this pathway. In turn, these proteins, such as CBF-A, then represent putative drug targets for controlling the expression of genes, such as AVP, presumed to underlie the phenotype.

4.2 HAB mouse

It remains unclear whether the behaviour of the HAB mice pertains to the HPA axis, and whether this model correlates with the HAB rat line. AVP levels in the PVN do significantly differ to non-anxiety bred animals, though whether this AVP increase is causal or inconsequential remains to be tested *in vivo*. Moreover, the hypothesis that the SNPs residing in the AVP promoter might lead to the similar effects we discovered in the HAB rat line, concerning gene regulation, remains tempting and mandatory to be studied.

4.3 LAB mouse

Familial neurohypophyseal DI is an autosomal dominant disorder caused by a deficiency of AVP. Symptoms of DI, such as polyuria, polydipsia, and thirst, usually manifest several months or years after birth. A limited number of autopsy studies have reported a paucity of AVP-producing neurons in the hypothalamus of patients with DI, leading to the hypothesis that progressive degeneration of AVP-producing cells might be involved in the pathogenesis of the disease (for review see Maghnie, 2003). The AVP precursor (prepro-AVP) is synthesized in magnocellular and parvocellular neurons of the hypothalamus and is converted to pro-AVP by the removal of the signal peptide and the addition of carbohydrate side chains within the ER. After trafficking to the ER, precursors are further glycosylated and packaged into dense core granules. Subsequent proteolytic processing during axonal transport to the posterior pituitary results in the generation of AVP, neurophysin II, and glycoprotein, all of which are stored within neurosecretory vesicles in the nerve terminals and released into the blood in response to osmotic stimuli. AVP then binds to the V2-type receptors in the kidney and controls serum osmolarity by reducing renal water excretion.

In patients with DI, 48 distinct mutations have been found in the AVP gene encoding the AVP precursor (GenBank accession number M11166) (for review see Christensen et al., 2004). Most of the mutations occur within the signal peptide and the NPII domain. Among

Discussion

the signal peptide mutations, a substitution of threonine for alanine at the -1 position, A(-1)T, has been reported in several different ethnic groups (Ito et al., 1993; Krishnamani et al., 1993; McLeod et al., 1993; Kawakami et al., 1998). For the most part, genotype-phenotype correlations are not apparent, and most mutations lead to a similar clinical presentation, although there is some variation even within the same family. An exception, however, is the aforementioned A(-1)T signal peptide mutation, which is frequently associated with delayed-onset or milder DI (for review see Hansen, 1997). These signal peptide mutations have been suspected to interfere with cleavage of the signal peptide and consequently inhibiting release of the functional 9aa AVP peptide. It remains to be determined if the polymorphism in the LAB mice in this study might also be subjected to a similar mechanism, although, to date, no such mutations in this part of the AVP gene have been reported. This can be tested for by expressing both the prepro-AVP constructs in AVP-expressing cell lines and measuring for AVP secretion into the medium. Further studies might also be followed up to investigate the role of the peptides in cell degeneration studies. It should also further be noticed that partial DI in human patients has received little attention, and the existence of individuals presenting with less severe mutations in this AVP gene and showing less evident DI symptoms is fully feasible. This idea is shared with experts in the field, notably David Jentsch (Los Angeles) (personal correspondence).

The relevance of DI to psychiatric research might be questioned at this point. Nevertheless, one has to appreciate the role of AVP, and in specific, the PVN neurons in regulation of the HPA axis. Of the vasopressinergic neurons, the magoncellular cells might secrete far greater levels of AVP than the parvocellular neurons, in response to osmotic challenges, but degeneration of these neurons might well accompany the parvocellular neurons, which processes AVP in an identical mechanism. One further has to appreciate, that this event, as well as disturbing AVP expression, would also disrupt the further co-expression of CRH from a large number of these parvocellular AVP/CRH co-expressing neurons. As described in the introduction, there is evidence that high levels of AVP expression in the PVN present with the development of affective disorders. It is further well documented that high numbers of CRH expressing neurons in this region also result in depressive behaviour. These results in itself provide evidence of tentative a relationship between vasopressinergic and CRH-expressing neuron density in affective disorders, where low AVP/CRH-containing neuron density, on the contrary, may result in an individual being less prone to developing HPA-axis dysregulation.

5 Summary

Two inbred rat lines have been developed that show either high (HAB) or low (LAB) anxiety-related behavior. The behavioral phenotype correlates with arginine vasopressin (AVP) expression at the level of the hypothalamic paraventricular nucleus (PVN), but not supraoptic nucleus, with HAB animals overexpressing the neuropeptide in both magnocellular and parvocellular subdivisions of the PVN.

This study aimed to investigate the molecular cause of the AVP overexpression in the PVN of the HAB animals. Sequencing of the AVP locus resulted in the detection of a number of single nucleotide polymorphisms (SNPs) in the promoter differing between the HAB and LAB animals. Two of the SNPs were embedded in *cis*-regulatory elements. Genotyping further revealed that the HAB-specific allele of the AVP gene promoter occurs in 1.5% of outbred Wistar rats. An assay was developed to address the question of differential allele-specific transcription rates between the LAB and HAB alleles using cross-mated HAB/LAB F1 animals. Results from the experiment revealed the HAB AVP promoter to be more transcriptionally active *in vivo*. EMSA assays confirmed that one specific SNP [A(-1276)G] conferred reduced binding of the transcriptional repressor CARG binding factor A (CBF-A) in the HAB allele. Reporter gene assays supported the view that the A(-1276)G transition in the CARG element impairs CBF-A repression in the HAB allele, which in turn relates to a weakened repression of the intact HAB AVP promoter by CBF-A. Furthermore, CBF-A is highly co-expressed in AVP-containing neurons of the PVN supporting an important role for regulation of AVP gene expression *in vivo*. Taken together, these results demonstrate a role for an AVP gene polymorphism and CBF-A in elevated AVP expression in the PVN of HAB rats likely to contribute to their behavioral and neuroendocrine phenotype.

Phenotypic variation among organisms is central to evolutionary adaptations underlying natural and artificial selection, and also determines individual susceptibility to common diseases including cardiovascular, metabolic and age related and psychiatric diseases. Most phenotypic diversity in natural populations is characterised by differences in degree rather than in kind. In accordance with this view, HAB rats lacked changes in the coding part of the vasopressin gene, but instead were homozygous for the polymorphic promoter region. Therefore, the HAB specific AVP promoter represents a natural model for AVP overexpression and highlights, in turn, cognate molecular pathways which potentially fuel the resulting pathologies. Specifically, our finding that the SNP in position 1276 of the AVP gene promoter underlies AVP overexpression in the PVN of HAB rats, makes this SNP a potential

Summary

target for further studies aimed at improving therapeutic tools. Finally, further studies are necessary to understand to which degree and in concert with which vulnerability loci vasopressin overexpression underlies the complex neuroendocrine and behavioural stigmata in the HAB line. Certainly, such studies will yield important insights into gene-gene interactions between susceptibility genes and shed light on additional pathways suitable for therapeutic interventions. In conclusion, this present work exemplifies that selective inbreeding for behavioural traits and combined phenotypic and molecular analysis of candidate genes is an important step and tool to address these issues.

6 Abbreviations

6.1 Standard

aa	Amino acids	A	Adenine
Amps	Ampere	Bp	Base pair
C	Cytosine	cDNA	Complementary DNA
cR	CentiRays	Ci	Curie
cm,mm	Centimeter, Millimeter	cpm	Counts per Minute
DNA	Deoxyribonucleic acid	EMSA	Electrophoretic mobility shift assay
G	Guanine	g	Gram
h, min, sec	Hour, Minute, Second	kb	Kilobase
kDa	Kilodalton	l	Litre
μ	Micro	m	Milli
min	Minute(s)	Mb	Megabase
M	Molar	mRNA	Messenger-RNA
n	Nano	OD	Optical density
PCR	Polymerase chain reaction	RNA	Ribonucleic acid
rRNA	Ribosomal RNA	RT	Room temperature
RT-PCR	Reverse transcription-PCR	sec(s)	Second(s)
T	Thymine	T _m	Melting temperature
U	Uracil	Vol	Volume
W	Watt	Zn	Zinc

6.2 Buffers and substances

Ac	Acetate	AMCA	7-amino-4-methylcoumarin-3-acetic acid
Amps	Ammoniumperoxodisulphate	ATP	Adenosine TriPhosphate
BSA	Bovine serum albumin	Cy2	Cyanine (spectrum green)
Cy3	Indocarbocyanine (texas red)	ddH ₂ O	Distilled water
DEPC	1ethylpyrocarbonate	DH5 ^α	<i>Escherichia coli</i>
DMEM	Dulbecco's Modified Eagle Medium	DMSO	Dimethylsulphoxide
DdNTP	Dideoxyribonucleoside triphosphate	dNTP	Deoxyribonucleoside triphosphate
DTT	Dithiothreitol	EDTA	Ethylendiamintetraacetate
EGTA	[ethylenebis(oxonitrilo)]tetra-acetate	EtBr	Ethidium Bromide
EtOH	Ethanol	FCS	Foetal calf serum
HEPES	N-2-Hydroxyethylpiperazin-N'-2'-Ethansulfate	IPTG	Isopropyl-β-d-thiogalactopyranoside
M-PVA	Magnetic poly(vinyl alcohol)	MetOH	Methanol
MOPS	3(N-Morpholine)propane-sulfonic acid	³² P	Phosphor-Isotope 32
³³ P	Phosphor-isotope 33	PAGE	Polyacrylamide gel electrophoresis
PBS	Phosphate buffered saline	PMSF	Phenylmethylsulfonylfluoride
PNK	Polynucleotide kinase	SDS	Sodium dodecyl sulphate
SSC	Sodium chloride sodium citric acid	tRNA	Transfer RNA
TE	Tris Ethylenediaminetetraacetic acid	TAE	Tris acetic acid
TBE	Tris boric acid	TEMED	N,N,N',N'-Tetramethyl-ethylenediamine
Tris	Tris-(hydroxymethyl)-aminomethane	X-Gal	5-bromo-4-chloro-3-indoyl-β-D-galactosidase

6.3 Non standard

ACTH	Corticotropin	AML-1	Acute myeloid leukaemia gene
API	Activating protein 1	APOE	Apolipoprotein E
Arg	Arginine	Arnt2	Aryl hydrocarbon receptor nuclear translocator 2
ATG	Start codon sequence	AVP	Arginine Vasopressin
AVP1aR	Arginine Vasopressin 1a receptor	BAFLs	Band across four lanes
B-element	Nopaline synthase promoter (bacteria)	β-gal	β-galactosidase
bHLH	Basic helix-loop-helix protein family	Bmal1	Arnt-like protein1, brain and muscle
BRCA1	Breast cancer 1 gene	CAAT	Sequence involved in trans-activating
cAMP	Cyclic AMP adenosine (3',5'-phosphate)	CArG	C, A/T repeat (6), G
CAT	Chloramphenicol acetyltransferase	CBF-A	CArG binding factor-A
c-domain	Cleavage domain (signal peptide)	c-fos	Murine osteosarcoma viral oncogene homolog
CFTR	Cystic fibrosis transmembrane conductance regulator	CLOCK	Circadian locomotor output cycle kaput
CNS	Central Nervous system	COMP	Cartilage oligomeric matrix protein
ColE1	Colicinogenic factor E1 bacterial plasmid	CORT	Cortisol/Corticosterone
CRE	cAMP responsive element	CREB	cAMP responsive element binding protein
CRH	Corticotropin releasing hormone	CSF	Cerebral spinal fluid
Cyr61	Cysteine-rich, angiogenic inducer, 61	d(CH ₂) ₅ Tyr(Me)AVP	AVP V1 receptor antagonist

Abbreviations

DEX	Dexamethasone	DI	Diabetes Insipidus
dsDNA	Double stranded DNA	E-box	Enhancer element
<i>E.coli</i>	<i>Escherichia coli</i>	EGF	Epidermal growth factor
Egr1	Early growth response factor 1	EMSA	Electrophoretic mobility shift assay
EPM	Elevated plus maze	ER	Endoplasmic reticulum
ERDBP-1	EGF responsive DNA-binding protein	EST	Expressed sequence tag
FBE-A	Drosophila yolk protein fat body enhancer element	F-element	Promoter of Drosophila LINE element
FLAG	DYKDDDDK	FosB	FBJ murine osteosarcoma viral oncogene homolog B
FS	Forced swim	FUSE	Polykaryocytosis inducer gene
GAD	Generalised anxiety disorder	GAPDH	Glyceraldehyde-3-phosphate dehydrogenase
GLO1/2	Glyoxalase ½	GR	Glucocorticoid receptor
GRE	Glucocorticoid receptor DNA binding element	GST	Glutathione-S-transferase
H4TF-1	Histone H4 gene-specific transcription factor	HA	High-anxiety-related-behaviour (non-anxiety bred)
HAB	High-anxiety-related-behaviour (anxiety bred)	h-domain	Hydrophobic domain (signal peptide)
HES1	Hairy/enhancer of split (drosophila homologue)	HiNF-A	Histone 4 nuclear factor A
His	Histone	HNF1a	Hepatocyte nuclear factor 1a
hnRNA	Heteronuclear RNA	hnRNP	Heteronuclear RNA binding protein
HPA	Hypothalamic-pituitary-adrenocortical axis	HS40	Alpha-globin gene element
IEGs	Immediate-early response genes	IGR	Intergenic region (AVP and oxytocin)
IHC	Immunohistochemistry	IL	Interleukin
IRF3	Interferon regulatory factor 3	ISH	<i>In situ</i> -hybridisation
JKTBP	AU-rich element RNA binding factor	LA	Low-anxiety-related-behaviour (non-anxiety bred)
LAB	Low-anxiety-related-behaviour (anxiety bred)	Lyf1	Ikaros, zinc finger protein
MaoA	Monoamine oxidase A	MBP	Myelin basic protein
Mertk	Mer tyrosine kinase protooncogene	MSY-1	Mouse Y-box protein-1
MuLV	Moloney murine leukemia virus	Myc	Avian myelocytomatosis viral oncogene homolog
NAB	Non-anxiety bred	N-box	Neuregulin element
n-domain	Amino-terminal region (signal peptide)	NF-1	Neurofibromatosis type 1
NF-Zz	IFN-gamma inducible element	NGFI-B	nerve growth factor I-B
NPII	Neurophysin II	NRF	Nuclear respiratory factor
Nur1/77	Orphan receptor family nuclear proteins	Pax3	Paired box gene 3
P-box	Element in phenylpropanoid biosynthetic genes	PCR	Polymerase chain reaction
PDE5	Phosphodiesterase 5	Pea3	ETS transcription factor
Pip92	Proline-rich induced protein 92	PKA	cAMP-protein dependent kinase
Pou	Pou-domain transcription factor	POZ	Zinc finger protein 278
Pro	Proline	PTSD	Posttraumatic stress disorder
Puralpha	PUR element binding protein	PVN	Paraventricular nucleus
QTL	Quantitative trait locus	R121919	CRH 1 receptor antagonist
RAP1	Ras-related protein	Ras	GTPase activating protein
RBD	RNA binding domain	RFLP	Restriction fragment length polymorphism
SCLC	Small cell lung cancer	SCN	Suprachiasmatic nucleus
Sim1	Single-minded, drosophila, homolog 1	Smad3	Mothers against deapentaplegic (drosophila)
Sm22	Smooth muscle protein 22	SMN1	Survival of motor neuron 1 gene
SNP	Single nucleotide polymorphism	Snrpb	Small nuclear ribonucleoprotein polypeptide B
SON	Supraoptic nucleus	SP6	Salmonella bacteriophage
Sp1	Transcription factor Sp1	Src	Avian sarcoma viral oncogene homolog
SRE	Serum response element	SRF	Serum response factor
SRP	Signal peptide recognition protein	SSCP	Single stranded conformation polymorphism
ssDBF	Single-stranded DNA binding proteins	ssDNA	Single stranded DNA
SSLP	Sequence length polymorphism	SSRI	Selective serotonin re-uptake inhibitor
T3R	Thyroid hormone receptor	TATA	Sequence involved in trans-activating
TCF11	Nuclear factor reythroid 2-like 1	TF	Transcription factor
Thing1	bHLH factor Hand	TS	Tail suspension
UCR	Upstream conserved region	UTR	Untranslated region
Val	Valine	W	A/T nucleotide
Y-box	Inverted CCAAT box	YY1	Yin Yang 1 protein
zif268	Zinc-finger transcription factor 268		

7 Reference List

1. Adan RA, Burbach JP (1992) Regulation of vasopressin and oxytocin gene expression by estrogen and thyroid hormone. *Prog Brain Res* 92: 127-136.
2. Altemus M, Pigott T, Kalogeras KT, Demitrack M, Dubbert B, Murphy DL, Gold PW (1992) Abnormalities in the regulation of vasopressin and corticotropin releasing factor secretion in obsessive-compulsive disorder. *Arch Gen Psychiatry* 49: 9-20.
3. Altemus M, Swedo SE, Leonard HL, Richter D, Rubinow DR, Potter WZ, Rapoport JL (1994) Changes in cerebrospinal fluid neurochemistry during treatment of obsessive-compulsive disorder with clomipramine. *Arch Gen Psychiatry* 51: 794-803.
4. Angel P, Imagawa M, Chiu R, Stein B, Imbra RJ, Rahmsdorf HJ, Jonat C, Herrlich P, Karin M (1987) Phorbol ester-inducible genes contain a common cis element recognized by a TPA-modulated trans-acting factor. *Cell* 49: 729-739.
5. Bahnsen U, Oosting P, Swaab DF, Nahke P, Richter D, Schmale H (1992) A missense mutation in the vasopressin-neurophysin precursor gene cosegregates with human autosomal dominant neurohypophyseal diabetes insipidus. *EMBO J* 11: 19-23.
6. Bebien M, Salinas S, Becamel C, Richard V, Linares L, Hipskind RA (2003) Immediate-early gene induction by the stresses anisomycin and arsenite in human osteosarcoma cells involves MAPK cascade signaling to Elk-1, CREB and SRF. *Oncogene* 22: 1836-1847.
7. Beck JA, Lloyd S, Hafezparast M, Lennon-Pierce M, Eppig JT, Festing MF, Fisher EM (2000) Genealogies of mouse inbred strains. *Nat Genet* 24: 23-5.
8. Becker KG, Jedlicka P, Templeton NS, Liotta L, Ozato K (1994) Characterization of hUCRBP (YY1, NF-E1, delta): a transcription factor that binds the regulatory regions of many viral and cellular genes. *Gene* 150: 259-266.
9. Bemark M, Olsson H, Heinegard D, Leanderson T (1998) Purification and characterization of a protein binding to the SP6 kappa promoter. A potential role for CArG-box binding factor-A in kappa transcription. *J Biol Chem* 273: 18881-18890.
10. Bennett PM (2004) Genome plasticity: insertion sequence elements, transposons and integrons, and DNA rearrangement. *Methods Mol Biol* 266: 71-113.
11. Benoist C, Chambon P (1981) *In vivo* sequence requirements of the SV40 early promoter region. *Nature* 290: 304-310.
12. Bird P, Gething MJ, Sambrook J (1990) The functional efficiency of a mammalian signal peptide is directly related to its hydrophobicity. *J Biol Chem* 265: 8420-8425.
13. Blume A, Seifert K, Lebrun CJ, Mollenhoff E, Gass P, Unger T, Herdegen T (1998) Differential time course of angiotensin-induced AP-1 and Krox proteins in the rat lamina terminalis and hypothalamus. *Neurosci Lett* 241: 87-90.

Reference List

14. Burbach JP, De Hoop MJ, Schmale H, Richter D, De Kloet ER, Ten Haaf JA, De Wied D (1984) Differential responses to osmotic stress of vasopressin-neurophysin mRNA in hypothalamic nuclei. *Neuroendocrinology* 39:582-4.
15. Burbach JP, Luckman SM, Murphy D, Gainer H (2001) Gene regulation in the magnocellular hypothalamo-neurohypophysial system. *Physiol Rev* 81:1197-267.
16. Burbach JP (2002) Regulation of gene promoters of hypothalamic peptides. *Front Neuroendocrinol* 23: 342-369.
17. Changelian PS, Feng P, King TC, Milbrandt J (1989) Structure of the NGFI-A gene and detection of upstream sequences responsible for its transcriptional induction by nerve growth factor. *Proc Natl Acad Sci U S A* 86: 377-381.
18. Chen H, Hewison M, Hu B, Adams JS (2003) Heterogeneous nuclear ribonucleoprotein (hnRNP) binding to hormone response elements: a cause of vitamin D resistance. *Proc Natl Acad Sci U S A* 100: 6109-6114.
19. Chen H, Hu B, Gacad MA, Adams JS (1998) Cloning and expression of a novel dominant-negative-acting estrogen response element-binding protein in the heterogeneous nuclear ribonucleoprotein family. *J Biol Chem* 273: 31352-31357.
20. Chen LL, Clawson ML, Bilgrami S, Carmichael G (1993) A sequence-specific single-stranded DNA-binding protein that is responsive to epidermal growth factor recognizes an S1 nuclease-sensitive region in the epidermal growth factor receptor promoter. *Cell Growth Differ* 4: 975-983.
21. Chermat R, Thierry B, Mico JA, Steru L, Simon P (1986) Adaptation of the tail suspension test to the rat. *J Pharmacol* 17: 348-350.
22. Christensen JH, Siggaard C, Corydon TJ, deSanctis L, Kovacs L, Robertson GL, Gregersen N, Rittig S (2004) Six novel mutations in the arginine vasopressin gene in 15 kindreds with autosomal dominant familial neurohypophyseal diabetes insipidus give further insight into the pathogenesis. *Eur J Hum Genet* 12: 44-51.
23. Chomczynski P, Sacchi N (1987) Single-step method of RNA isolation by acid guanidinium thiocyanate-phenol-chloroform extraction. *Anal Biochem* 162: 156-9.
24. Coccaro EF, Kavoussi RJ, Hauger RL, Cooper TB, Ferris CF (1998) Cerebrospinal fluid vasopressin levels: correlates with aggression and serotonin function in personality-disordered subjects. *Arch Gen Psychiatry* 55: 708-714.
25. Cok SJ, Acton SJ, Sexton AE, Morrison AR. (2004) Identification of RNA-binding proteins in RAW 264.7 cells that recognize a lipopolysaccharide-responsive element in the 3'-untranslated region of the murine cyclooxygenase-2 mRNA. *J Biol Chem* 279: 8196-205.
26. Coles LS, Diamond P, Lambrusco L, Hunter J, Burrows J, Vadas MA, Goodall GJ (2002) A novel mechanism of repression of the vascular endothelial growth factor promoter, by single strand DNA binding cold shock domain (Y-box) proteins in normoxic fibroblasts. *Nucleic Acids Res* 30: 4845-4854.

Reference List

27. Conkright MD, Canettieri G, Sreaton R, Guzman E, Miraglia L, Hogenesch JB, Montminy M (2003) TORCs: transducers of regulated CREB activity. *Mol Cell* 12: 413-423.
28. Cota D, Marsicano G, Tschop M, Grubler Y, Flachskamm C, Schubert M, Auer D, Yassouridis A, Thone-Reineke C, Ortmann S, Tomassoni F, Cervino C, Nisoli E, Linthorst AC, Pasquali R, Lutz B, Stalla GK, Pagotto U (2003) The endogenous cannabinoid system affects energy balance via central orexigenic drive and peripheral lipogenesis. *J Clin Invest* 112: 423-431.
29. Coulson JM, Fiskerstrand CE, Woll PJ, Quinn JP (1999a) Arginine vasopressin promoter regulation is mediated by a neuron-restrictive silencer element in small cell lung cancer. *Cancer Res* 59: 5123-5127.
30. Coulson JM, Fiskerstrand CE, Woll PJ, Quinn JP (1999b) E-box motifs within the human vasopressin gene promoter contribute to a major enhancer in small-cell lung cancer. *Biochem J* 344: 961-970.
31. Courtois G, Morgan JG, Campbell LA, Fourel G, Crabtree GR (1987) Interaction of a liver-specific nuclear factor with the fibrinogen and alpha 1-antitrypsin promoters. *Science* 238: 688-692.
32. Cvekl A, McDermott JB, Piatigorsky J (1995) cDNA encoding a chicken protein (CRP1) with homology to hnRNP type A/B. *Biochim Biophys Acta* 1261: 290-292.
33. De Bellis MD, Gold PW, Geraciotti TD, Listwak SJ, Kling MA (1993) Association of fluoxetine treatment with reductions in CSF concentrations of corticotropin-releasing hormone and arginine vasopressin in patients with major depression. *Am J Psychiatry* 150: 656-657.
34. Dean JL, Sully G, Wait R, Rawlinson L, Clark AR, Saklatvala J (2002) Identification of a novel AU-rich-element-binding protein which is related to AUF1. *Biochem J* 366: 709-719.
35. Demitrack MA, Kalogeras KT, Altemus M, Pigott TA, Listwak SJ, Gold PW (1992) Plasma and cerebrospinal fluid measures of arginine vasopressin secretion in patients with bulimia nervosa and in healthy subjects. *J Clin Endocrinol Metab* 74: 1277-1283.
36. DiPetrillo K, Tsaih SW, Sheehan S, Johns C, Kelmenson P, Gavras H, Churchill GA, Paigen B (2004) Genetic analysis of blood pressure in C3H/HeJ and SWR/J mice. *Physiol Genomics*.
37. Dou QP, Fridovich-Keil JL, Pardee AB (1991) Inducible proteins binding to the murine thymidine kinase promoter in late G1/S phase. *Proc Natl Acad Sci U S A* 88: 1157-1161.
38. du Vigneaud V (1954) Hormones of the posterior pituitary gland: oxytocin and vasopressin. *Harvey Lect* 50: 1-26.
39. Dunn FL, Brennan TJ, Nelson AE, Robertson GL (1973) The role of blood osmolality and volume in regulating vasopressin secretion in the rat. *J Clin Invest* 52: 3212-3219.

Reference List

40. Dutil J, Moujahidine M, Lemieux C, Jankowski M, Gutkowska J, Deng AY (2001) Chromosomal and comparative mapping of rat oxytocin, oxytocin receptor and vasopressin genes. *Cytogenet Cell Genet* 93: 57-59.
41. Ellis PD, Martin KM, Rickman C, Metcalfe JC, Kemp PR (2002) Increased actin polymerization reduces the inhibition of serum response factor activity by Yin Yang 1. *Biochem J* 364: 547-554.
42. Engelmann M, Wotjak CT, Neumann I, Ludwig M, Landgraf R. (1996) Behavioral consequences of intracerebral vasopressin and oxytocin: focus on learning and memory. *Neurosci Biobehav Rev* 20: 341-58.
43. Falconer DS, Mackay TFC (1996) Introduction to quantitative genetics. Essex, UK: Longman.
44. Fields RL, House SB, Gainer H (2003) Regulatory domains in the intergenic region of the oxytocin and vasopressin genes that control their hypothalamus-specific expression in vitro. *J Neurosci* 23: 7801-7809.
45. Flanagan JR, Becker KG, Ennist DL, Gleason SL, Driggers PH, Levi BZ, Appella E, Ozato K (1992) Cloning of a negative transcription factor that binds to the upstream conserved region of Moloney murine leukemia virus. *Mol Cell Biol* 12: 38-44.
46. Fogh J, Fogh JM, Orfeo T (1977) One hundred and twenty-seven cultured human tumor cell lines producing tumors in nude mice. *J Natl Cancer Inst* 59: 221-226.
47. Frank GK, Kaye WH, Altemus M, Greeno CG (2000) CSF oxytocin and vasopressin levels after recovery from bulimia nervosa and anorexia nervosa, bulimic subtype. *Biol Psychiatry* 48: 315-318.
48. Gainer H, Fields RL, House SB (2001) Vasopressin gene expression: experimental models and strategies. *Exp Neurol* 171: 190-199.
49. Galvagni F, Cartocci E, Oliviero S (1998) The dystrophin promoter is negatively regulated by YY1 in undifferentiated muscle cells. *J Biol Chem* 273: 33708-33713.
50. Gazdar AF, Carney DN, Russell EK, Sims HL, Baylin SB, Bunn PA, Jr., Guccion JG, Minna JD (1980) Establishment of continuous, clonable cultures of small-cell carcinoma of lung which have amine precursor uptake and decarboxylation cell properties. *Cancer Res* 40: 3502-3507.
51. Gilman MZ, Wilson RN, Weinberg RA (1986) Multiple protein-binding sites in the 5'-flanking region regulate c-fos expression. *Mol Cell Biol* 6: 4305-4316.
52. Gold PW, Goodwin FK, Post RM, Robertson GL (1981) Vasopressin function in depression and mania [proceedings]. *Psychopharmacol Bull* 17: 7-9.
53. Gold PW, Kaye W, Robertson GL, Ebert M (1983) Abnormalities in plasma and cerebrospinal-fluid arginine vasopressin in patients with anorexia nervosa. *N Engl J Med* 308: 1117-1123.
54. Gorwood P (2004) Generalized anxiety disorder and major depressive disorder comorbidity: an example of genetic pleiotropy? *Eur Psychiatry* 19: 27-33.

Reference List

55. Grace CO, Fink G, Quinn JP (1999) Characterization of potential regulatory elements within the rat arginine vasopressin proximal promoter. *Neuropeptides* 33: 81-90.
56. Greco O, Marples B, Dachs GU, Williams KJ, Patterson AV, Scott SD (2002) Novel chimeric gene promoters responsive to hypoxia and ionizing radiation. *Gene Ther* 9: 1403-1411.
57. Griebel G, Simiand J, Serradeil-Le Gal C, Wagnon J, Pascal M, Scatton B, Maffrand JP, Soubrie P (2002) Anxiolytic- and antidepressant-like effects of the non-peptide vasopressin V1b receptor antagonist, SSR149415, suggest an innovative approach for the treatment of stress-related disorders. *Proc Natl Acad Sci U S A* 99: 6370-6375.
58. Gustafson TA, Kedes L (1989) Identification of multiple proteins that interact with functional regions of the human cardiac alpha-actin promoter. *Mol Cell Biol* 9: 3269-3283.
59. Hai T, Curran T (1991) Cross-family dimerization of transcription factors Fos/Jun and ATF/CREB alters DNA binding specificity. *Proc Natl Acad Sci U S A* 88: 3720-3724.
60. Hansen LK, Rittig S, Robertson GL (1997) Genetic basis of familial neurohypophyseal diabetes insipidus. *Trends Endocrinol Metab* 8: 363-372.
61. Hara Y, Battey J, Gainer H (1990) Structure of mouse vasopressin and oxytocin genes. *Brain Res Mol Brain Res* 8: 319-324.
62. Hariharan N, Kelley DE, Perry RP (1991) Delta, a transcription factor that binds to downstream elements in several polymerase II promoters, is a functionally versatile zinc finger protein. *Proc Natl Acad Sci U S A* 88: 9799-9803.
63. Henderson ND, Turri MG, DeFries JC, Flint J (2004) QTL Analysis of Multiple Behavioral Measures of Anxiety in Mice. *Behav Genet* 34: 267-293.
64. Henniger MS, Ohl F, Holter SM, Weissenbacher P, Toschi N, Lorsch P, Wigger A, Spanagel R, Landgraf R (2000) Unconditioned anxiety and social behaviour in two rat lines selectively bred for high and low anxiety-related behaviour. *Behav Brain Res* 111: 153-163.
65. Herdegen T, Blume A, Buschmann T, Georgakopoulos E, Winter C, Schmid W, Hsieh TF, Zimmermann M, Gass P (1997) Expression of activating transcription factor-2, serum response factor and cAMP/Ca response element binding protein in the adult rat brain following generalized seizures, nerve fibre lesion and ultraviolet irradiation. *Neuroscience* 81: 199-212.
66. Herdegen T, Leah JD (1998) Inducible and constitutive transcription factors in the mammalian nervous system: control of gene expression by Jun, Fos and Krox, and CREB/ATF proteins. *Brain Res Brain Res Rev* 28: 370-490.
67. Hettema JM, Neale MC, Kendler KS (2001) A review and meta-analysis of the genetic epidemiology of anxiety disorders. *Am J Psychiatry* 158: 1568-1578.
68. Heuser I, Yassouridis A, Holsboer F (1994) The combined dexamethasone/CRH test: a refined laboratory test for psychiatric disorders. *J Psychiatr Res* 28: 341-356.

Reference List

69. Hilakivi LA, Ota M, Lister RG (1989) Effect of isolation on brain monoamines and the behavior of mice in tests of exploration, locomotion, anxiety and behavioral 'despair'. *Pharmacol Biochem Behav* 33: 371-374.
70. Hirschfeld RM (2001) The Comorbidity of Major Depression and Anxiety Disorders: Recognition and Management in Primary Care. *Prim Care Companion J Clin Psychiatry* 3: 244-254.
71. Hofbauer KG, Studer W, Mah SC, Michel JB, Wood JM, Stalder R (1984) The significance of vasopressin as a pressor agent. *J Cardiovasc Pharmacol* 6: S429-38.
72. Hoffmann A, Ciani E, Boeckardt J, Holsboer F, Journot L, Spengler D (2003) Transcriptional activities of the zinc finger protein Zac are differentially controlled by DNA binding. *Mol Cell Biol* 23: 988-1003.
73. Holsboer F, Lauer CJ, Schreiber W, Krieg JC (1995) Altered hypothalamic-pituitary-adrenocortical regulation in healthy subjects at high familial risk for affective disorders. *Neuroendocrin* 62: 340-347.
74. Holsboer F (2000) The corticosteroid receptor hypothesis of depression. *Neuropsychopharmacology* 23: 477-501.
75. Holsboer F (2003) Corticotropin-releasing hormone modulators and depression. *Curr Opin Investig Drugs* 4: 46-50.
76. Holsboer F, von Bardeleben U, Wiedemann K, Muller OA, Stalla GK (1987) Serial assessment of corticotropin-releasing hormone response after dexamethasone in depression. Implications for pathophysiology of DST nonsuppression. *Biol Psychiatry* 22: 228-234.
77. Hsieh TY, Matsumoto M, Chou HC, Schneider R, Hwang SB, Lee AS, Lai MM (1998) Hepatitis C virus core protein interacts with heterogeneous nuclear ribonucleoprotein K. *J Biol Chem* 273: 17651-17659.
78. Hurd YL, Yakovleva T, Nussenzweig A, Li GC, Terenius L, Bakalkin G (1999) A novel neuron-specific DNA end-binding factor in the murine brain. *Mol Cell Neurosci* 14: 213-224.
79. Inder WJ, Prickett TC, Mulder RT, Donald RA, Joyce PR (2001) Reduction in basal afternoon plasma ACTH during early treatment of depression with fluoxetine. *Psychopharmacology (Berl)* 156: 73-78.
80. Innis MA and Gelfand DH (1990) *PCR Protocols*. Academic Press, New York.
81. Ishibashi M, Moriyoshi K, Sasai Y, Shiota K, Nakanishi S, Kageyama R (1994) Persistent expression of helix-loop-helix factor HES-1 prevents mammalian neural differentiation in the central nervous system. *EMBO J* 13: 1799-1805.
82. Ito M, Oiso Y, Murase T, Kondo K, Saito H, Chinzei T, Racchi M, Lively MO (1993) Possible involvement of inefficient cleavage of preprovasopressin by signal peptidase as a cause for familial central diabetes insipidus. *J Clin Invest* 91: 2565-71.

Reference List

83. Itoh S, Katoh Y, Konishi H, Takaya N, Kimura T, Periasamy M, Yamaguchi H (2001) Nitric oxide regulates smooth-muscle-specific myosin heavy chain gene expression at the transcriptional level-possible role of SRF and YY1 through CArG element. *J Mol Cell Cardiol* 33:95-107.
84. Ivell R, Richter D (1984) Structure and comparison of the oxytocin and vasopressin genes from rat. *Proc Natl Acad Sci U S A* 81: 2006-2010.
85. Iwasaki Y, Oiso Y, Saito H, Majzoub JA (1997) Positive and negative regulation of the rat vasopressin gene promoter. *Endocrinology* 138: 5266-5274.
86. Jarman AP, Wood WG, Sharpe JA, Gourdon G, Ayyub H, Higgs DR (1991) Characterization of the major regulatory element upstream of the human alpha-globin gene cluster. *Mol Cell Biol* 11: 4679-4689.
87. Kamada S, Miwa T (1992) A protein binding to CArG box motifs and to single-stranded DNA functions as a transcriptional repressor. *Gene* 119: 229-236.
88. Karolewicz B, Paul IA (2001) Group housing of mice increases immobility and antidepressant sensitivity in the forced swim and tail suspension tests. *Eur J Pharmacol* 415: 197-201.
89. Katon W, von Korff M, Lin E, Lipscomb P, Russo J, Wagner E, Polk E (1990) Distressed high utilizers of medical care. DSM-III-R diagnoses and treatment needs. *Gen Hosp Psychiatry* 12: 355-362.
90. Kawakami A, Okamoto Y, Yamamoto T, Tatsumi Y, Miki T, Tanaka S, Fujii S (1998) Central diabetes insipidus associated with a missense mutation in the arginine vasopressin gene that replaces Ala at the carboxyterminus of the signal peptide with Thr. *Intern Med* 37: 683-6.
91. Kawamura H, Tomozoe Y, Akagi T, Kamei D, Ochiai M, Yamada M (2002) Identification of the nucleocytoplasmic shuttling sequence of heterogeneous nuclear ribonucleoprotein D-like protein JKTBP and its interaction with mRNA. *J Biol Chem* 277: 2732-2739.
92. Keck ME, Welt T, Muller MB, Uhr M, Ohl F, Wigger A, Toschi N, Holsboer F, Landgraf R (2003) Reduction of hypothalamic vasopressinergic hyperdrive contributes to clinically relevant behavioral and neuroendocrine effects of chronic paroxetine treatment in a psychopathological rat model. *Neuropsychopharmacology* 28: 235-43.
93. Keck ME, Welt T, Wigger A, Renner U, Engelmann M, Holsboer F, Landgraf R (2001) The anxiolytic effect of the CRH(1) receptor antagonist R121919 depends on innate emotionality in rats. *Eur J Neurosci* 13: 373-380.
94. Keck ME, Wigger A, Welt T, Muller MB, Gesing A, Reul JM, Holsboer F, Landgraf R, Neumann ID (2002) Vasopressin mediates the response of the combined dexamethasone/CRH test in hyper-anxious rats: implications for pathogenesis of affective disorders. *Neuropsychopharmacology* 26: 94-105.
95. Kendler KS (2001) Twin studies of psychiatric illness: an update. *Arch Gen Psychiatry* 58: 1005-1014.

Reference List

96. Kessler RC, McGonagle KA, Zhao S, Nelson CB, Hughes M, Eshleman S, Wittchen HU, Kendler KS (1994) Lifetime and 12-month prevalence of DSM-III-R psychiatric disorders in the United States. Results from the National Comorbidity Survey. *Arch Gen Psychiatry* 51: 8-19.
97. Kessler RC, Sonnega A, Bromet E, Hughes M, Nelson CB (1995) Posttraumatic stress disorder in the National Comorbidity Survey. *Arch Gen Psychiatry* 52: 1048-1060.
98. Khagai II, Ivanov SV (1994) [Mapping of the gene for antidiuretic hormone in *Rattus norvegicus*]. *Genetika* 30: 1560-1562.
99. Kim JK, Summer SN, Wood WM, Schrier RW (2001) Role of glucocorticoid hormones in arginine vasopressin gene regulation. *Biochem Biophys Res Commun* 289: 1252-1256.
100. Kim KH, Min YK, Baik JH, Lau LF, Chaqour B, Chung KC (2003) Expression of angiogenic factor Cyr61 during neuronal cell death via the activation of c-Jun N-terminal kinase and serum response factor. *J Biol Chem* 278: 13847-13854.
101. Kirmayer LJ, Robbins JM, Dworkind M, Yaffe MJ (1993) Somatization and the recognition of depression and anxiety in primary care. *Am J Psychiatry* 150: 734-741.
102. Klebe RJ RF (1969) Neuroblastoma: cell culture analysis of a differentiating stem cell system. *J Cell Biol* 43: 69A.
103. Koolhaas JM, Korte SM, de Boer SF, van der Vegt BJ, van Reenen CG, Hopster H, de Jong IC, Ruis MA, Blokhuis HJ (1999) Coping styles in animals: current status in behavior and stress-physiology. *Neurosci Biobehav Rev* 23: 925-935.
104. Kovacs KJ, Sawchenko PE (1996) Regulation of stress-induced transcriptional changes in the hypothalamic neurosecretory neurons. *J Mol Neurosci* 7: 125-133.
105. Krishnamani MR, Phillips JAI, Copeland KC (1993) Detection of a novel arginine vasopressin defect by dideoxy fingerprinting. *J Clin Endocrinol Metab* 77:596-598
106. Kurokawa R, Yu VC, Naar A, Kyakumoto S, Han Z, Silverman S, Rosenfeld MG, Glass CK (1993) Differential orientations of the DNA-binding domain and carboxy-terminal dimerization interface regulate binding site selection by nuclear receptor heterodimers. *Genes Dev* 7: 1423-1435.
107. Kyte J, Doolittle RF (1982) A simple method for displaying the hydropathic character of a protein. *J Mol Biol* 157: 105.
108. Landgraf R (2001) Neuropeptides and anxiety-related behavior. *Endocr J* 48: 517-533.
109. Landgraf R, Wigger A (2002) High vs low anxiety-related behavior rats: an animal model of extremes in trait anxiety. *Behav Genet* 32: 301-314.
110. Landgraf R, Wigger A (2003) Born to be anxious: neuroendocrine and genetic correlates of trait anxiety in HAB rats. *Stress* 6: 111-119.
111. Laszlo FA, Laszlo F, De Wied D (1991) Pharmacology and clinical perspectives of vasopressin antagonists. *Pharmacol Rev* 43: 73-108.

Reference List

112. Latinkic BV, Lau LF (1994) Transcriptional activation of the immediate early gene *pip92* by serum growth factors requires both Ets and CArG-like elements. *J Biol Chem* 269: 23163-23170.
113. Lazo PS, Dorfman K, Noguchi T, Mattei MG, Bravo R (1992) Structure and mapping of the *fosB* gene. *FosB* downregulates the activity of the *fosB* promoter. *Nucleic Acids Res* 20: 343-350.
114. Lewin B (2000) *Genes VII*. Oxford University Press Inc., New York.
115. L'honore A, Lamb NJ, Vandromme M, Turowski P, Carnac G, Fernandez A (2003) MyoD distal regulatory region contains an SRF binding CArG element required for MyoD expression in skeletal myoblasts and during muscle regeneration. *Mol Biol Cell* 14: 2151-2162.
116. Li L, He S, Sun JM, Davie JR (2004) Gene regulation by Sp1 and Sp3. *Biochem Cell Biol* 82: 460-471.
117. Liebsch G, Linthorst AC, Neumann ID, Reul JM, Holsboer F, Landgraf R (1998) Behavioral, physiological, and neuroendocrine stress responses and differential sensitivity to diazepam in two Wistar rat lines selectively bred for high- and low-anxiety-related behavior. *Neuropsychopharmacology* 19: 381-396.
118. Lohmueller KE, Pearce CL, Pike M, Lander ES, Hirschhorn JN (2003) Meta-analysis of genetic association studies supports a contribution of common variants to susceptibility to common disease. *Nat Genet* 33: 177-182.
119. Lucki I (1997) The forced swimming test as a model for core and component behavioral effects of antidepressant drugs. *Behav Pharmacol* 8: 523-532.
120. Mack DR, Chiu TK, Dickerson RE (2001) Intrinsic bending and deformability at the T-A step of CCTTTAAAGG: a comparative analysis of T-A and A-T steps within A-tracts. *J Mol Biol* 312: 1037-1049.
121. Maghnie M (2001) Diabetes insipidus. *Horm Res* 59: 42-54.
122. Marck C (1988) 'DNA Strider': a 'C' program for the fast analysis of DNA and protein sequences on the Apple Macintosh family of computers. *Nucleic Acids Res* 6:1829-1836.
123. Marez D, Legrand M, Sabbagh N, Guidice JM, Spire C, Lafitte JJ, Meyer UA, Broly F (1997) Polymorphism of the cytochrome P450 CYP2D6 gene in a European population: characterization of 48 mutations and 53 alleles, their frequencies and evolution. *Pharmacogenetics* 7: 193-202.
124. Marini JC, Nelson KK, Battey J, Siracusa LD (1993) The pituitary hormones arginine vasopressin-neurophysin II and oxytocin-neurophysin I show close linkage with interleukin-1 on mouse chromosome 2. *Genomics* 15:200-202.
125. Marsicano G, Lutz B (1999) Expression of the cannabinoid receptor CB1 in distinct neuronal subpopulations in the adult mouse forebrain. *Eur J Neurosci* 11: 4213-4225.

Reference List

126. Martin KA, Gualberto A, Kolman MF, Lowry J, Walsh K (1997) A competitive mechanism of CArG element regulation by YY1 and SRF: implications for assessment of Phox1/MHox transcription factor interactions at CArG elements. *DNA Cell Biol* 16: 653-661.
127. Martin Y, Valero A, del Castillo E, Pascual SI, Hernandez-Chico C (2002) Genetic study of SMA patients without homozygous SMN1 deletions: identification of compound heterozygotes and characterisation of novel intragenic SMN1 mutations. *Hum Genet* 110: 257-263.
128. Masquilier D, Sassone-Corsi P (1992) Transcriptional cross-talk: nuclear factors CREM and CREB bind to AP-1 sites and inhibit activation by Jun. *J Biol Chem* 267: 22460-22466.
129. McKinney WT, Bunney WE (1969) Animal model of depression. I. Review of evidence: implications for research. *Arch Gen Psychiatry* 21: 240-248.
130. McLeod JF, Kovacs L, Gaskill MB, Rittig S, Bradley GS, Robertson GL (1993) Familial neurohypophyseal diabetes insipidus associated with a signal peptide mutation. *J Clin Endocrinol Metab* 77: 599A-599G.
131. Meaney MJ (2001) Maternal care, gene expression, and the transmission of individual differences in stress reactivity across generations. *Annu Rev Neurosci* 24:1161-92.
132. Meyers S, Downing JR, Hiebert SW (1993) Identification of AML-1 and the (8;21) translocation protein (AML-1/ETO) as sequence-specific DNA-binding proteins: the runt homology domain is required for DNA binding and protein-protein interactions. *Mol Cell Biol* 13: 6336-6345.
133. Michelotti EF, Michelotti GA, Aronsohn AI, Levens D (1996a) Heterogeneous nuclear ribonucleoprotein K is a transcription factor. *Mol Cell Biol* 16: 2350-2360.
134. Michelotti GA, Michelotti EF, Pullner A, Duncan RC, Eick D, Levens D (1996b) Multiple single-stranded cis elements are associated with activated chromatin of the human c-myc gene in vivo. *Mol Cell Biol* 16: 2656-2669.
135. Mikheev AM, Mikheev SA, Zhang Y, Aebersold R, Zarbl H (2000) CArG binding factor A (CBF-A) is involved in transcriptional regulation of the rat Ha-ras promoter. *Nucleic Acids Res* 28: 3762-3770.
136. Minty A, Kedes L (1986) Upstream regions of the human cardiac actin gene that modulate its transcription in muscle cells: presence of an evolutionarily conserved repeated motif. *Mol Cell Biol* 6: 2125-2136.
137. Miyata T, van Ypersele dS, Imasawa T, Yoshino A, Ueda Y, Ogura H, Kominami K, Onogi H, Inagi R, Nangaku M, Kurokawa K (2001) Glyoxalase I deficiency is associated with an unusual level of advanced glycation end products in a hemodialysis patient. *Kidney Int* 60: 2351-2359.
138. Mongeau R, Blier P, de Montigny C (1997) The serotonergic and noradrenergic systems of the hippocampus: their interactions and the effects of antidepressant treatments. *Brain Res Brain Res Rev* 23: 145-195.

Reference List

139. Morgenstern B, Dress A, Werner T (1996) Multiple DNA and protein sequence alignment based on segment-to-segment comparison. *Proc Natl Acad Sci USA* 93: 12098-12103.
140. Murgatroyd CA, Wigger A, Frank E, Singewald N, Bunck M, Holsboer F, Landgraf R, Spengler D (2004) Impaired Repression at a Vasopressin Promoter Polymorphism Underlies Overexpression of Vasopressin in a Rat Model of Trait Anxiety. *J Neurosci* 24: 7762-7770.
141. Murray CJL, Lopez AD (1996) Harvard School of Public Health, World Health Organization and World Bank, "The Global Burden of Disease: A Comprehensive Assessment of Mortality and Disability from Diseases, Injuries, and Risk Factors in 1990 and Projected to 2020 (Global Burden of Disease and Injury, Vol 1)", Harvard University Press.
142. Nagai K, Oubridge C, Kuglstatter A, Menichelli E, Isel C, Jovine L (2003) A Structure, function and evolution of the signal recognition particle. *EMBO* 22: 3479-3485.
143. Nestler EJ, Barrot M, DiLeone RJ, Eisch AJ, Gold SJ, Monteggia LM (2002) Neurobiology of depression. *Neuron* 34: 13-25.
144. Nicholas FW (1987) *Veterinary Genetics*. New York: Oxford Univ. Press.
145. Nickel T, Sonntag A, Schill J, Zobel AW, Ackl N, Brunbauer A, Murck H, Ising M, Yassouridis A, Steiger A, Zihl J, Holsboer F (2003) Clinical and neurobiological effects of tianeptine and paroxetine in major depression. *J Clin Psychopharmacol* 23: 155-168.
146. Nielsen H, Engelbrecht J, Brunak S, von Heijne G (1997) Identification of prokaryotic and eukaryotic signal peptides and prediction of their cleavage sites. *Protein Eng* 10: 1-6.
147. Nilsson I, Whitley P, von Heijne G (1994) The COOH-terminal ends of internal signal and signal-anchor sequences are positioned differently in the ER translocase. *J Cell Biol* 126: 1127-1132.
148. Norman C, Runswick M, Pollock R, Treisman R (1988) Isolation and properties of cDNA clones encoding SRF, a transcription factor that binds to the c-fos serum response element. *Cell* 55: 989-1003.
149. Ouagazzal AM, Moreau JL, Pauly-Evers M, Jenck F (2003) Impact of environmental housing conditions on the emotional responses of mice deficient for nociceptin/orphanin FQ peptide precursor gene. *Behav Brain Res* 144: 111-117.
150. Patten M, Wang W, Aminololama-Shakeri S, Burson M, Long CS (2000) IL-1 beta increases abundance and activity of the negative transcriptional regulator yin yang-1 (YY1) in neonatal rat cardiac myocytes. *J Mol Cell Cardiol* 32: 1341-1352.
151. Pellow S, Chopin P, File SE, Briley M (1985) Validation of open:closed arm entries in an elevated plus-maze as a measure of anxiety in the rat. *J Neurosci Methods* 14: 149-167.

Reference List

152. Peskind ER, Raskind MA, Leake RD, Ervin MG, Ross MG, Dorsa DM (1987) Clonidine decreases plasma and cerebrospinal fluid arginine vasopressin but not oxytocin in humans. *Neuroendocrinology* 46: 395-400.
153. Pirnik Z, Mravec B, Kiss A (2004) Fos protein expression in mouse hypothalamic paraventricular (PVN) and supraoptic (SON) nuclei upon osmotic stimulus: colocalization with vasopressin, oxytocin, and tyrosine hydroxylase. *Neurochem Int* 45: 597-607.
154. Pitts AF, Samuelson SD, Meller WH, Bissette G, Nemeroff CB, Kathol RG (1995) Cerebrospinal fluid corticotropin-releasing hormone, vasopressin, and oxytocin concentrations in treated patients with major depression and controls. *Biol Psychiatry* 38: 330-335.
155. Porsolt RD, Le Pichon M, Jalfre M (1977) Depression: a new animal model sensitive to antidepressant treatments. *Nature* 266: 730-732.
156. Potter E, Behan DP, Fischer WH, Linton EA, Lowry PJ, Vale WW (1991) Cloning and characterization of the cDNAs for human and rat corticotropin releasing factor-binding proteins. *Nature* 349: 423-426.
157. Purba JS, Hoogendijk WJ, Hofman MA, Swaab DF (1996) Increased number of vasopressin- and oxytocin-expressing neurons in the paraventricular nucleus of the hypothalamus in depression. *Arch Gen Psychiatry* 53: 137-143.
158. Quandt K, Frech K, Karas H, Wingender E, Werner T (1995) MatInd and MatInspector: new fast and versatile tools for detection of consensus matches in nucleotide sequence data. *Nucleic Acids Res* 23: 4878-4884.
159. Raadsheer FC, Sluiter AA, Ravid R, Tilders FJ, Swaab DF (1993) Localization of corticotropin-releasing hormone (CRH) neurons in the paraventricular nucleus of the human hypothalamus; age-dependent colocalization with vasopressin. *Brain Res* 615: 50-62.
160. Ramkumar T, Adler S (1999) A requirement for the POU transcription factor, Brn-2, in corticotropin-releasing hormone expression in a neuronal cell line. *Mol Endocrinol* 13: 1237-1248.
161. Ratty AK, Jeong SW, Nagle JW, Chin H, Gainer H, Murphy D, Venkatesh B (1996) A systematic survey of the intergenic region between the murine oxytocin- and vasopressin-encoding genes. *Gene* 174: 71-78.
162. Rao VV, Loffler C, Battey J, Hansmann I (1992) The human gene for oxytocin-neurophysin I (OXT) is physically mapped to chromosome 20p13 by in situ hybridization. *Cytogenet Cell Genet* 61: 271-273.
163. Ritchie SA, Pasha MK, Batten DJ, Sharma RK, Olson DJ, Ross AR, Bonham K (2003) Identification of the SRC pyrimidine-binding protein (SPy) as hnRNP K: implications in the regulation of SRC1A transcription. *Nucleic Acids Res* 31: 1502-13.
164. Rodgers RJ, Cole JC (1993) Influence of social isolation, gender, strain, and prior novelty on plus-maze behaviour in mice. *Physiol Behav* 54: 729-736.

Reference List

165. Romey MC, Pallares-Ruiz N, Mange A, Mettling C, Peytavi R, Demaille J, Claustres M (2000) A naturally occurring sequence variation that creates a YY1 element is associated with increased cystic fibrosis transmembrane conductance regulator gene expression. *J Biol Chem* 275: 3561-3567.
166. Rost B (1996) PHD: predicting 1D protein structure by profile based neural networks *Meth in Enzym* 266: 525-539.
167. Rost B, Fariselli P, Casadio R (1996) Topology prediction for helical transmembrane proteins at 86% accuracy. *Protein Sci* 5: 1704-1718.
168. Rost B, Sander C (1993) Secondary structure prediction of all-helical proteins in two states. *Protein Eng* 6: 831-836.
169. Rushlow W (1997) Elevated levels of CARG-binding protein mRNA in the striatum in neuroleptic-induced dyskinesia. *Society Neuroscience Abstract* 23.
170. Rushlow WJ, Rajakumar B, Flumerfelt BA, Naus CC, Rajakumar N (2000) Changes in CARG-binding protein A expression levels following injection(s) of the D1-dopamine agonist SKF-82958 in the intact and 6-hydroxydopamine-lesioned rat. *Neuroscience* 98: 69-78.
171. Rushlow WJ, Rajakumar N, Flumerfelt BA, Naus CC (1999) Characterization of CARG-binding protein A initially identified by differential display. *Neuroscience* 94: 637-649.
172. Ryan P, Robbins A, Whealy M, Enquist LW (1993) Overall signal sequence hydrophobicity determines the in vivo translocation efficiency of a herpesvirus glycoprotein. *Virus Genes* 7: 5-21.
173. Ryan P, Edwards CO (1995) Systematic introduction of proline in a eukaryotic signal sequence suggests asymmetry within the hydrophobic core. *J Biol Chem* 270: 27876-27879.
174. Sadakata T, Kuo C, Ichikawa H, Nishikawa E, Niu SY, Kumamaru E, Miki N (2000) Puralpha, a single-stranded DNA binding protein, suppresses the enhancer activity of cAMP response element (CRE). *Brain Res Mol Brain Res* 77: 47-54.
175. Sage D, Maurel D, Bosler O (2002) Corticosterone-dependent driving influence of the suprachiasmatic nucleus on adrenal sensitivity to ACTH. *Am J Physiol Endocrinol Metab* 282: E458-465.
176. Salchner P, Singewald N (2002) Neuroanatomical substrates involved in the anxiogenic-like effect of acute fluoxetine treatment. *Neuropharmacology* 43: 1238-1248.
177. Sanger F, Nicklen S, Coulson AR (1977) DNA sequencing with chain-terminating inhibitors. *Proc Natl Acad Sci USA* 74: 5463-5467.
178. Sawchenko PE (1987) Adrenalectomy-induced enhancement of CRF and vasopressin immunoreactivity in parvocellular neurosecretory neurons: anatomic, peptide, and steroid specificity. *J Neurosci* 7: 1093-1106.

Reference List

179. Scherer WF Hoogasian AF (1954) Preservation at subzero temperatures of mouse fibroblasts (Strain L) and human epithelial cells (Strain HeLa). *Proc Soc Exp Biol Med* 87: 480-487.
180. Schmitz E, Mohr E, Richter D (1991) Rat vasopressin and oxytocin genes are linked by a long interspersed repeated DNA element (LINE): sequence and transcriptional analysis of LINE. *DNA Cell Biol* 10: 81-91.
181. Schug J, Overton C (1997) Transcription Element Search Software on the WWW. Technical Report CBIL-TR-1997-1001-v0.0.
182. Schwartzbauer G, Yu JH, Cheng H, Menon RK (1998) Transcription factor MSY-1 regulates expression of the murine growth hormone receptor gene. *J Biol Chem* 273: 24760-24769.
183. Scott LV, Dinan TG (2002) Vasopressin as a target for antidepressant development: an assessment of the available evidence. *J Affect Disord* 72: 113-124.
184. Scott SD, Joiner MC, Marples B (2002) Optimizing radiation-responsive gene promoters for radiogenetic cancer therapy. *Gene Ther* 9: 1396-1402.
185. Segurado R, Detera-Wadleigh SD, Levinson DF, Lewis CM, Gill M, Nurnberger JI, Jr., Craddock N, DePaulo JR, Baron M, Gershon ES, Ekholm J, Cichon S, Turecki G, Claes S, Kelsoe JR, Schofield PR, Badenhop RF, Morissette J, Coon H, Blackwood D, McInnes LA, Foroud T, Edenberg HJ, Reich T, Rice JP, Goate A, McInnis MG, McMahon FJ, Badner JA, Goldin LR, Bennett P, Willour VL, Zandi PP, Liu J, Gilliam C, Joo SH, Berrettini WH, Yoshikawa T, Peltonen L, Lonqvist J, Nothen MM, Schumacher J, Windemuth C, Rietschel M, Propping P, Maier W, Alda M, Grof P, Rouleau GA, Del Favero J, van Broeckhoven C, Mendlewicz J, Adolfsson R, Spence MA, Luebbert H, Adams LJ, Donald JA, Mitchell PB, Barden N, Shink E, Byerley W, Muir W, Visscher PM, Macgregor S, Gurling H, Kalsi G, McQuillin A, Escamilla MA, Reus VI, Leon P, Freimer NB, Ewald H, Kruse TA, Mors O, Radhakrishna U, Blouin JL, Antonarakis SE, Akarsu N (2003) Genome scan meta-analysis of schizophrenia and bipolar disorder, part III: Bipolar disorder. *Am J Hum Genet* 73: 49-62.
186. Shapiro RA, Xu C, Dorsa DM (2000) Differential transcriptional regulation of rat vasopressin gene expression by estrogen receptor alpha and beta. *Endocrinology* 141: 4056-4064.
187. Sherman TG, Day R, Civelli O, Douglass J, Herbert E, Akil H, Watson SJ (1988) Regulation of hypothalamic magnocellular neuropeptides and their mRNAs in the Brattleboro rat: coordinate responses to further osmotic challenge. *J Neurosci* 8: 3785-96.
188. Shrivastava A, Calame K (1994) An analysis of genes regulated by the multi-functional transcriptional regulator Yin Yang-1. *Nucleic Acids Res* 22: 5151-5155.
189. Solberg LC, Ahmadiyeh N, Baum AE, Vitaterna MH, Takahashi JS, Turek FW, Redei EE (2003) Depressive-like behavior and stress reactivity are independent traits in a Wistar Kyoto x Fisher 344 cross. *Mol Psychiatry* 8: 423-433.

Reference List

190. Sorensen PS, Gjerris A, Hammer M (1985) Cerebrospinal fluid vasopressin in neurological and psychiatric disorders. *J Neurol Neurosurg Psychiatry* 48: 50-57.
191. Spengler D, Waeber C, Pantaloni C, Holsboer F, Bockaert J, Seeburg PH, Journot L (1993) Differential signal transduction by five splice variants of the PACAP receptor. *Nature* 365: 170-175.
192. Stauffer DR, Chukwumezie BN, Wilberding JA, Rosen ED, Castellino FJ (1998) Characterization of transcriptional regulatory elements in the promoter region of the murine blood coagulation factor VII gene. *J Biol Chem* 273: 2277-2287.
193. Stringer JL, Belaguli NS, Iyer D, Schwartz RJ, Balasubramanyam A (2002) Developmental expression of serum response factor in the rat central nervous system. *Brain Res Dev Brain Res* 138: 81-86.
194. Taira E, Baraban JM (1997) Identification of a strand-specific Egr response element binding complex enriched in rat brain. *J Neurochem* 68: 2255-62.
195. Takiguchi M, Mori M (1991) In vitro analysis of the rat liver-type arginase promoter. *J Biol Chem* 266: 9186-9193.
196. Tasken K, Aandahl EM (2004) Localized effects of cAMP mediated by distinct routes of protein kinase A. *Physiol Rev* 84: 137-167.
197. Terasaki T, Matsuno Y, Shimosato Y, Yamaguchi K, Ichinose H, Nagatsu T, Kato K (1994) Establishment of a human small cell lung cancer cell line producing a large amount of anti-diuretic hormone. *Jpn J Cancer Res* 85: 718-722.
198. Thompson RC, Seasholtz AF, Herbert E (1987) Rat corticotropin-releasing hormone gene: sequence and tissue-specific expression. *Mol Endocrinol* 1: 363-370.
199. Thornalley PJ (2003) Glyoxalase I--structure, function and a critical role in the enzymatic defence against glycation. *Biochem Soc Trans* 31: 1343-1348.
200. Todaro GJaGH (1963) Quantitative studies of the growth of mouse embryo cells in culture and their development into established lines. *J Cell Biol* 17: 299-313.
201. Tominaga K, Shinohara K, Otori Y, Fukuhara C, Inouye ST (1992) Circadian rhythms of vasopressin content in the suprachiasmatic nucleus of the rat. *Neuroreport* 3: 809-812.
202. Tornatzky W, Miczek KA (1994) Behavioral and autonomic responses to intermittent social stress: differential protection by clonidine and metoprolol. *Psychopharmacology (Berl)* 116: 346-356.
203. Treisman R (1987) Identification and purification of a polypeptide that binds to the c-fos serum response element. *EMBO J* 6: 2711-2717.
204. Trimmer EE, Zamble DB, Lippard SJ, Essigmann JM (1998) Human testis-determining factor SRY binds to the major DNA adduct of cisplatin and a putative target sequence with comparable affinities. *Biochem* 37: 352-62.

Reference List

205. Tsang SY, Nakanishi M, Peterlin BM (1990) Mutational analysis of the DRA promoter: cis-acting sequences and trans-acting factors. *Mol Cell Biol* 10: 711-719.
206. Uhl GR, Grow RW (2004) The burden of complex genetics in brain disorders. *Arch Gen Psychiatry* 61: 223-229.
207. Umar A, Luider TM, Berrevoets CA, Grootegoed JA, Brinkmann AO (2003) Proteomic analysis of androgen-regulated protein expression in a mouse fetal vas deferens cell line. *Endocrinology* 144: 1147-1154.
208. Uzan G, Prenant M, Prandini MH, Martin F, Marguerie G (1991) Tissue-specific expression of the platelet GPIIb gene. *J Biol Chem* 266: 8932-8939.
209. van Londen L, Goekoop JG, van Kempen GM, Frankhuijzen-Sierevogel AC, Wiegant VM, van der Velde EA, De Wied D (1997) Plasma levels of arginine vasopressin elevated in patients with major depression. *Neuropsychopharmacology* 17: 284-292.
210. van Londen L, Kerkhof GA, van den BF, Goekoop JG, Zwinderman KH, Frankhuijzen-Sierevogel AC, Wiegant VM, De Wied D (1998) Plasma arginine vasopressin and motor activity in major depression. *Biol Psychiatry* 43: 196-204.
211. van Loo PL, Mol JA, Koolhaas JM, van Zutphen BF, Baumans V (2001) Modulation of aggression in male mice: influence of group size and cage size. *Physiol Behav* 72: 675-683.
212. van West D, Del Favero J, Aulchenko Y, Oswald P, Souery D, Forsgren T, Sluijs S, Bel-Kacem S, Adolfsson R, Mendlewicz J, van Duijn C, Deboutte D, van Broeckhoven C, Claes S (2004) A major SNP haplotype of the arginine vasopressin 1B receptor protects against recurrent major depression. *Mol Psychiatry* 9: 287-292.
213. Vargas ML, Abella C, Hernandez J (2001) Diazepam increases the hypothalamic-pituitary-adrenocortical (HPA) axis activity by a cyclic AMP-dependent mechanism. *Br J Pharmacol* 133: 1355-1361.
214. Vassileva MT, Matunis MJ (2004) SUMO modification of heterogeneous nuclear ribonucleoproteins. *Mol Cell Biol* 24: 3623-3632.
215. Verbalis JG (2003) Diabetes insipidus. *Rev Endocr Metab Disord* 4: 177-185.
216. Verbeeck MA, Adan RA, Burbach JP (1990) Vasopressin gene expression is stimulated by cyclic AMP in homologous and heterologous expression systems. *FEBS Lett* 272: 89-93.
217. Verger A, Perdomo J, Crossley M, Verbeeck MA, Adan RA, Burbach JP (2003) Modification with SUMO. A role in transcriptional regulation. *EMBO* 4: 137-142.
218. Vincent CK, Gualberto A, Patel CV, Walsh K (1993) Different regulatory sequences control creatine kinase-M gene expression in directly injected skeletal and cardiac muscle. *Mol Cell Biol* 13: 1264-72.
219. von Heijne G (1998) Life and death of a signal peptide. *Nature* 396: 111-113.

Reference List

220. Wada K, Inoue K, Hagiwara M (2002) Identification of methylated proteins by protein arginine N-methyltransferase 1, PRMT1, with a new expression cloning strategy. *Biochim Biophys Acta* 1591: 1-10.
221. Wahlbeck K, Sundblom M, Kalso E, Tigerstedt I, Rimon R (1996) Elevated plasma vasopressin and normal cerebrospinal fluid angiotensin-converting enzyme in chronic pain disorder. *Biol Psychiatry* 40: 994-999.
222. Weaver DR (1998) The suprachiasmatic nucleus: a 25-year retrospective. *J Biol Rhythms* 13:100-112.
223. Weaver IC, Cervoni N, Champagne FA, D'Alessio AC, Sharma S, Seckl JR, Dymov S, Szyf M, Meaney MJ (2004) Epigenetic programming by maternal behavior. *Nat Neurosci* 7: 847-54.
224. Weisman-Shomer P, Cohen E, Fry M (2002) Distinct domains in the CArG-box binding factor A destabilize tetraplex forms of the fragile X expanded sequence d(CGG)_n. *Nucleic Acids Res* 30: 3672-3681.
225. Wigger A, Loerscher P, Weissenbacher P, Holsboer F, Landgraf R (2001) Cross-fostering and cross-breeding of HAB and LAB rats: a genetic rat model of anxiety. *Behav Genet* 31: 371-382.
226. Wigger A, Sanchez MM, Mathys KC, Ebner K, Frank E, Liu D, Kresse A, Neumann ID, Holsboer F, Plotsky PM, Landgraf R (2004) Alterations in central neuropeptide expression, release, and receptor binding in rats bred for high anxiety: critical role of vasopressin. *Neuropsychopharmacology* 29: 1-14.
227. Will CC, Aird F, Redei EE (2003) Selectively bred Wistar-Kyoto rats: an animal model of depression and hyper-responsiveness to antidepressants. *Mol Psychiatry* 8: 925-932.
228. Williams GT, Lau LF (1993) Activation of the inducible orphan receptor gene *nur77* by serum growth factors: dissociation of immediate-early and delayed-early responses. *Mol Cell Biol* 13: 6124-6136.

8 Acknowledgments

For providing me with the opportunity of performing this study and their valuable support I am extremely grateful to Dr. Spengler, Professor Landgraf and Professor Holsboer. For further stimulatory discussions and encouragement I am again thankful to Dr. Spengler. In help with DNA and protein experiments I am further in debt to Anke Hoffmann and Dr. Spengler. I would also like to acknowledge the work of Elisabeth Frank, in supplying the brain material for RNA extraction, important help with the CBF-A *in situ*-hybridisation, and data regarding CBF-A and AVP immunohistochemistry and the rat behavioural analysis used in the association and correlation studies. I am also grateful to Dr. Wigger for help with the CBF-A *in situ*-hybridisation and access to further behavioural and neuroendocrine data. For all the CBF-A and AVP fluorimmunohistochemistry work I am thankful to Dr. Nicolas Singewald. For further technical help with immunohistochemistry and *in situ*-hybridisation experiments I would like to thank Dr. Paez-Pereda and Dr. Daniela Cota respectively and Dr. Marily Theodoropoulou and Dr. Georgos Vlotides for further valuable support. For statistical advice and the expert multiple regression analysis of the association study I am extremely grateful to Dr. Bertram Müller-Myhsok. I would like to acknowledge for the provision of materials; Dr. Takeo Terasaki and Dr. Judy Coulson for the Lu-165 cells, Dr. Shinji Kamada and Dr. Akira Inoue for the CBF-A cDNA, Dr. Alaitz Aranburu, Dr. Thomas Leanderson for the CBF-A antibody and CBF-A deletion constructs and Dr. Fry for additional CBF-A antibodies. For much appreciated advise and correspondence, I would like to thank Dr. Richard Treisman, Dr. Bob Schwartz, Dr. Blume, Dr. Janet Stringer, Dr. Peter Burbach, Dr. Alaitz Aranburu, Dr. Robert Jentsch, Dr. Shi, Dr. Oei, Dr. Edward Seto, Dr. Wayne Vedeckis, Dr. Amy Lee, Dr. Judy Coulson and Dr. Daniela Glatz.

9 Curriculum Vitae

Christopher Anthony Murgatroyd

Isartalstr. 45a
80469 München
+49-01742504249
murgatroyd@mpipsykl.mpg.de

Born on 5th June 1975 in Plymouth, UK.

EDUCATION

- Feb 2000 - **Max-Planck-Institut für Psychiatrie, München, Germany.**
AG Molecular Neuroendocrinology
Doctoral thesis submitted “Impaired repression at a vasopressin promoter polymorphism in a rat model of trait anxiety and depression”
- Sept 1997 - Sept 1998 **University of Newcastle upon Tyne, UK.**
Dept. Human Genetics
M.Sc Medical Genetics. Research; alpha-synuclein mutations and Dementia with Lewy bodies.
- Sept 1994 – Sept 1997 **Swansea University, Wales, UK.**
Dept. Genetics
B.Sc Genetics. Research; Genetic control of plant height in *Pelargonium*.

RESEARCH EXPERIENCE

- Sept 1998- Nov 1999 Research assistant. Dept. Human Genetics, University of Newcastle upon Tyne, UK.
Research; molecular cause of Lewy body formation in Dementia with Lewy bodies.